DOE/ER/13491--709

Progress Report

for

Grant No: DE-FG02-86ER13491
Reporting Period: FY 1991–94

Submitted to

U.S. Department of Energy

Title: "Atomic Physics with Highly Charged Ions"

Institution: Kansas State University
Department of Physics
J.R. Macdonald Laboratory
Manhattan, Kansas 66506-2604

Principal Investigator: Patrick Richard
Patrick Richard
Director, J.R. Macdonald Laboratory

August 1994

DISCLAIMER

Table of Contents

1. Foreword

This report presents a review of the research performed by the personnel of the J. R. Macdonald Laboratory and of the technical assessments of the laboratory over the three-year period of this Department of Energy grant. The report is prepared for the Atomic Physics Program of the Fundamental Interactions Branch of the Division of Chemical Sciences, Office of Energy Research.

This three-year grant period has been an extremely productive and busy one in which 94 papers were published in refereed journals, 15 papers have been accepted or submitted for publication, and 110 papers were given at conferences or meetings. Seven of the latter papers were invited talks.

The KSU CRYEBIS, which was put into use during the previous three-year grant period, has been used extensively for experiments during the present reporting period and has seen a gradual improvement in its operational capabilities. The KSU superconducting LINAC, which was put into operation after its initial beam tests during the previous reporting period, has been in routine use for experiments during the present reporting period. The tandem Van de Graaff continues to be used for many experiments as well as for injecting beams into the LINAC.

The new initiative of building an ion-ion collision research facility proposed by J. Giese in the last three-year proposal has progressed very well with the help of a DOE Instrumentation Grant. The ECR ion source for this facility has been installed and tested. The interaction region and other peripherals are presently being installed. We anticipate that this system will be put into operation during the proposed three-year grant period.

On October 15-16, 1991, KSU hosted the annual Department of Energy Atomic Physics Program Workshop. Twenty-one oral presentations were made and a total of forty-one research summaries were submitted.

The VIth International Conference on the Physics of Highly Charged Ions was hosted by KSU September 28-October 2, 1992 and Co-chaired by P. Richard and M. Stockli. The proceedings were published in AIP Conference Proceedings 274, pp. 1-700, ed. by P. Richard, M. Stockli, C. L. Cocke, and C. D. Lin (1993) AIP, New York. Over 190 participants gathered for the conference with nearly 50% being from abroad.

During this reporting period, Dr. U. Thumm was hired as an Assistant Professor in the vacancy left by Prof. J. McGuire. He is working primarily on the theory of ion-solid interactions. In addition, P. E. Gibson was hired in the needed staff position to assist in the CRYEBIS maintenance and operation. The remainder of the faculty and staff positions were unchanged during this three-year period. There are 13 faculty members and 14 full-time staff members. This translates into a 20 FTE effort.

During the reporting period, we graduated 7 Ph.D. students and 2 M.S. students. At the present time we have 14 students doing Ph.D. research, and 7 undergraduate students working on a part-time basis.

P. Richard
Laboratory Director
August 10, 1994

2. JRM Laboratory Schematic

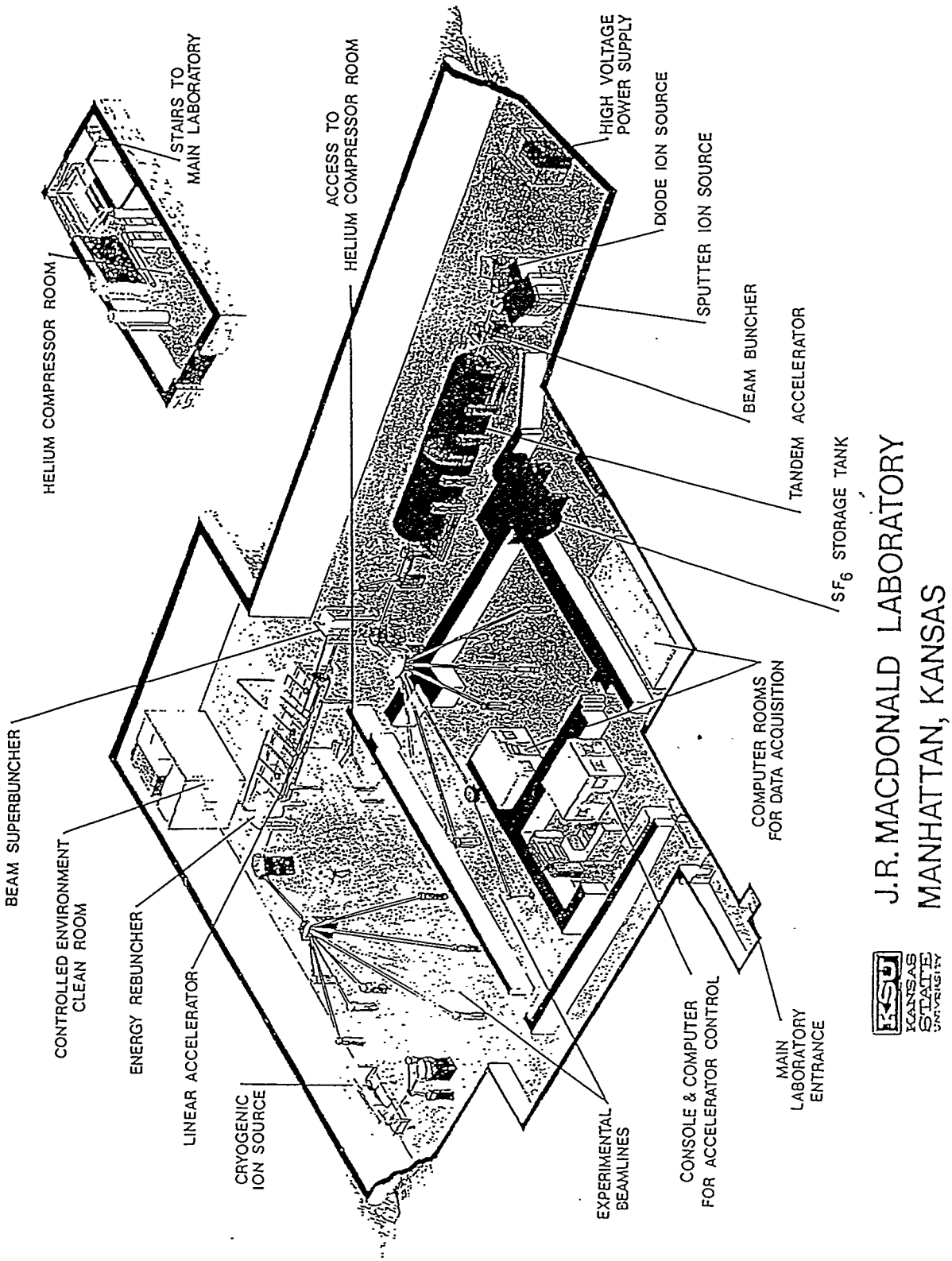

3. Introduction

The study of inelastic collision phenomena with highly charged projectile ions and the interpretation of spectral features resulting from these collisions remain as the major focal points in the atomic physics research at the J. R. Macdonald Laboratory, Kansas State University, Manhattan, Kansas. The title of the research project, "Atomic Physics with Highly Charged Ions," speaks to these points. The experimental work in the past few years has divided into collisions at high velocity using the primary beams from the tandem and LINAC accelerators and collisions at low velocity using the CRYEBIS facility. Theoretical calculations have been performed to accurately describe inelastic scattering processes of the one-electron and many-electron type, and to accurately predict atomic transition energies and intensities for x rays and Auger electrons.

The list of laboratory personnel involved in this project is given in Section 4 and brief summaries of the research performed during this reporting period are presented in Section 5 of this report. Each summary writeup refers to the publications that have resulted from the research. They are referred to by the publication number, as given in Section 7 of the report, List of Publications. A report on the laboratory operations is given in Section 6.

4. JRM Laboratory Personnel

J.R. Macdonald Laboratory Personnel
February 15, 1992 - July 14, 1994

Faculty

Itzhak Ben-Itzhak, Assistant Professor
Chander P. Bhalla, Professor
Kevin Carnes, Assistant Research Professor
C. Lewis Cocke, Professor and Associate Director for Research Planning
Brett DePaola, Associate Professor
John P. Giese, Assistant Professor
Tom J. Gray, Professor and Associate Director for Accelerator Operations
Siegbert Hagmann, Professor
James C. Legg, Professor and Department Head
Chii-Dong Lin, Distinguished Professor
Patrick Richard, Cortelyou-Rust Professor and Laboratory Director
Martin P. Stockli, Assistant Research Professor
Uwe Thumm, Assistant Professor

Research Associates

Zheng Chen
Emanuel Kamber, Present address: Western Michigan University, Kalamazoo
K.R. Karim, Present address: Illinois State University, Normal
Vidhya Krishnamurthi
Dan Parks
Mark Raphaelian, Present address: Alcedo, Sunnyvale, CA
Harald Schone, Present address: Sandia National Laboratories, Albuquerque
Michael Schulz, Present address: University of Missouri, Rolla
Rajiv Shingal, Present address: Philadelphia, PA
Jack Straton, Present address: California State University, Fresno
Theodore Zouros, Present address: University of Crete, Heraklion, Greece
Keith Wong

Technical Staff

Paul Gibson, Assistant Scientist
Chrysostomos Hadjistamoulou, Assistant Scientist
Present address: Lincoln, Nebraska
Vince Needham, Assistant Scientist
Carol Regehr, Assistant Scientist
Tracy Tipping, Assistant Scientist - Lab Safety Officer

Laboratory Staff

Megan Maskill, Draftsperson*, until May 1993
Shauna Schauf, Draftsperson*
Dave Hill,[1] Machine Shop Foreman
Steve Kelly, Electronics Technician
Chris Koci, Secretary
Robert Krause, Research Technician
Al Rankin, Research Technician
Dea Richard, Administrative Assistant
Mark Ross,[1] Electronics Shop Foreman
Daphne Sand, Secretary*
Mike Wells,[1] Research Technician

Visiting Scientists

Scott Arko, Colorado State University, Ft. Collins, CO
Yohko Awaya, Institute of Physical and Chemical Research, RIKEN, Saitama, Japan
Robert Bastasz, Sandia National Laboratory, Livermore, California
J.P. Briand, Université Pierre et Marie Curie, Paris, France
Robert Cowan, Los Alamos National Laboratory, NM
Lucille de Billy, Université Pierre et Marie Curie, Paris, France
Evgeni Donets, JINR, Dubna, Russia
Reinhard Dorner, University of Frankfurt, Germany
Charles Fehrenbach, Colorado State University, Ft. Collins, CO
Ralf Herrman, University of Frankfurt, Germany
Egon Jans, University of Aarhus, Denmark
Tadashi Kambara, Institute of Physical and Chemical Research, RIKEN, Saitama, Japan
Emanuel Kamber, Western Michigan University, Kalamazoo, MI
Dinakar Kanjilal, Nuclear Science Centre, New Delhi, India
Yasuyuki Kanai, Institute of Physical and Chemical Research, RIKEN, Saitama, Japan
K.R. Karim, Illinois State University, Normal, IL
Helge Knudsen, University of Aarhus, Denmark
Bertold M. Krassig, University of Freiburg, Germany
D.H. Lee, Brookhaven National Lab, NY/Oak Ridge National Lab, TN
Stephen Lundeen, Colorado State University, Ft. Collins, CO
Frank Melchert, University of Giessen, Germany
Stefan Meuser, University of Giessen, Germany
Eduardo Montenegro, Pontificia Universidade Catholica do Rio de Janeiro, Rio de Janeiro, Brasil
Robert Moshammer, Buettelborn, Germany
Masaki Oura, RIKEN, Hachioji, Tokyo, Japan
R. Parameswaran, Texas A & M University, College Station, TX
Edward S. Parilis, California Institute of Technology, Pasadena, CA
Tricia Reeves, University of Kentucky, Lexington, KY

Robert Schmeider, Sandia National Laboratory, Albuquerque, NM
H. Schmidt-Böcking, University of Frankfurt, Germany
Michael Schulz, University of Missouri, Rolla, MO
Hisham Sharabati, University of Jordan, Amman, Jordan
Alexander Skutlartz, East Carolina University, Greenville, NC
Nico Stolterfoht, Hahn-Meitner Institute, Berlin, Germany
John Tanis, Western Michigan University, Kalamazoo, Michigan
S.L. Varghese, University of South Alabama, Mobile, AL
Mike Wilson, Royal Holloway and New Bedford College, Egham, England
Theodoros Zouros, University of Crete, Heraklion, Greece

Visiting Students

Graduate

Peter Grübling, University of Dresden, Germany
Stefan Lampenscherf, University of Dresden, Germany
Jesper Lauritsen, University of Copenhagen, Denmark
Ullrick Mikkelsen, University of Aarhus, Denmark
Liesl Neale, University of London, United Kingdom
Jörg Opitz, University of Dresden, Germany
Lars Rebohle, University of Dresden, Germany
Nathalie Renard, University of Paris, France
Anders Waananen, University of Copenhagen, Denmark

Undergraduate

Summer 1992 NSF REU Participants
Christopher Bevin, Middlebury, VT
Jason Breitweg, Brunswick, ME
Zoltan Cseri, Northbrook, IL
Chris Ferris, Sarasota, FL
Joseph Kaufman, Des Moines, IA
Damon Johnson, Pearl River, IA
Allen Landers, Manhattan, KS
Clinton Miller, Thomas, OK
Peter Norris, Denver, CO
Marc Troike, Oxford, OH

Summer 1993 NSF REU Participants:
Sean Armster, Montgomery, AL
Bryan Barnes, Laurel, MS
David Berry, Estes Park, CO
Kristana Bloom, Cedar Rapids, IA
Peter Bronk, Salisbury, CT
Joseph Kaufman, Portsmouth, IA
Diana Ling, Albuquerque, NM
Michael Payne, Florissant, MO
Joanna Randall, Milwaukee, WI

Joseph Roberts, Columbus, OH
Kenneth Ruchala, Valley Stream, NY
Roger Smith, Dixon, MO
Eric Wells, Axtell, NE

Summer 1994 NSF REU Participants
Bryce Anson, University of Missouri-Rolla
Jia Ming Chen, Boston University
Scott Cowherd, Met. St. College of Denver
John Eaton, Carleton College
Gilbert Feke, Boston University
Russell Fields, SW Oklahoma State University
David Fischbach, NE Missouri State University
Danny Fry, Texas A & M University
Harvard Harding, Clarkson University
Rebecca Harlan, Kansas State University
Natalia Kuznetsova, Kenyon College
Charles (Chris) Polly, University of Missouri-Rolla
Robert Quinn, University of Arkansas-Fayetteville
Joseph Roberts, Colorado Springs
David Seematter, Kansas State University
Amy Sutton, Bryn Mawr

Graduate Research Assistants and Advanced Degrees Awarded
Mohammad Abdallah
Habib Aliabadi
Rami Ali, Ph.D., 1993
Present address: Argonne National Laboratory, Illinois
Chun-Yen Chen
Song Cheng, Ph.D., 1991
Present address: Argonne National Laboratory
Vickie Frohne, Ph.D., 1994
Present address: Western Illinois University, Macomb
Shon Grabbe
Stuart Ginther, M.S., 1992
Hisham Hidmi, Ph.D., 1993
Present address: Islamic University-Gaza, Israel
Ming-Tie Huang
Xiaohua Huang, Present address: UCLA
Allen Landers
Chunlei Liao
Morten Lundsgaard
Suzanne Maleki, M.S., 1993, Kansas State University, Manhattan
Nabil Malhi, Ph.D., 1991
Present address: Jordan University of Science and Technology, Irbid, Jordan

Ulrik Mikkelsen
R. Parameswaran, Ph.D., 1992
Present address: College Station, Texas
Lamya Saleh
Justin Sanders, Ph.D., 1992
Present address: Oak Ridge National Laboratory, Tennessee
Gabor Toth
Bernhard Walch
Slawek Winecki
Wuchun Wu

Undergraduate Research Assistants

Keith Beyer
Brett D. Esry
Christopher Hunt
James Lock
Richard Mack
Megan Maskill
James Miller
Darin Neufeld
Ted Pope
Michael Rediger
David Seematter
Jason Werick
Mark Whitfield
Mike Wiley
Kirk Wolleson

---

*Part-time
[1]Supported by Kansas State University

5.1 Electron Production in Ion-Atom Collisions

5.1.1 The Enhancement of the Binary Encounter Peak for q=1 to Z in Collisions of Fast C^{q+} and O^{q+} on H_2

C.P. Bhalla

DDCS for the production of the binary encounter electrons in collisions of 8 MeV C^{q+} ions and 10 MeV O^{q+} ions with H_2 were calculated in the impulse approximation. The contribution of exchange[1] was included in the Hartree-Fock calculations of the phase shifts. These calculations are compared with the experimental data[2] in Fig. 5.1.1.1. The calculations and measurements are in fairly good agreement. For the lowest charge state, however, the cross section is clearly smaller than predicted by the calculations. The reasons for this discrepancy are not clear at this time. [See Publication #83.]

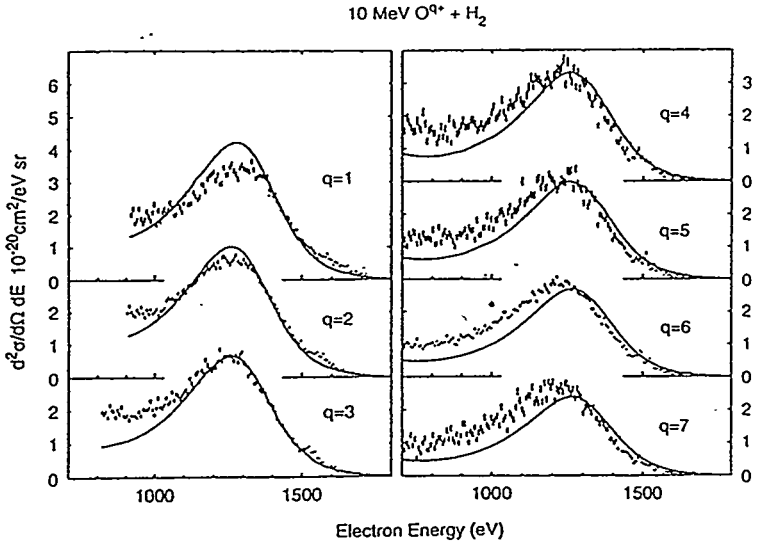

Figure 5.1.1.1.

References for Section 5.1.1

1. C.P. Bhalla and R. Shingal, J. Phys. B 24, 3187 (1991).
2. J.H. Posthumus, B. Christensen, N. Glargaard, J.N. Madsen, L.H. Anderson, P. Hvelplund, S.R. Grabbe, and C.P. Bhalla, J. Phys. B 27, L97 (1994).

5.1.2 Contribution of Exchange on Charge-State Dependence of Large-Angle Electron-Ion Elastic Scattering

C.P. Bhalla and R. Shingal

Taulbjerg[1] considered the electron-F^{8+} elastic scattering, and found that the electron exchange provides an important contribution to the backscattering cross section.

Fig. 5.1.2.1 shows the dependence of the ratio, defined as DCS divided by the corresponding Rutherford cross section with Z equal to the atomic number, as a function of the scattering angle. These calculations were performed with the static Hartree-Fock potential, and with the inclusion of the electron exchange contributions. We note that this ratio increases starting from $(q/Z)^2$ at zero scattering angle to larger than unity for large scattering angles, in particular at 180° that corresponds to zero degree laboratory angle in ion-atom collisions.

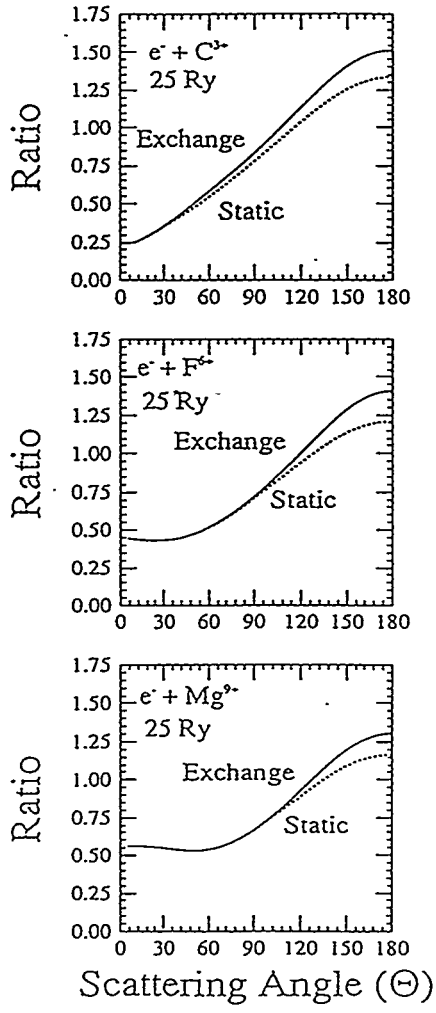

Figure 5.1.2.1. Ratio, DCS(q)/DCS(Z), versus scattering angle at 25 Ry electron energy for various three-electron ions.

The effects of the inclusion of electron exchange on the ratio is shown in Fig. 5.1.2.2 for a scattering angle of 180° (zero degree laboratory frame for BEe) as a function of the incident electron energy for carbon and magnesium ions.

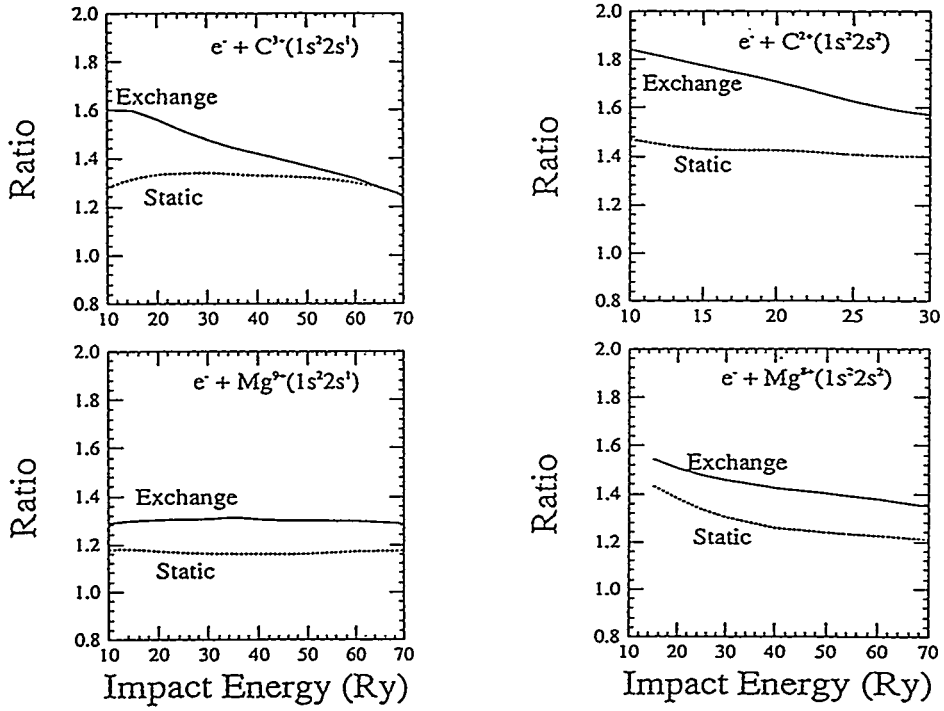

Figure 5.1.2.2. Calculated ratios of differential elastic cross section for carbon and magnesium ions and Rutherford cross sections for bare ions at a scattering angle equal to 180° plotted versus electron impact energy. The full and broken curves represent respectively the ratio with the inclusion of exchange contribution and the ratio with only static potential.

The exchange contribution of the continuum with the bound orbitals of the ion is more pronounced at large electron scattering angles and it is insignificant at smaller θ values. Such contributions increase in all cases with decreasing charge state of the ion. [See Publication #8.]

References for Section 5.1.2

1. K. Taulbjerg, J. Phys. B 23, L761 (1990).

5.1.3 Resonant Inelastic Scattering of Quasi-Free Electrons in $C^{5+}(1s)$

C.P. Bhalla

The process considered in this paper [see Publication #82] is analogous to a free-electron inelastic scattering from a hydrogen-like ion. In addition to the direct inelastic process, where the initial electron (1s) of the ion is excited to 2ℓ states, manifolds of doubly excited helium-like states such as $3\ell 3\ell'$ that predominantly de-excite to 2ℓ exist. In general, interference is found between the two processes, and one expects a Fano-type profile in the differential inelastic cross section at electron energies that can populate the doubly excited states. Only the contributions of $3\ell 3\ell'$ resonances in the calculations of the electron differential inelastic cross sections $d\sigma/(d\Omega)$ for $C^{5+}(1s)$ were considered.

The calculations are simplified because of the observation that for $e^- + C^{5+}(1s)$ collisions, all the doubly excited states ($3\ell 3\ell'$) produced can have only orbital magnetic quantum number M_L equal to zero when the axis of quantization is chosen as the electron-beam direction. Since the different M_L values are not statistically populated, de-excitation of these doubly excited states by electron emission (autoionization) leads to a non-isotropic electron angular distribution. We have calculated this angular distribution $W(\theta)$ for all states belonging to the $3\ell 3\ell'$ complex (for details, see Ref. 1) and the resonance strengths $\Omega(2\ell)$ defined below

$$\Omega(2\ell) = \frac{2.475\ 10^{-30}}{E} \quad \frac{(2L_d+1)(2S_d+1)}{2} \times A_a(d-g) \cdot \frac{A_a(d-2\ell)}{\sum A_a + \sum A_r} \ cm^2 \cdot$$

The doubly excited states, the ground state, and the states for n=2 are denoted by d, g, and 2ℓ, respectively. A_a and A_r are the autoionization rates and the radiative rates in units of s^{-1}. E represents the electron energy, i.e., the difference between the energy of the doubly excited state and the ground state of the initial ion (C^{5+}).

In the impulse approximation, the bound electrons of the target (H_2) are treated as 'quasi'-free electrons with a characteristic momentum distribution, where the projectile (C^{5+}) ion velocity is much larger than the typical electron velocity of the target atom.

The differential electron cross section, with final electron energy epsilon in the projectile frame, can be written in the impulse approximation (in units of cm^2/sr) as:

$$\frac{d\sigma}{d\Omega}(d \rightarrow 2\ell, \epsilon, \theta) = \Omega(2\ell)\, W(\theta)\, \left[\frac{J(Q)}{(Q+V_p)\,\epsilon_0}\right]$$

where

$$Q = (2E + 2E_I)^{1/2} - V_p.$$

The Compton profile of the target (H_2), J(Q), Q, and the velocity of the projectile V_p are in a.u., ϵ_0 = 27.21 eV, and E_I is the electron-binding energy of H_2. The normalized angular distribution of the electron is W(θ).

The differential electron cross section in the laboratory frame, with electron energy ϵ_L and angle θ_L, is given by standard transformations.[1]

All the calculations were performed using the Hartree-Fock atomic model with the inclusion of electron-configuration mixing in the same complex.

The experimental data[2] of 8.6 MeV C^{5+} ions on H_2 were obtained by the Aarhus group (Hvelplund, González, and Dahl), and are compared with theory in Fig. 5.1.3.1.

The Hartree-Fock calculation compares well for the angular dependence of most of the Auger lines. However, a large deviation is found for two states, 3s3d ^{3}D and 3p3d ^{1}F. There is evidence for strong electron correlation for the 3p3d ^{1}F state autoionization rate to the ground state. When this rate, calculated with the truncated-diagonalization method,[3] is used in the present calculations, the agreement between theory and experiment is excellent. It is probable that the 3s3d ^{3}D autoionization rate to the ground state may be influenced also by electron-correlation effects.

It should be noted that a comparison between experiment and theoretical calculations of relative line intensities is not straightforward. The data may be influenced by state mixing, and also interferences with the direct non-resonant channel most likely make problematic a detailed comparison of line intensities based on the present measurements and theory. The experimental data clearly indicate that the $3s^2$ ^{1}S state has a Fano profile, and accordingly, the Gaussian-peak area is not an accurate measure of the line intensity related to the population of the $3s^2$ ^{1}S state. Similar effects may influence some of the other lines.

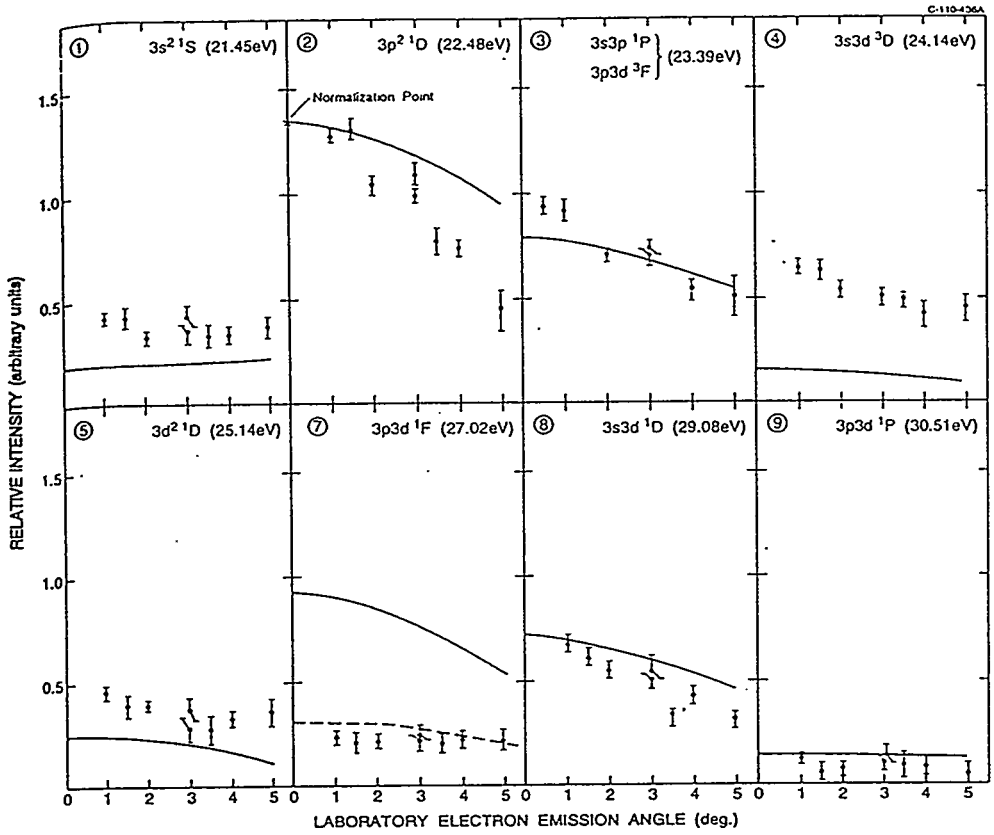

Figure 5.1.3.1. The relative intensities of electrons from the doubly-excited states versus laboratory angle. The solid lines is the result of the Hartree-Fock calculations normalized to $3p^2\ ^1D$ peak at 0°. The dashed line is calculated using the autoionization rate to the ground state from Ref. 3.

References for Section 5.1.3

1. C.P. Bhalla, Phys. Rev. Lett 64, 1103 (1990).
2. P. Hvelplund, A.D. González, P. Dahl, and C.P. Bhalla, Phys. Rev. A 49, 2535 (1994).
3. H.W. van der Hart and J.E. Hansen, J. Phys. B 26, 641 (1993); (private communication).

5.1.4 Dielectronic Recombination from High-Lying Resonance States in H-like Silicon, Calcium, and Iron

K.R. Karim, M. Ruesink, and C.P. Bhalla

The dielectronic recombination (DR) of a H-like ion involves the following steps: (i) the capture of a free electron $\epsilon\ell_c$ by an ion in the state $|i> = 1s\ ^2S_{1/2}>$ with simultaneous excitation of the 1s electron to a higher orbit to form a doubly excited autoionizing state $|s> = |2\ell n\ell' SLJ>$, and (ii) the radiative decay of the state $|s> = |2\ell n\ell' SLJ>$ to a low-lying state $|f> = |1sm\ell'' S'L'J'>$, which is stable against autoionization. This process can be represented schematically as

$$1s + \epsilon\ell_c \rightarrow (2\ell n\ell')^* \rightarrow 1sm\ell'' + \gamma \qquad (1)$$

The intensity of a satellite line originating in the DR process as represented in Eq. (1) is given by

$$\alpha_d(s\rightarrow f) = N_e N_i \alpha_d(s\rightarrow f), \qquad (2)$$

where N_e and N_i are, respectively, the densities of electrons and hydrogenlike ions in the initial state $|i> = 1s\ ^2S_{1/2}>$ and $\alpha_d(s\rightarrow f)$ are the DR rate coefficients. Assuming a Maxwellian electron-energy distribution, the DR rate coefficients can be expressed as

$$\alpha_d(s\rightarrow f) = \tfrac{1}{2}(2\pi\hbar^2/mkT_e)^{3/2}\, F_2^*(s\rightarrow f) \times \exp(-E_a/kT_e), \qquad (3)$$

where E_a is the Auger electron energy, k is Boltzmann's constant, T_e is the electron temperature, and $F_2^*(s\rightarrow f)$ are the satellite intensity factors. The satellite intensity factors are related to the ratio of the intensity of the satellite to the resonance line and are given by

$$F_2^*(s\rightarrow f) = \frac{(2J_s+1)}{(2J_i+1)} \frac{\Gamma_a(s\rightarrow i)\Gamma_r(s\rightarrow f)}{\Gamma(s)} \qquad (4)$$

Here, J_s and J_i are, respectively, the total angular momentum quantum numbers of the autoionizing states $|2>$ and the initial state $|i>$, $\Gamma_a(s\rightarrow i)$ is the rate of autoionization of the state $|s>$, $\Gamma_r(s\rightarrow f)$ is the rate for radiative transition, and $\Gamma(s)$ is the total rate for the state $|s>$ in all possible radiative and autoionizing channels.

We performed calculations[1] of the radiative and Auger rates within the Hartree-Fock atomic model for all intermediate states up to n=8 for H-like silicon, calcium, and iron. The DR rates were calculated where the $1/n^3$ scaling law was used beyond n=8. The results are presented in Figs. 5.1.4.1-3.

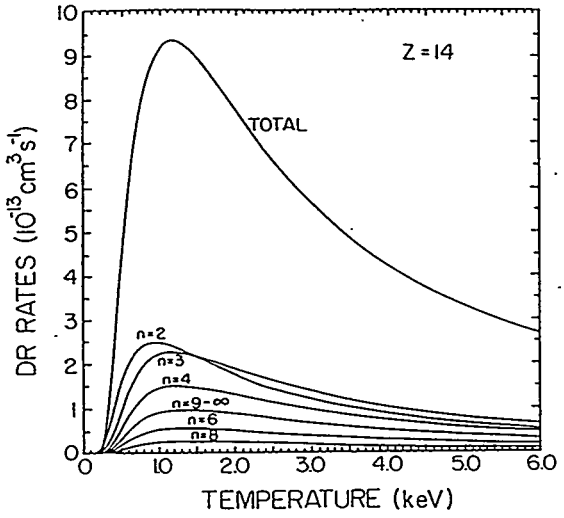

Figure 5.1.4.1. Partial and total dielectronic recombination rate coefficients of H-like silicon as a function of electron temperature T_e.

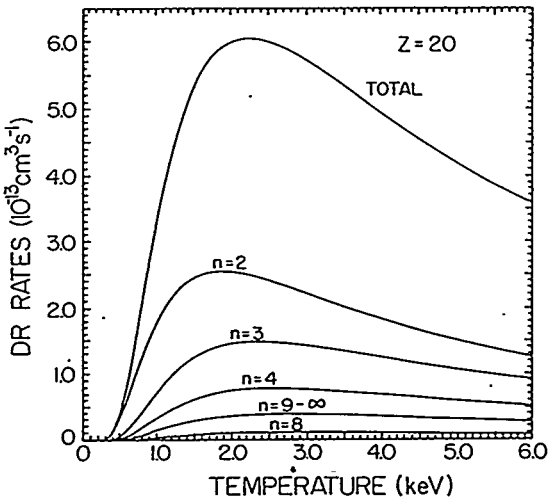

Figure 5.1.4.2. Partial and total dielectronic recombination rate coefficients of H-like calcium as a function of electron temperature T_e.

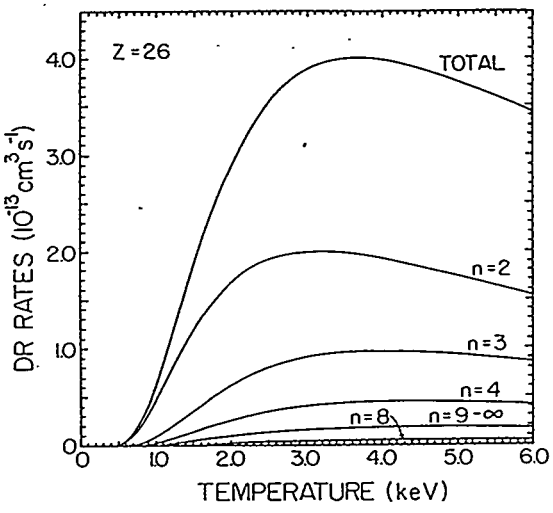

Figure 5.1.4.3. Partial and total dielectronic recombination rate coefficients of H-like iron as a function of electron temperature T_e.

A critical examination of the errors in DR values when the calculations are only performed up to n=4, and the $1/n^3$ scaling law is used for high-lying states is given elsewhere.[1] [See Publication #35.]

Reference for Section 5.1.4

1. K.R. Karim, M. Ruesink, and C.P. Bhalla, Phys. Rev. A 46, 3904 (1992).

5.1.5 Theoretical Auger Spectra of Selected Doubly Excited Li-like Ions

K.R. Karim and C.P. Bhalla

The Auger-electron energies, Auger transition rates, life times, and non-radiative branching ratios for double excited Li-like ions with Z=10, 14, 18, 20, 22, 24, 26, and 28 were calculated for all atomic states $|\tau SLJ>$ for configurations $1s2\ell n\ell'$ with n=2-4. Effects of electron configuration and spin-orbit coupling mixing were included in the Hartree-Fock approximation. There is an excellent agreement between our calculations and those of Chen[1] who used the multi-configuration Dirac-Fock model. The detailed results have been published.[2] [See Publication #84.]

References for Section 5.1.5

1. M.H. Chen, Atom. Data Nucl. Data Tables 34, 301 (1986).
2. K.R. Karim and C.P. Bhalla, J. Quant. Spectrosc. Radiat. Transfer 51, 557 (1994).

5.1.6 Binary Encounter Electron, BEe, Production Systematics

P. Richard

Zero Degree Double Differential Cross Sections, DDCS

Introduction: Electron production in ion atom collisions can proceed via first order scattering events and via second order scattering events. This is demonstrated in the data of Lee *et al.*[1] for 1.5 MeV/u F^{9+} + He when compared to several calculations as depicted in Fig 5.1.6.1. The dots are the data of Lee *et al.*[1] The dotted line is the first Born approximation result which agrees with the experimental DDCS near the BEe peak but underestimates the cross sections below the BEe peak. The dashed line, the solid line and the heavy solid line are the results of distorted wave calculations. These second order calculations predict the DDCS cross sections between the BEe peak and the cusp peak fairly well but underestimate the cross section below the cusp. The squares are classical trajectory Monte Carlo calculations which predict the data amazingly well over the entire energy range of the DDCS. The calculations are taken from Schultz and Reinhold.[2]

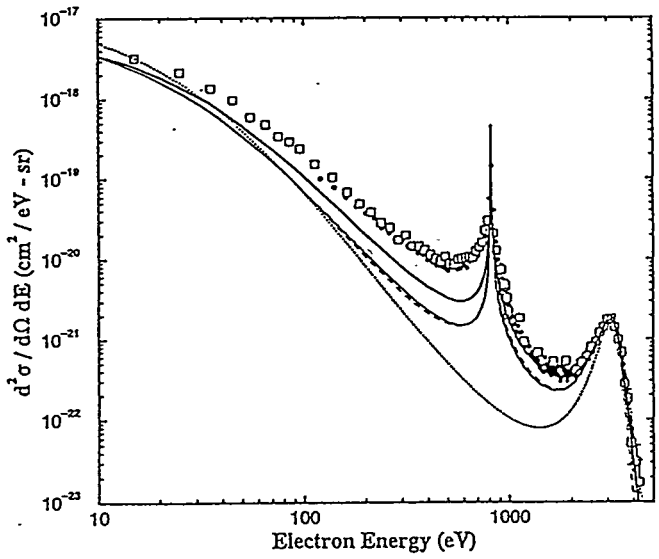

Figure 5.1.6.1. 1.5 MeV/u F^{9+}+He; • • • data Lee *et al.*, □□□ CTMC, —— CDW-EIS, —— model potential CDW-EIS, --- DSPB, · · · FBA from Schultz and Reinhold.

A pictorial view of three prominent collision mechanisms is attempted in Fig. 5.1.6.2 for bare ions on an atomic hydrogen target. Depicted here are 1) binary projectile-target electron collisions producing BEe electrons at twice the velocity of the incident projectile (at zero degrees in the lab, in general at $v_e = 2v_p \cos\theta_L$), 2) capture to the continuum producing electrons with the velocity of the projectile

primarily at zero degrees in the lab frame, and 3) two center collisions producing a broad range of electron velocities at all angles. A well known example of this mechanism is the so-called Thomas mechanism leading to electron capture. Most scattering events of this type do not satisfy the rather strict kinematic conditions for electron capture and thus lead to pure ionization.

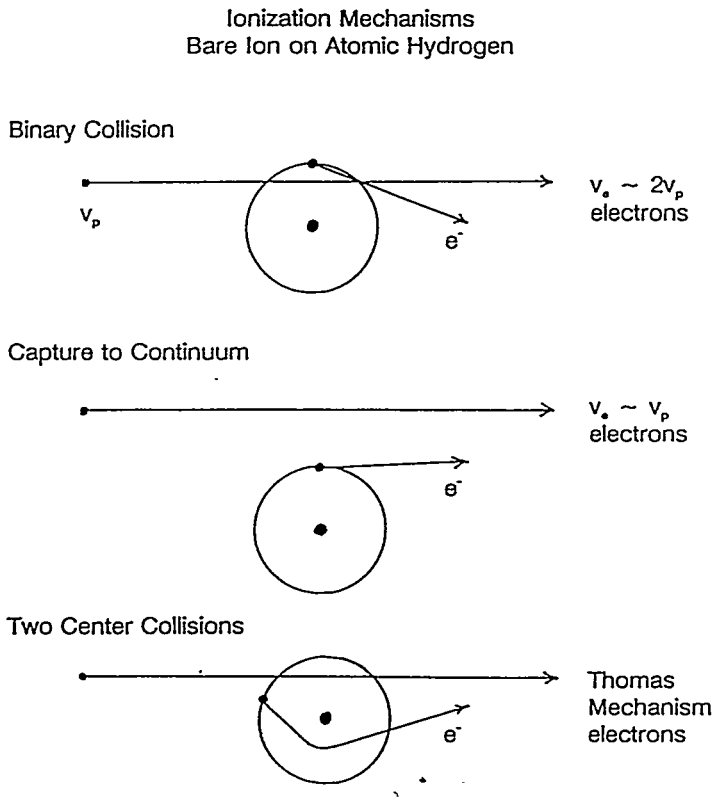

Figure 5.1.6.2. Mechanisms for projectile ionization in bare-ion atomic-hydrogen collisions.

We have developed a quasi free electron, bare-ion elastic scattering model, ESM, to describe the BEe DDCS[1,3-4] for bare ion projectiles which fit the data of Lee *et al.* very well. In this model, the Compton profile of the target electron accounts for the various possible projectile frame energies of the quasi-free target electrons and gives rise to the broad peak of the BEe. The model predicts a Z_p^2 projectile Z dependence of the cross section and an $E_p^{-2.5}$ projectile energy dependence. The Z_p^2 behavior for light projectiles on H_2 and He targets was confirmed. The ESM model was extended so as to apply in principle to all projectiles on all targets by doing the full screened electron-ion Coulomb scattering[5-7] problem and to include the effect of electron exchange.[8-9] See Publication #8 Bhalla and Shingal.

The latter development was motivated by our experimental results which showed that the BEe DDCS decreases as the projectile charge increases.[10] This is

often referred to as the inverse q-scaling. What seems a surprising result, since it does not follow a normal screening behavior, i.e., the cross section increasing with increasing charge state, was shown in fact to be due to the short range static potential of the projectile bound electrons.[5-7]

The initial work on zero degree binary encounter electron production was done in the previous progress reporting period and consists of the basic data for projectile ions of H^+, C^{q+}, N^{q+}, O^{q+}, and F^{q+} on H_2 and He, the comparisons with ESM calculations, and the observation of the inverse q-scaling. The work completed in this reporting period is an extension of the previous work and is discussed below.

Projectile energy dependence: One important and time-consuming study that was performed was the experimental check of the projectile energy dependence of BEe DDCS for the case of light ion projectiles. We observed an energy dependence of $\sim E_p^{-2.4}$ which is very good agreement with the ESM prediction of $E_p^{-2.5}$. The results are shown in Fig. 5.1.6.3 for 3 charge states of F. See Publication #66, Lee, Zouros, Sanders, Hidmi, and Richard.

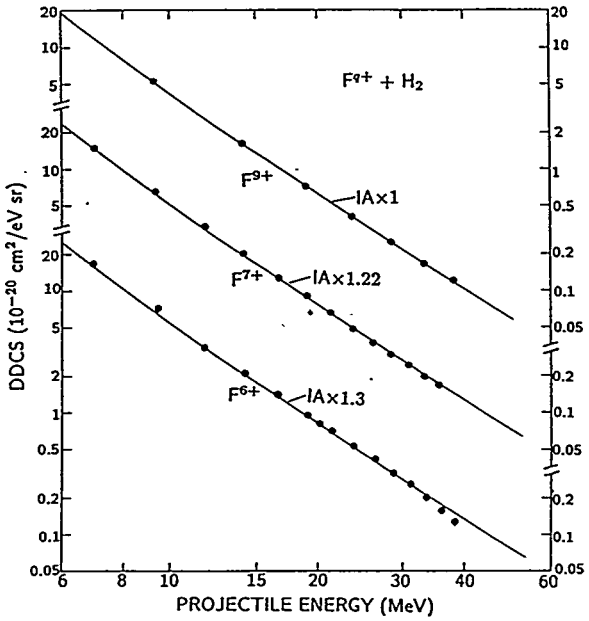

Figure 5.1.6.3. Zero degree BEe peak values measured (data points) and calculated by a scaled IA (solid lines) versus projectile energy in collisions of 7-38 MeV $F^{6,7,9+}$ ions on H_2 targets. The scaling factor for the clothed ions shows BEe production enhancement. From Lee *et al.*, see Publication #66.

BEe energy shifts: When we began studying more highly charged projectiles with Z>10, we observed that the ESM model did not fit the peak positions as they did for the lower Z projectiles. We reported this first for Cu projectiles, see Publication #50, Hidmi, Richard, Sanders, and Zouros. We observed that the peak shifts to lower energy as the projectile q is increased. The ESM predicts the BEe

peak independent of q. Fig. 5.1.6.4a shows the typical result for low Z projectiles where the shift is approximately 90-100 eV, whereas in Fig. 5.1.6.4b the shift for Si^{q+} varies from 115 to 150 eV in going from q = 4 to q = 13 (see Publication #77, Hidmi, Richard, Sanders, Schöne, Giese, Lee, Zouros, and Varghese). The solid line is the result of a Bohr-Lindhard model,[9] which predicts $\Delta E = 53 \sqrt{q}$ eV. This model clearly does not fit all the data in Fig. 5.1.6.4.

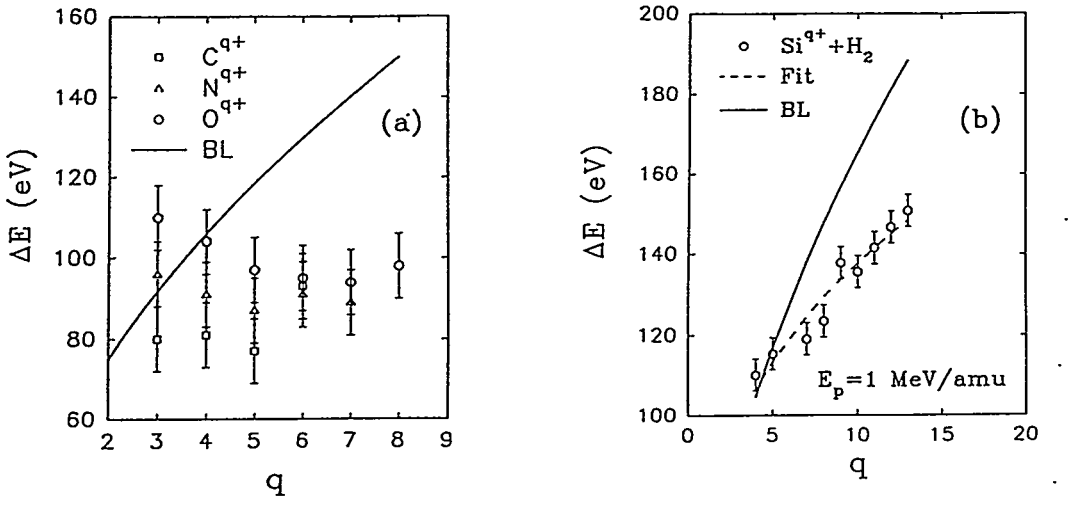

Figure 5.1.6.4. Energy shifts $\Delta E = 4t - E_{peak}$ (see text) as a function of the charge state q for 1 MeV/amu (a) C, N, and O, and (b) Si. Circles, present data; dashed line, fit to the data, $\Delta E(eV) = aq^n$; solid line, Bohr-Lindhard (BL) model. From Hidmi *et al.*, see Publication #77.

Electron Exchange: We performed a very accurate determination of the DDCS of BEe for $C^{q+} + H_2$ at 0.75 Mev/u where we expected to be able to clearly identify the contribution of electron exchange by comparing with the ESM prediction. Fig. 5.1.6.5 (next page) shows the comparison of the ESM with and without the static potential, and the calculation including static and electron exchange to the measurements. Excellent agreement is found between the data and the full calculation. See Publication #61, Hidmi, Bhalla, Grabbe, Sanders, Richard, and Shingal.

Inverse q-scaling: We also extended the inverse q-scaling studies to Si^{q+}, $C\ell^{q+}$, and Cu^{q+}. In the case of Cu we observed enhancements as large as 350% above the bare ion prediction. These results are also presented in Publication #77. The comparisons of these data with the ESM predictions are in progress at this writing. Fig. 5.1.6.6 (next page) shows the data obtained to date together with a Z_p^2 prediction. All data show the inverse q-scaling.

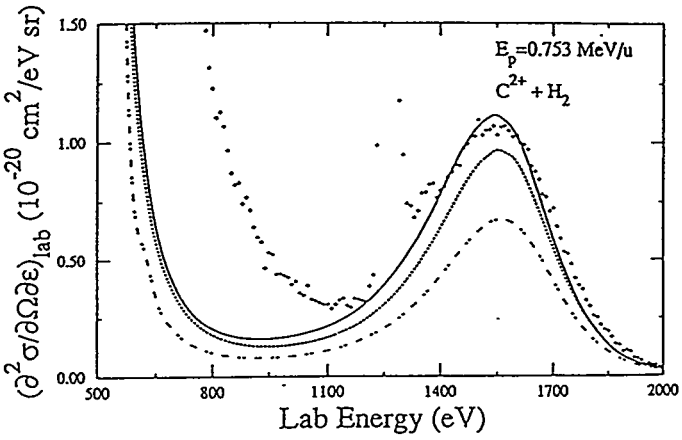

Figure 5.1.6.5. Comparison of ESM calculation of DDCS with experiment: ♦♦♦, data; theory: •• — ••, pure Coulomb potential; •••, static potential; ——, static plus exchange. From Hidmi *et al.*, see Publication #77.

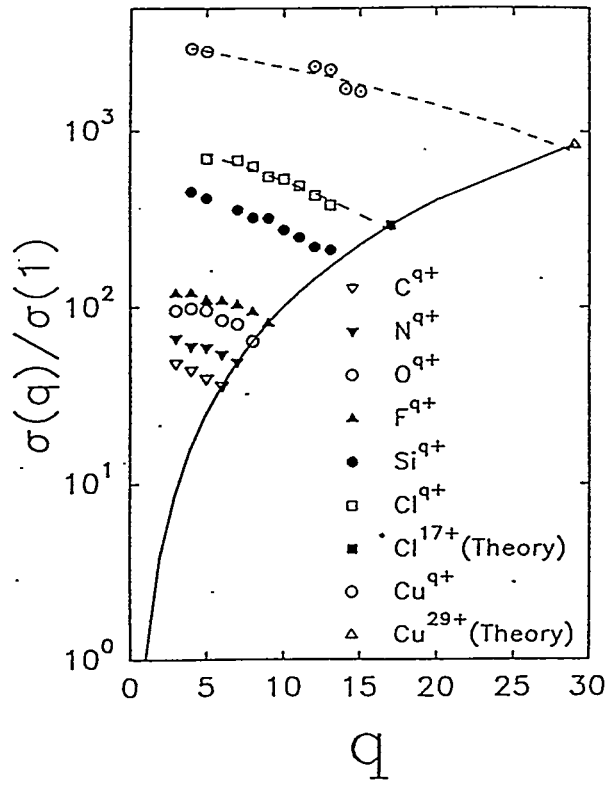

Figure 5.1.6.6. Ratio of DDCS for ions of charge state q on H_2 relative to the DDCS for protons on H_2. Cu projectile ions have an energy equal to 0.5 MeV/u and all other ions have a beam energy of 1 MeV/u. The solid line is the Z_p^2 prediction for $q=Z_p$, and the dashed lines are the best fits to the Cℓ and Cu data extrapolated to the bare ions for each case. From Hidmi *et al.*, see Publication #77.

Many electron targets: In a hallmark paper by Stolterfoht *et al.*[11] in 1974 BEe production by light ions on molecular oxygen targets showed a normal q-dependence due to screening as opposed to an inverted q-scaling. Theory[5-7] and several experiments[12] (see Accepted for Publication #4 and references therein) have demonstrated that for He and H_2 targets the switch from a normal scaling to an inverted q-scaling occurs at a laboratory angle of about 20° depending somewhat on the projectile. Stolterfoht's data were for laboratory angles equal to, or greater than

25°. To confirm the ideas of screening in many electron targets we studied the q-scaling of the BEe production for O^{q+} on O_2 and Ne targets. We did obtain the inverted q-scaling predicted by the ESM, however the ESM calculations did not agree very well with the results of Stolterfoht. Fig. 5.1.6.7 shows the results of the two experiments and the ESM prediction. The preliminary results of this study can be found in Publication #88, Zouros, Richard, Wong, Hidmi, Sanders, Liao, Grabbe, and Bhalla.

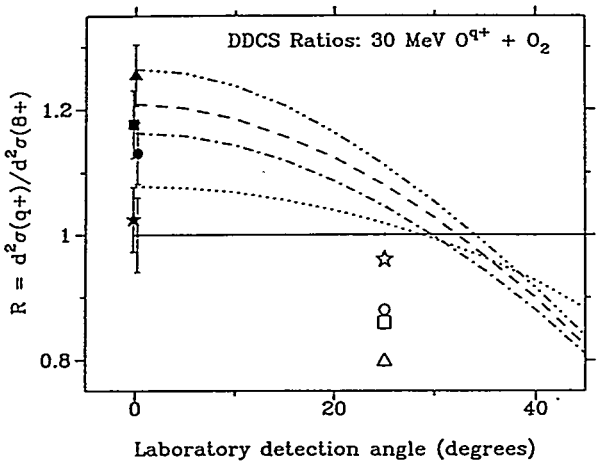

Figure 5.1.6.7. Ratios of the BEE DDCS's relative to bare ion BEE DDCS's for 30-MeV O^{q+} + O_2 plotted as a function of laboratory angle θ. The symbol $d^2\sigma$ denotes $d^2\sigma/d\epsilon d\Omega$. Lines, IA calculations; solid symbols, present 0° data; open symbols, older 25° data of Stolterfoht *et al.* q=4, triangles and dash-dot-dot-dot-dashed lines; q=5, squares and dashed line; q=6, circles and dot-dashed line; q=7, stars and dotted line; q=8, dot and solid line. Taken from Zouros *et al.*, see Publication #88.

References for Section 5.1.6

1. D.H. Lee, P. Richard, T.J.M Zouros, J.M. Sanders, J.L Shinpaugh, and H. Hidmi, Phys. Rev. A 41, 4816 (1990).
2. D.R. Schultz and C.O. Reinhold, to be published (1994).
3. D. Bruch, H. Wieman, and W.B. Ingalls, Phys. Rev. Lett. 30, 823 (1973).
4. H. Böckl and F. Bell, Phys. Rev. A 28, 3207 (1983).
5. C.O. Reinhold, D.R. Schultz, and R.E. Olson, J. Phys. B 23, L591 (1990).
6. R. Shingal, Z. Chen, K.R. Karim, C.D. Lin, and C.P. Bhalla, J. Phys. B 23, L637 (1990).
7. D.R. Schultz and R.E. Olson, J. Phys. B 24, 3409 (1991).

8. K. Taulbjerg, J. Phys. B 23, L761 (1990).
9. C.P. Bhalla and R. Shingal, J. Phys. B 24, 3187 (1991).
10. P. Richard, D.H. Lee, T.J.M. Zouros, J.M Sanders, and J.L. Shinpaugh, J. Phys. B 23, L213 (1990).
11. N. Stolterfoht *et al.*, Phys. Rev. Lett. 33, 59 (1974).
12. A.D. González, P. Dahl, P. Hvelplund, and P.D. Fainstein, J. Phys. B 26, L135 (1993).

5.1.7 Diffraction Structure in the Doubly Differential Cross Section for Electron Emission for 0.2 MeV/u to 3.6 MeV/u Au Impinging on Noble Gases

S. Hagmann and C.P. Bhalla

(in collaboration with A. Wolf, MPI for Kernphysik, Heidelberg,
R. Mann *et al.*, GSI-Darmstadt, and
H. Schmidt-Böcking, IKF, Frankfurt, Germany)

We have investigated electron diffraction in the binary encounter electron spectra for collisions of 0.20 MeV/u to 3.6 MeV/u Au projectiles with gas targets ranging from H to Xe. As no present accelerator is able to cover the whole collision velocity range desired for the experiment, it was performed at three different laboratories: the J.R Macdonald Lab tandem (0.2 MeV/u), the MPI-Emperor (0.42 MeV/u to 0.62 MeV/u), and GSI-Unilac (1.4 to 3.6 MeV/u). The electron spectra display a three peak structure at low collision energies which changes to a two peak structure at high energies. Binary encounter electron peak energies are found to be nearly invariant over the angular range where they appear instead of displaying the characteristic $\cos^2(\theta)$ dependence. However, their intensity varies strongly with the observation angle θ. The intensity appears to be shifted from the higher energy peak to the respective lower energy peak with increasing laboratory angle θ (see Fig. 5.1.7.1). This constitutes a strong discrepancy between experimental BE centroid energies and cross sections and the predictions based on first order Born calculations treating this as a collision of quasi-free target-electrons with a point projectile core charge. A satisfactory description of the cross section and energies is given, however, when for the scattering of the quasi-free target electron in the projectile potential a Hartree-Fock atomic model is used and the resulting doubly differential cross sections are folded with the Compton profile of the target atom. The multi-peak structure is then seen as resulting from a kinematic transformation of the scattered

electron angular distribution from the projectile frame into the laboratory frame: BE electron emission in heavy ion-light atom collision is the kinematically inverted process to elastic electron atom scattering (Fig. 5.1.7.2). This is clearly seen for collision energies up to 1.4 MeV/u (see Fig. 5.1.7.3). In velocity space laboratory frame angular distributions are straightforwardly compared to projectile frame electron-atom elastic scattering angular distributions;[1] the equivalence of patterns in electron-Hg and Au-He is thus easily established. Impulse approximation (IA) calculations reproduce all the major features seen in the experiments. The calculations also show that the sensitivity to the form of the target Compton profile varies strongly with laboratory electron energy, as can be seen in the calculation for 0.62 MeV/u $Au^{11+} \rightarrow Ar$ in Fig. 5.1.7.4. This may open new doors for investigating the role electrons from different parts of the target Compton profile play in the collision and to assess their respective contribution to the total cross section (see also proposal).

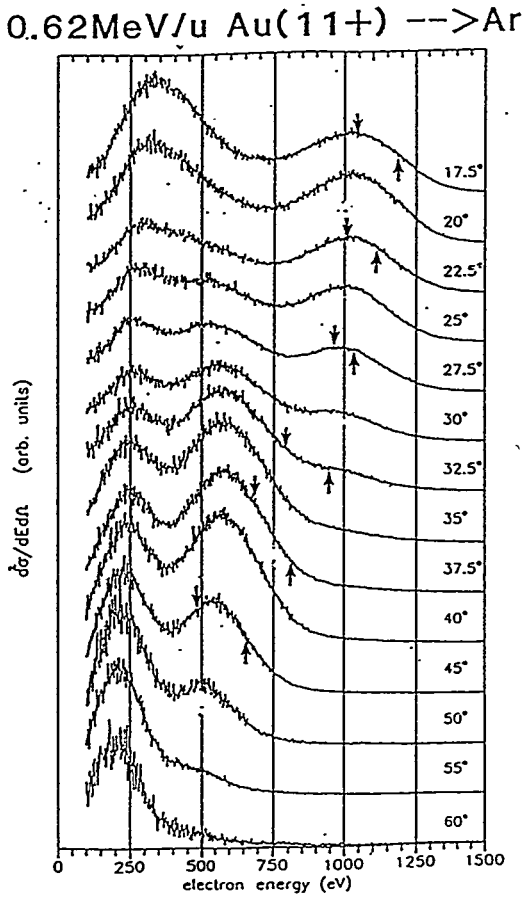

Figure 5.1.7.1. Double differential cross sections for 0.62 MeV/u Au^{11+} on Ar, measured between 17.5 and 60 degrees laboratory observation angle. The upward arrows indicate the position of the 2-body binary encounter peak; the downward arrow indicates the energy given by nCTMC calculations.

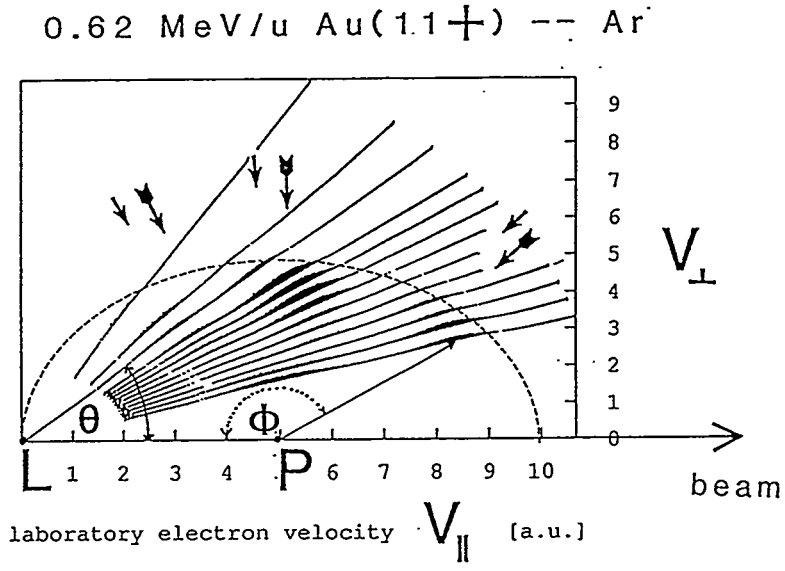

Figure 5.1.7.2. Comparison in velocity space of extrema in the angular distribution of electrons emitted in Au^{11+} on Ar with laboratory reference L with those from elastic electron-Hg scattering in projectile reference P; the large arrows indicate maxima found in the experimental e-Hg angular distribution, the short arrows those calculated for e-Au^{11+} by Olson; the dotted line is the location of the 2-body binary encounter.

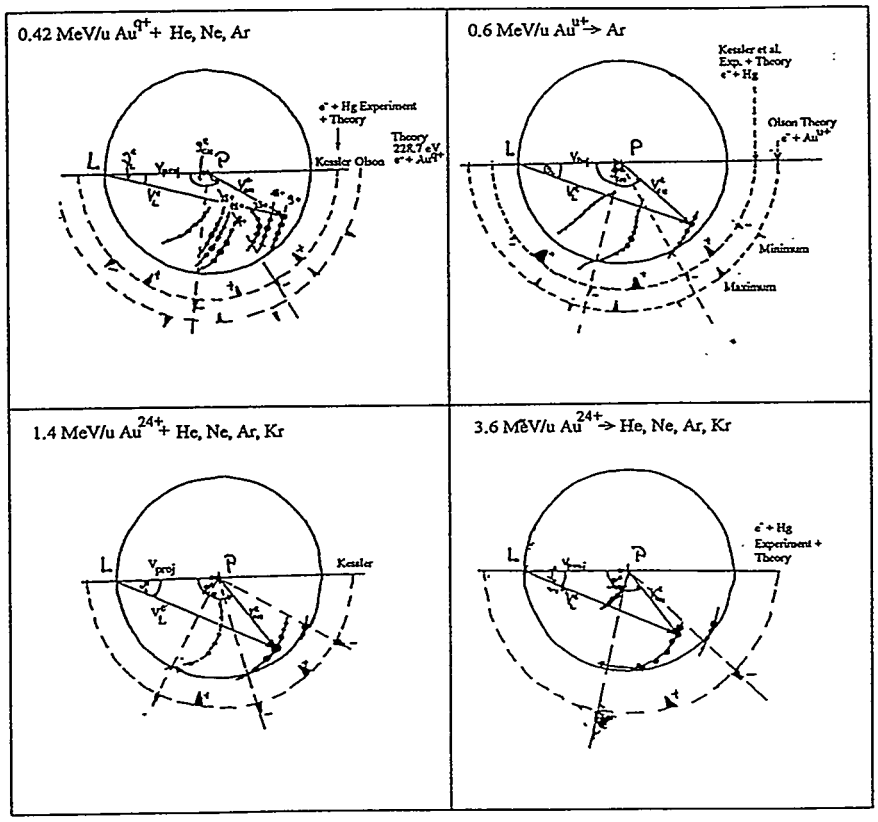

Figure 5.1.7.3. Comparison in velocity space of binary encounter maxima for 0.42 MeV/u to 3.6 MeV/u Au → noble gases with those found for elastic electron-Hg collisions and for electron-Au^{q+}.

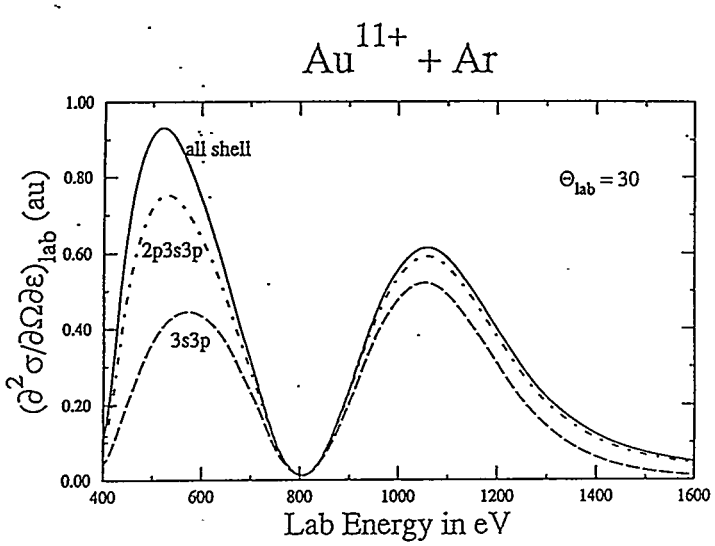

Figure 5.1.7.4. Theoretical doubly differential cross section for binary encounter electron emission at 30 degrees for 0.62 MeV/u Au^{11+} on Ar with contributions from electrons from different shells in Ar resolved.

In a second part the dependence of the observed diffraction structure on the screening of the projectile potential was investigated via variation of the projectile charge state. For the higher charge state q=23+ the diffraction did not appear to be dominating the cross section (Fig. 5.1.7.5) as it does for the low charge state q=9+ and indeed a systematic analysis over all observation angles shows a strong violation of the q^2 scaling law of the doubly differential cross sections, DDCS, (predicted by first order Born approximation) almost everywhere, i.e. for all angles and all electron energies (see Fig. 5.1.7.6).[2,3]

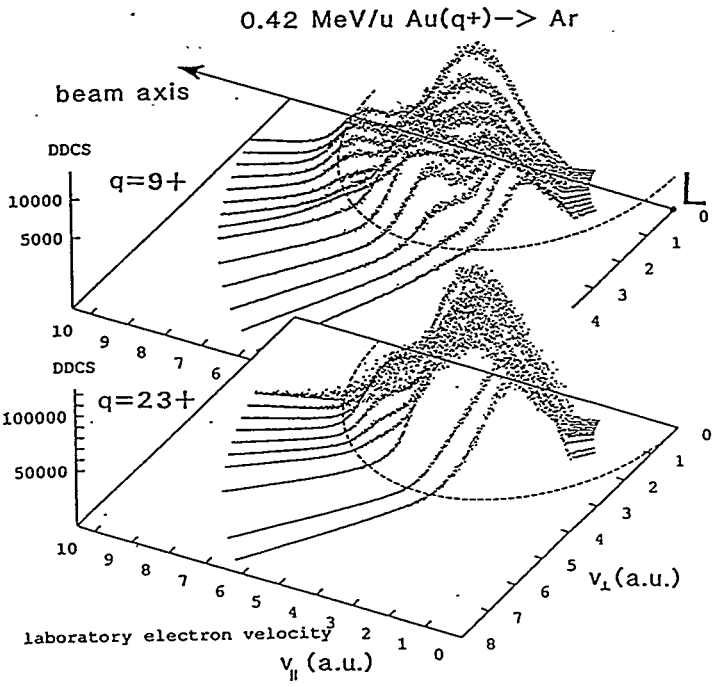

Figure 5.1.7.5. Comparison of the doubly differential cross section for electron emission for 0.42 MeV/u Au → Ar for projectile charge states 9+ and 23+.

It is interesting to note that contrary to the good agreement experiment and theory have for Au^{11+} projectiles, which have a closed shell [$4f^{14}$] electronic configuration, agreement for Au^{9+} with 2 electrons outside a closed shell [$5d^2$] electronic configuration is less than satisfactory at present. In light of the well known observation that elastic scattering from open shell systems requires significant amounts of polarization in theory to generate agreement with experiment (Massey and Burhop: Electronic and Ionic Collision Phenomena, Vol. I) we presently work towards a more quantitative understanding of this case. We wish to explore whether inversely the observed diffraction structure can provide information concerning polarization and other perturbations and interactions with open shells in the projectile, in collisions of heavy ions with atoms.

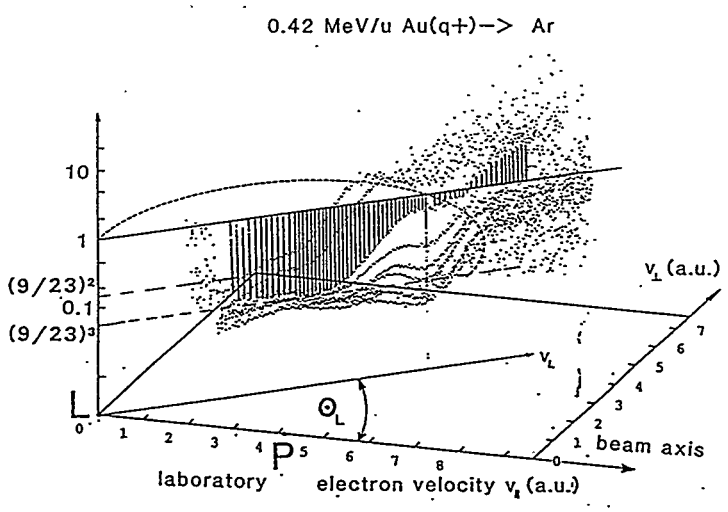

Figure 5.1.7.6. Ratio of doubly differential cross sections for electron emission for 0.42 MeV/u Au^{q+} → Ar for 9+ and 23+ projectiles in velocity space. For a q^2 dependence of the cross section all data would lie in the plane $(9/23)^2$.

References for Section 5.1.7

1. S. Hagmann *et al.*, J. Phys. B 25, L287 (1992). See Publication #30.
2. S. Hagmann *et al.*, Radiation Effects and Defects in Solids 126, 35 (1993). See Publication #60.
3. S. Hagmann, to be published.

5.1.8 Diffraction Structure in Binary Encounter Electron Spectra for Projectiles with Z down to Chlorine (Z=17)

S. Hagmann and C.P. Bhalla

After a systematic investigation had established that diffraction effects in collision systems with very heavy projectiles could be well understood using well known elastic scattering angular distributions of electrons from heavy atoms, we initiated a search for how low a projectile Z would still show these phenomena and give structure in the emitted electron spectra. So far we have established clear diffraction patterns in collisions of projectiles as low as $C\ell^{2+}$ with H; strong diffraction effects have been found also for Cu^{q+}, Br^{q+}, and I^{q+} projectiles (see Figs. 5.1.8.1 and 5.1.8.2; for fluorine see next section).

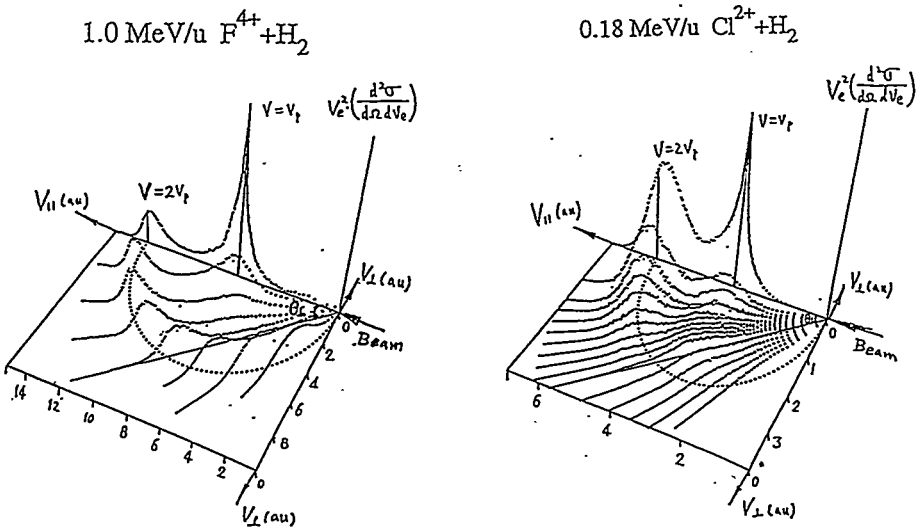

Figure 5.1.8.1. Doubly differential cross sections for electron emission for 1.0 MeV/u $F^{4+} \rightarrow H$ and 0.18 MeV/u $C\ell^{2+} \rightarrow H$. The monotonic distribution of the binary encounter for fluorine projectiles can be seen well; for $C\ell$ one sees clearly both the strongly forward peaked angular distribution and the diffraction pattern.

Our approach consists in measuring electron energy and angular distributions DDCS in collision velocity ranges where, in elastic electron atom collisions, the strongest diffraction is observed. This technique has already served us to find the regions of the strong diffraction spectra for Au projectiles (see report A). Using again collision velocities from electron→Z collisions where diffraction is known to be strong for lighter systems, e.g. Z^{q+}-H collisions, we invariably find multiple peaks in the

electron spectra with almost angle invariant energies which we again interpret as strong evidence for diffraction.[1] After transformation from laboratory to projectile frame we find in all cases reasonable agreement of the pattern of maxima and minima, characteristic for diffraction in elastic electron-atom collisions, with the extrema in the electron angular distribution in ion-atom collisions. For Cu projectiles where the tandem and LINAC allow a wider range of impact velocities to be covered, we investigated the velocity dependence of the diffraction and the effect of electronic configuration of the projectile with open and closed shells on the angular distribution (see also last paragraph of Section A). This work is still in progress.[2]

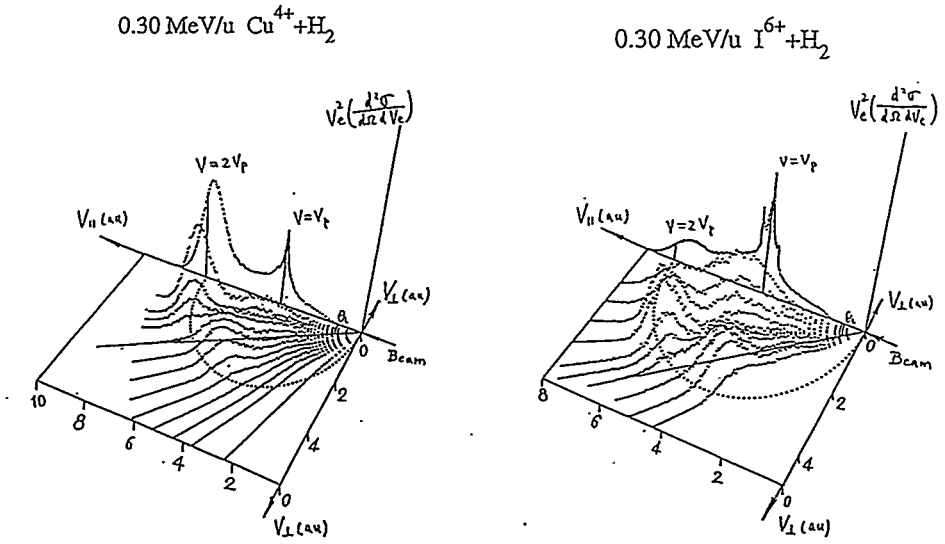

Figure 5.1.8.2. Comparison of the doubly differential cross sections for Cu^{4+} and I^{6+} both at 0.3 MeV/u. Note the strong forward peaking of the DDCS for Cu and the strong attenuation of the forward binary encounter peak for same velocity iodine.

References for Section 5.1.8

1. S. Hagmann *et al.*, Radiation Effects and Defects in Solids 126, 35 (1993). See Publication #60.
2. C. Liao *et al.*, accepted for publication. See Accepted for Publication #3.

5.1.9 Electron Emission Angle Dependence of the Violation of q^2 Scaling of the DDCS for BE Electron Emission for $F^{3+,\ldots 9+} \rightarrow H_2$

S. Hagmann and P. Richard

The surprising discovery of the violation of the q^2 scaling of the doubly differential cross section for 0 degree BE emission in collision systems $A^{q+} \rightarrow He, H_2$ for non-bare projectiles by P. Richard *et al.* has stimulated new interest in the fundamental mechanism of the electron emission processes in ion atom collisions.[1]

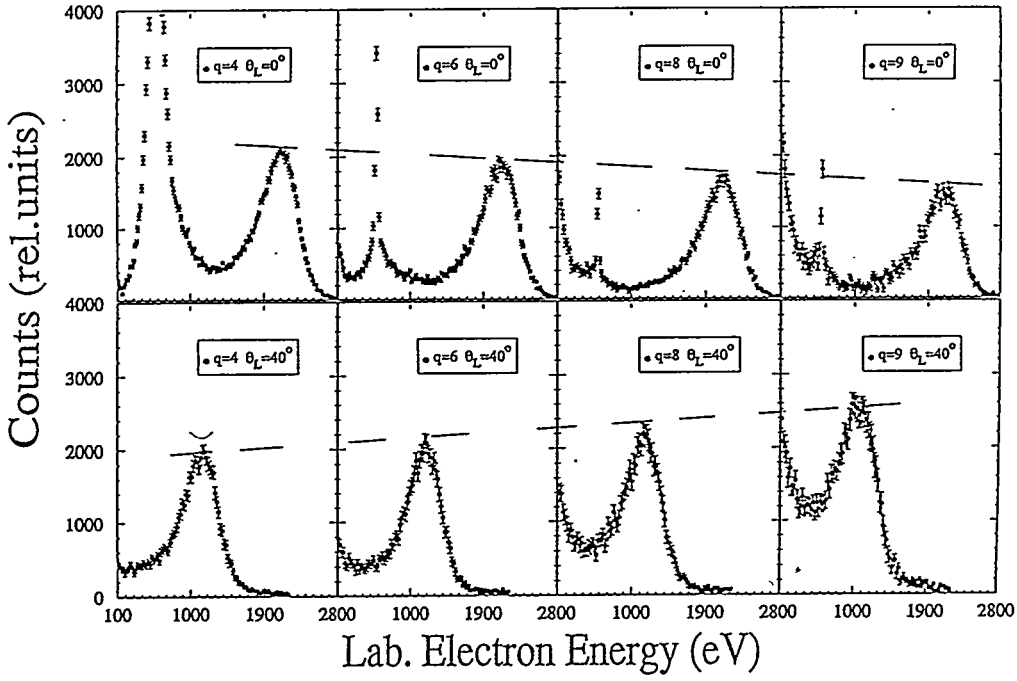

Figure 5.1.9.1. Comparison of the DDCS for binary encounter electron emission for 1 MeV/u $F^{q+} \rightarrow H$ for charge states between 4+ and 9+ for 0 degree emission showing the inverted q-scaling and for 40 degree emission with an opposite q dependence.

We have established that the reason for this violation of the q^2 scaling rule seen at 0 degree laboratory observation angle is the characteristic form of the screened projectile potential. We measured at 0 degree DDCS for pure target ionization for fluorine and Cu projectiles in various charge states using electron particle coincidence techniques showing that in the pure target ionization, where the

projectile does not change its charge state, the cross sections do not scale with q^2 but display even an inverted scaling. This eliminates speculations that contributions from projectile related capture and loss channels are important. It is now well confirmed, also theoretically, that the short range screening part of the projectile potential leads to strongly forward peaking of the DDCS in the laboratory frame. It was not clear, however, how the DDCS may depend on the projectile q for larger laboratory emission angles corresponding to smaller projectile frame scattering angles. This aspect we have now investigated for 1.0 MeV/u $F^{4+,6+,8+,9+}$ impinging on molecular hydrogen. As a first step we have measured DDCS for electron emission for laboratory emission angles between 0 and 70 degrees without imposing a condition on the final charge state of the projectile.[2] Besides the pure target ionization channel the spectra include contributions from projectile loss (particularly for the low charge state) and capture (for the high charge states). But already these data show, as can be seen in Fig. 5.1.9.1 above, that the inverted q scaling of the DDCS observed for 0 degrees has changed to a scaling more proportional with q for 40 degrees. For a more quantitative analysis it is intended to repeat the experiment with electron-projectile coincidences to isolate the pure target ionization.

References for Section 5.1.9

1. P. Richard *el al.*, J. Phys. B 23, L213 (1990).
2. C. Liao *et al.*, accepted for publication. See Accepted for Publication #3.

5.1.10 Large Solid Angle Electron Spectrometer for Coincidence Studies with Simultaneous Coverage of Angles between 0 and 180 Degrees

S. Hagmann

(in collaboration with J. Ullrich, *et al.*, GSI, Darmstadt, Germany)

Our recent studies of the mechanism of electron emission in ion atom collisions have shown that the simultaneous detection of electrons with scattered projectiles and/or recoiling target ions adds significantly to the information on the vacancy creating mechanism. For processes leading to continuous energy delta electron emission we have found that the impact parameter dependence of the electron

emission probability shows very strong anisotropies: at very small impact parameters the probability to emit an electron into the forward direction is up to 100 times bigger than at 90 degrees; similarly for high electron emission multiplicities we found that the spectra recorded at 90 degrees display different electron energy dependencies than those under forward direction.

For this reason we have designed a new electrostatic toroid electron analyzer following the principles first given by Wollnik[1] and applied by Engelhardt *et al.*[2] This instrument allows a highly efficient measurement of angle-resolved electron emission via energy dispersive simultaneous determination of the polar angular distribution of the emitted electrons. A small prototype has been used successfully with Xe and U beams from the UNILAC (see Fig. 5.1.10.1). A full size instrument is presently assembled and awaits being put into service in our beam line. In Fig. 5.1.10.2 is shown a doubly differential cross section for electron emission where a discrete target Auger line appears in the spectrum in addition to the continuum. The ring of electrons with velocity 6.4 a.u. contains fluorine K-Auger electrons. The spectrometer will be fitted with a pulsed recoil TOF spectrometer which has been used in previous electron recoil coincidence experiments.

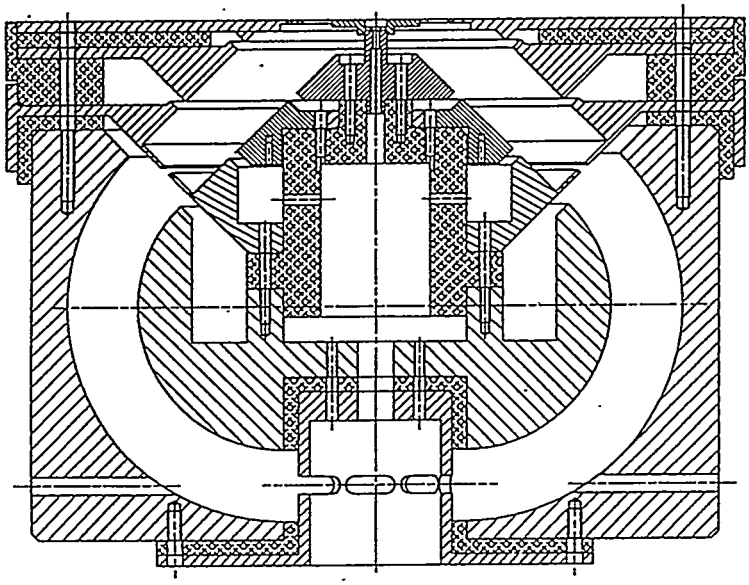

Figure 5.1.10.1. Cross section of the new electrostatic toroidal electron spectrometer, which allows the simultaneous measurement of electrons with emissions angles between 0 and 360 degrees onto a position sensitive detector.

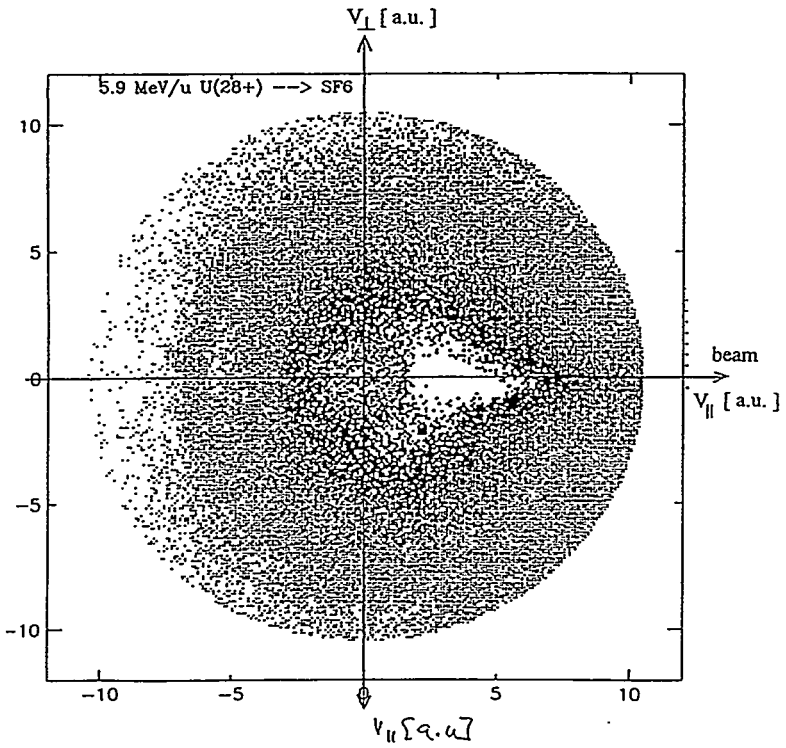

Figure 5.1.10.2. Doubly differential cross section for electron emission in 5.9 MeV/u $U^{28+} \rightarrow SF_6$; the circular ridge with a radius of approximately 6.4 a.u represents the F-K Auger lines.

References for Section 5.1.10

1. H. Wollnik, Focussing of Charged Particles, Vol II, p. 163 (1967).
2. H. Engelhardt *et al.*, Rev. Sci. Instr. 52, 835 (1981).

5.1.11 Two Electron Excitation to Rydberg States Populated in 0.3 MeV/u I^{6+} → Hydrogen Collisions

S. Hagmann, T.J.M. Zouros, E.C Montenegro, P. Richard, and C.P. Bhalla

In our study of diffraction effects in iodine → H_2 we discovered that the prominent cusp in the electron spectrum emitted at zero degrees is flanked by a few very strong autoionization lines associated with Rydberg states of the projectile on its wings. These lines only appear for incident charge state of the projectile 6+, i.e.

a configuration I^{6+} {....$4d^{10}$ 5s} but not for higher incident charge states. We did a combined high resolution and electron projectile coincidence study to investigate the origin of these prominent lines. Emitter frame energies are determined to be 0.03 eV, 1.15 eV, and 17.4 eV (see Fig. 5.1.11.1). A coincidence between electrons and outgoing charge state selected projectiles is used to determine the electronic configuration of the emitter. We find that all three peaks are associated with the 7+ outgoing projectile, whereas electron spectra coincident with other final charge states of the projectile are smooth and do not contain discrete lines (see Fig. 5.1.11.2). This points towards a double excitation process of electrons of the projectiles to Rydberg states ($4d^{10}$ 5s) → ($4d^9$ nℓ n$'\ell'$) with subsequent autoionization to ($4d^9$ 5ℓ) or ($4d^{10}$). Further studies concerning the mechanism for such selective population of doubly excited states are in progress.[1]

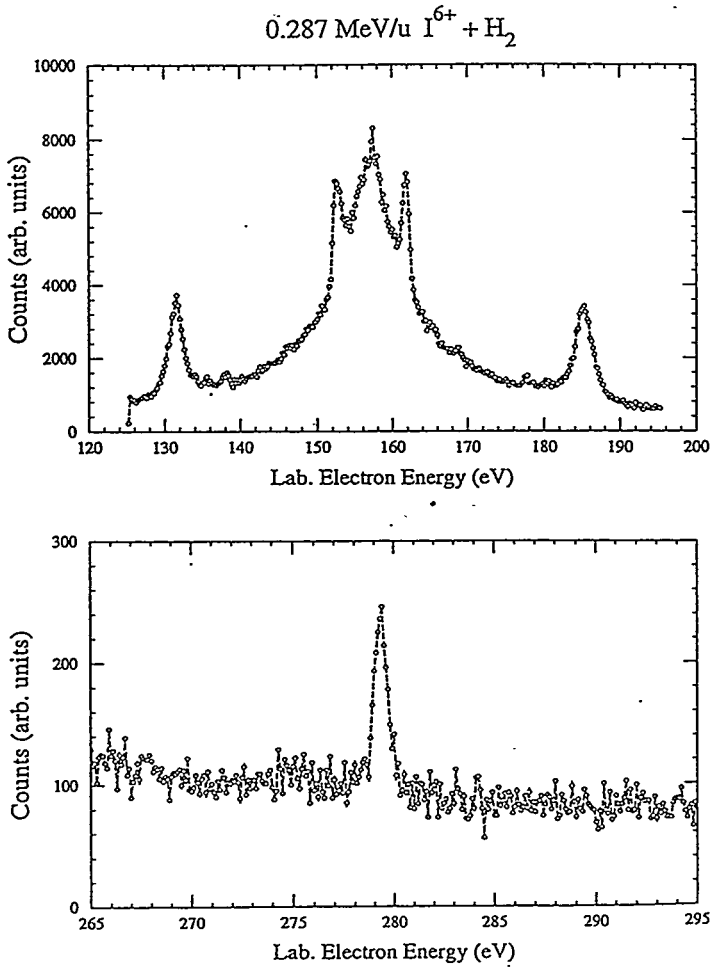

Figure 5.1.11.1. High resolution electron spectra at zero degree emission for 0.3 MeV/u I^{6+} → H. Around the cusp there appear symmetrically two lines with emitter frame energies of 0.03 eV and 1.15 eV. The line in the lower frame has an emitter frame velocity of 17.4 eV.

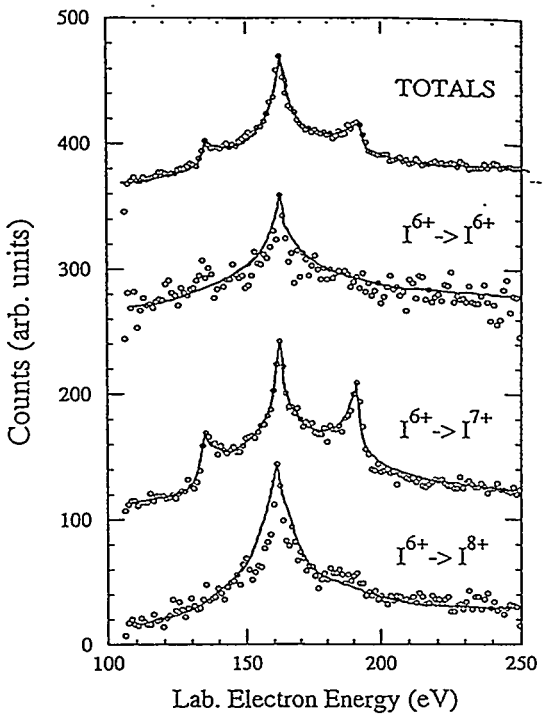

Figure 5.1.11.2. Comparison of 0 degree electron spectra for 0.3 MeV/u $I^{6+} \rightarrow H_2$; the top spectrum is the singles spectrum, the next the coincident electron spectrum with the 6+ outgoing charge state that is pure target ionization. The third electron spectrum was taken in coincidence with single electron loss by the projectile and the bottom spectrum was taken in coincidence with double electron loss by the projectile. It is apparent that the autoionization lines only appear with double excitation of the projectile.

References for Section 5.1.11

1. C. Liao *et al.*, to be published.

5.1.12 Binary Encounter Electron Studies at Relativistic Energies

B.D. DePaola and P. Richard

We have pursued our studies of binary encounter electron (BEe) production by measuring relativistic BEe peaks produced in collisions of very fast projectiles with carbon foil targets. At the projectile velocities investigated (135 MeV/u Ar^{18+}) the electrons produced were relativistic. At these velocities, the post-collision interactions of the carbon foil with the electrons was negligible. The BEe peaks were measured at lab frame angles from 0° to 60° using a magnetic electron spectrometer. The goal of these experiments, carried out at RIKEN, Japan, through a collaboration with the group of Dr. Yohko Awaya, is to see if the trends in BEe peak energy being

studied at the J.R. Macdonald laboratory at lower energies continue into the regime of very high energies. Preliminary results indicate that there are no surprises at these very high energies. However, further analysis of the data is required to be certain.

5.1.13 Stark Quantum Beats

B.D. DePaola and P. Richard

Work has continued on the study of final n distributions following fast ion-foil collisions using the technique of Stark beats spectroscopy. In this method one uses an electrostatic Rydberg analyzer to study the beat signal produced when adjacent n-manifolds are Stark shifted using a weak electric field. The specific system studied was 24 MeV C^{5+} on a 5 μgram/cm^2 carbon foil. At these energies the equilibrium charge states are 6+, 5+, and about 2% 4+ and lower. The principal quantum numbers investigated were near n=200. The results of these experiments were written up and will be submitted for publication.

5.1.14 Setting up of System for Determination of Final State (n, ℓ, and m) Following Fast Ion-Foil Collisions

B.D. DePaola

We have initiated experiments in which a laser is used to post-collisionally excite highly charged ions to very high n states followed by electric field ionization. The goal is to develop a technique by which we may learn the final state (n, ℓ and m) following processes like charge capture. The advantage of this system is that field ionization alone does not uniquely define the set of quantum numbers. That is, in general there exist many combinations of quantum numbers having the same threshold for electric field ionization. The key of this technique is that using the laser to excite to a specific n state uniquely determines the principal quantum number. Electric field ionization is then used to determine the other quantum numbers. In the experiments here the specific system studied was 24 MeV C^{5+} on a 5 μgram/cm^2 carbon foil. Hydrogen-like ions left in n=18 states were excited to

states near n=200 using a home-built tunable 50 mW diode laser. For the first run of experiments we concentrated only on determining if the procedure was even feasible. Therefore, instead of trying to find a specific 18-n transition, we electrically slewed the laser through approximately 20-30 resonances, and looked for an overall increase in the field ionization signal. This part of the technique worked. We will next carry out the specific 18-n transition and look for the family of spikes in the field ionization spectrum which should give us the distribution of final quantum numbers, for n=18.

5.2 Role of Electron-Electron Interaction in Two-Electron Processes

5.2.1 KLL Resonant Transfer Excitation of $F^{6+}(1s2\ell2\ell')$ Intermediate States

P. Richard and T.J.M. Zouros

Resonant transfer excitation (RTE) in energetic ion-atom collisions has been studied extensively in recent years. RTE is a two-electron e-e interaction process in which a weakly bound (quasi-free) target electron is transferred to an orbital ($n \geq 2$) of the projectile and simultaneously excites a projectile electron. The resulting doubly excited state must relax either by radiative (x-ray) decay (RTEX) or autoionization (Auger) decay (RTEA).

If the captured electron were truly free, RTEX and RTEA would be equivalent to dielectronic recombination (DR) and resonant excitation scattering (RES) in electron-ion collisions, respectively. DR is a process of fundamental interest in the high-temperature plasmas of laboratory or astrophysical environments. In particular, DR is thought to be an important energy-loss mechanism in fusion technology. DR has recently been observed in merged ion-electron beams, and in electron-beam ion traps (EBIT) sources (EBIS). RES is analogous to the well-known resonant scattering in electron-atom collisions. Since both RES and DR are deexcitation channels of the same doubly excited state, measurements of RES cross sections can complement DR cross sections.

In this work, we report on RTEA and its RES strength measured at $\theta_{lab} = 0°$ with respect to the projectile beam direction for $F^{6+}(1s2\ell2\ell')\ ^{(2S+1)}L$ intermediate states formed in collisions of 0.25-2 MeV/u F^{7+} with H_2 and He targets. All the $1s2\ell2\ell'\ ^{(2S+1)}L$ states were investigated, and their KLL RTEA cross sections were determined so far as their cross sections were measurable. These state-resolved cross sections showed a good agreement with theoretical calculations. The RTEA measurements for the ^2D and ^2P states, which have different total angular momentum L, complement the recent studies on the angular dependence of RTE, in which it was shown that the angular differential cross sections of RTEA are determined by the total angular momentum L in the LS coupling scheme. [See Publication #2 and references therein.] Part of this work is the Ph.D. thesis of D. H. Lee.

5.2.2 Interference Between RTEA and Elastically Scattered Target Electrons in 20 MeV F^{6+} + H_2 Collisions

C.P. Bhalla, P. Richard, and T.J.M. Zouros

High-resolution high-statistics Auger electron spectra were obtained in collisions of 20 MeV $F^{6+}(1s^22s)$ projectiles with H_2 targets using 0° projectile electron spectroscopy.

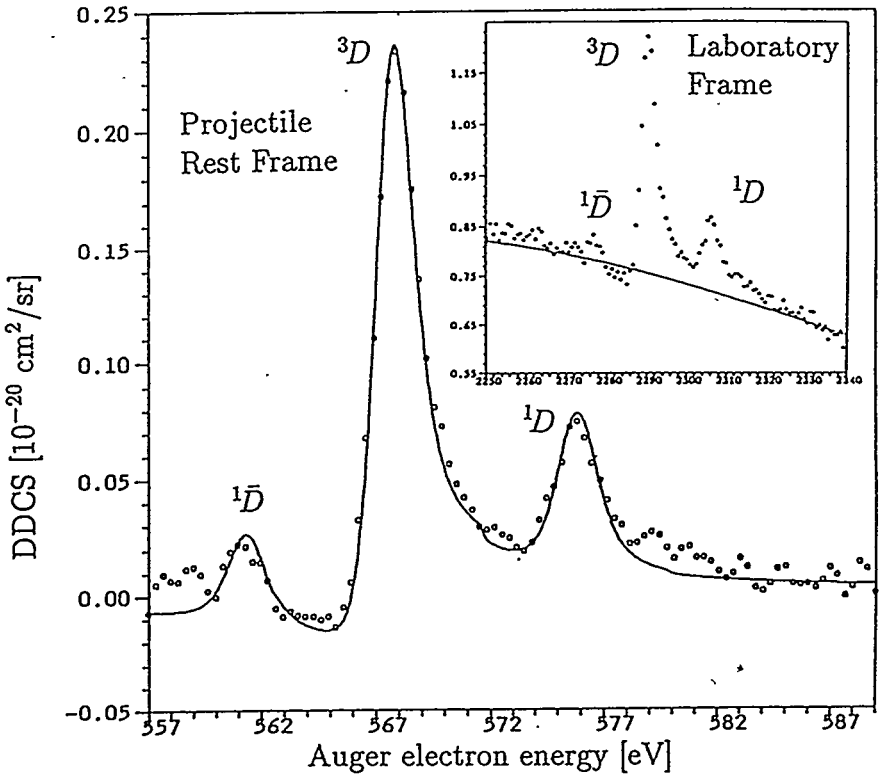

Figure 5.2.2.1. High statistics double differential cross section for F^{6+} + H_2 at 20 MeV taken at the J.R. Macdonald Laboratory using the zero-degree spectroscopy apparatus. Calculations of laboratory elastic electron production in the screened Coulomb potential model using a $Z_p^* = 10.42$ is shown in the inset (solid line). After subtracting it and transforming to the rest frame, the spectrum was fitted by Lorentzians with the full natural line width for each line folded by the spectrometer response function. The Fano profile of the strongest ^{3}D RTEA line is clearly seen. For the RTEA $^{3,1}\bar{D}$ lines, an asymmetry parameter $\tilde{q}^r$ was extracted and compared with theory. We note the barred line ($^1\bar{D}$ transition) can only interfere with inelastically scattered electrons. The ^{3}D transition is not shown in these figures as it was very weak.

The $1s2s2p^2\ ^{3,1}D \rightarrow 1s^22s$ (D-transitions) and the $1s2s2p^2\ ^1D \rightarrow 1s^22p$ ($\bar{D}$-transition) Auger transitions were clearly resolved. The $1s2s2p^2\ ^{3,1}D$ projectile states can be formed by Resonance Transfer and Excitation (RTE), and thus their Auger decay to the $1s^22s$ state can interfere with *elastically* scattered target electrons giving rise to characteristic Fano-like line shapes. Their Auger decay to the $1s^22p$ excited state can interfere with *inelastically* scattered target electrons. Comparisons with the results of existing RTEA-elastic electron scattering interference theory and asymmetry parameter were given. For the RTEA-inelastic electron scattering interference, calculations will soon be available. Fig. 5.2.2.1 (preceding page) shows the experimental results and the fit to the data. [See Publication #48 and references therein.]

5.2.3 Electron-Electron Interaction in the K-Shell Ionization of O^{4+} and C^{2+} Ions in Fast Collisions with H_2 and He Gas Targets

P. Richard and T.J.M. Zouros

Cross sections for 1s ionization of the $1s^22s^2$ and $1s^22s2p^3P$ (metastable) states of C^{2+} and O^{4+} ions in 0.5-1.8 MeV/u collisions with H_2 and He targets were measured using 0° projectile Auger electron spectroscopy. Calculations of K-shell ionization cross section, σ_K, were performed including contributions from projectile electron-target nuclear interactions, (σ_{enI}) within a Plane-Wave Born Approximation (PWBA), and contributions from projectile electron-target electron interactions, (σ_{eeI}) within an Impulse Approximation (IA). The theoretical total cross section $\sigma_K = \sigma_{enI} + \sigma_{eeI}$ was found to be in overall agreement with the K-shell ionization measurements indicating a contribution of up to ~30% due to electron-electron interactions. Separate screening-antiscreening calculations of σ_K were also performed and found to be in overall agreement with our data. Additionally, our PWBA-IA ionization calculation was also tested for H-like projectiles and found to be in agreement with recently published data. These results suggest that the IA calculation of σ_{eeI} when combined with a PWBA calculation of σ_{enI} is quite adequate for describing K-shell ionization, Fig. 5.2.3.1. [See Publication #31 and references therein.] Part of the work is the Ph.D. thesis of D.H. Lee.

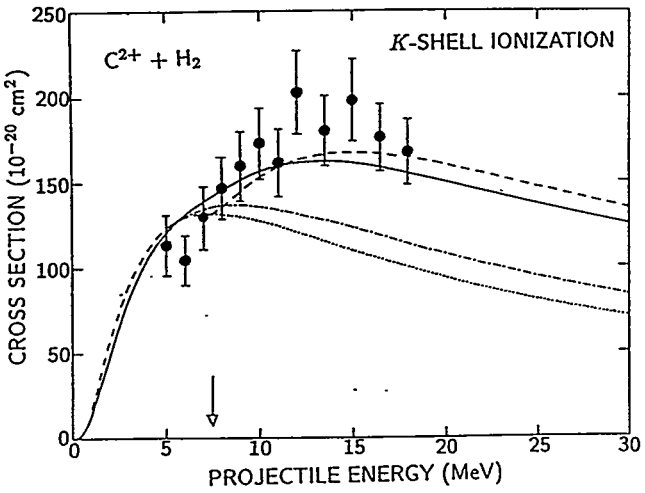

Figure 5.2.3.1. K-shell projectile ionization cross section, σ_K, for 5-18 MeV C^{2+} + H_2 collisions. Continuous line: PWBA-IA calculation of $\sigma_K = \sigma_{enI} + \sigma_{eeI}$. Dash-dot line: scaled PWBA calculation of σ_{enI}. Dotted line: PWBA calculation of σ_K (screening part only) considering only e-n interaction. Arrow indicates projectile energy corresponding to the 1s ionization threshold for electron impact of same velocity.

5.2.4 Experimental Separation of Electron-Electron and Electron-Nuclear Contributions to Ionization of Fast Hydrogenlike Ions Colliding with He

C.L. Cocke and J.P. Giese
(in collaboration with R. Dörner, V. Mergel, and H. Schmidt-Böcking, Univ. Frankfurt, Frankfurt, Germany, and W.E. Meyerhof, Stanford)

We have used longitudinal recoil momentum spectroscopy to experimentally distinguish between two mechanisms for the ionization of hydrogenlike O and F by a He target. The two mechanisms are ionization by the target nucleus (eN) and ionization by one of the target electrons (ee). If the ionization occurs through the eN process, the recoil is thrown forward by at least IP/v, where IP is the projectile ionization potential and v the beam velocity. If the ionization occurs through the ee process, the residual recoil ion is only a spectator and remains nearly at rest. Although too much discussion might convince the reader that this picture over-simplifies the kinematic situation, the experimental results show that the separation of the two mechanisms in this way is remarkably clean. Fig. 5.2.4.1 shows the results for both capture and loss from O^{7+} on He. The ee contribution is seen as a shoulder , almost a peak, growing in near a longitudinal momentum of 0 in the loss spectra for bombarding energies above 24 MeV, above the threshold for this process. From these data we have extracted the ratio of cross sections for the ee and

eN processes. The results are in good agreement with calculations based on an SCA description of ionization folded, via the impulse approximation formulation, into the Compton profile of the target. This experiment required a cold He gas jet to limit the thermal spread of the target, and the jet used for this work had a resolution superior to that used for Sections 5.3.1 and 5.3.3, but inferior to the supersonic jet described in the proposal. This work is published in Phys. Rev. Lett. as Publication #91.

Many of the technical developments, as well as some of the basic physics ideas, associated with this experiment, and indeed many of the recoil experiments appearing in both the progress report and proposal, have profited from a long standing collaboration between this laboratory and that of H. Schmidt-Böcking at the U. Frankfurt. A similar experiment, but for He^{++} on He, was carried out nearly simultaneously at Frankfurt by Dörner *et al.*, in which several personnel from KSU also participated during the early stages. This work is published as Publication #94.

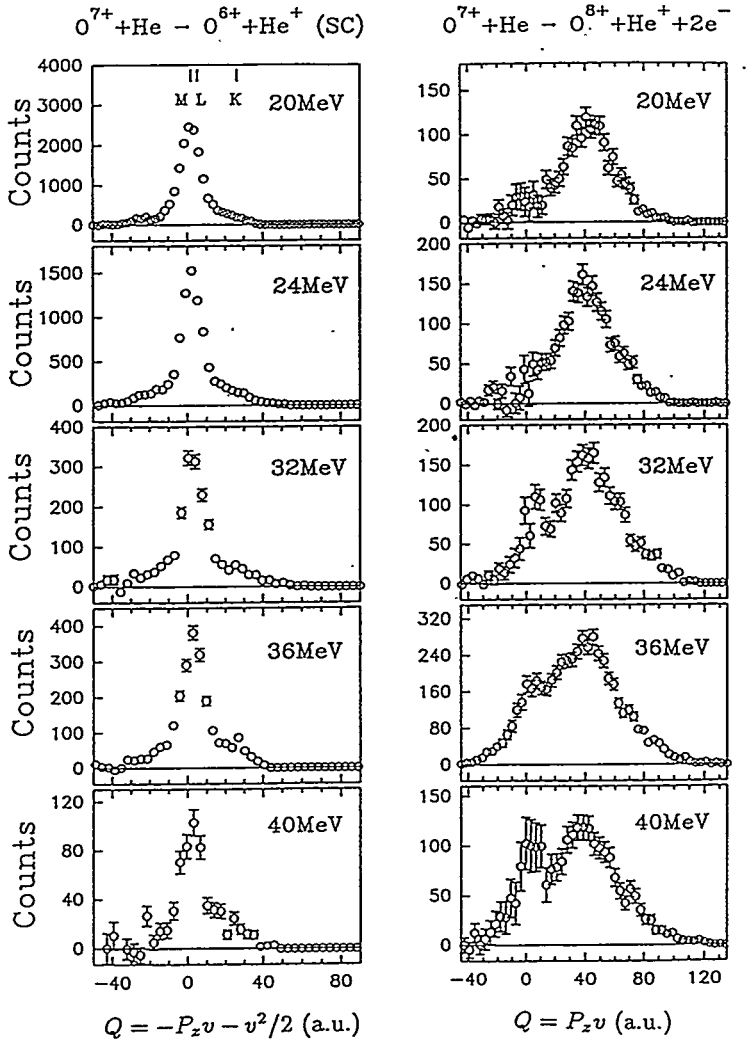

Figure 5.2.4.1. Spectra of longitudinal momentum transfer for O^{7+} on He for both single capture (SC) and projectile loss channels. The horizontal axis is transformed as indicated to represent the effective Q value for the reaction. The ee contribution in the loss channel appears above a projectile energy of 32 MeV, above the threshold for this process, for Q near 0.

5.3 Multi Electron Processes

5.3.1 Multi-Electron Processes in 10 keV/u Ar^{q+} (4<q<18) on Ar Collisions

M.P. Stockli and C.L. Cocke

We have measured cross sections for capture from Ar by slow multiply charged Ar^{q+} ions at a velocity of 0.63 a.u. The experiments were carried out at the EBIS using a warm gas jet and a geometry such that the charge states of both the projectile and the recoil, the full momentum vector of the recoil ion, and the transverse momentum of the projectile ion were all measured in coincidence for each event. A very comprehensive data set was thus obtained for a single collision system. The highly differential cross sections thus obtained were placed on an absolute scale using a single normalization from previous measurements. From these data, we have extracted:

1. Partial cross sections for capture, sorted according to recoil charge and projectile charge state. General conclusions which can be drawn from the data include: Autoionization from the multiply excited states is heavy in such capture processes. Capture of up to seven electrons is observed, but, for initial charge states for which ample L vacancies are present, the projectile seldom retains more than two, on the average. A distinct rise in the number of electrons lost into the continuum is seen as the projectile brings into the collision L vacancies, but no change is seen when an additional K vacancy is brought into the collision. This indicates that L Auger decays play an important role in the stabilization of the projectile, but that a single K vacancy plays little role, since the projectile charge state is essentially already determined by the time the decay reaches the K shell. The data show clearly that the recoil charge state is the major indicator of the number of electrons initially captured in the primary process. Measurements of projectile charge change for such collisions are of limited usefulness in understanding the capture process.

A detailed comparison of these data with the predictions of the molecular classical barrier model of Niehaus[1] has been carried out. The calculation is laborious, and includes the possibility that the target is left in a subsequently autoionizing excited state. More than one thousand final configurations predicted to be populated by the model had to be examined to determine its likely autoionization fate. The data are in excellent agreement with the predictions of the model, even for small impact parameter multielectron transfer, if target excitation

is allowed (but not if it is not). Sample comparisons are shown in Fig. 5.3.1.1. Cross sections for projectile charge change were also calculated within the framework of this model, with a simplified autoionization cascading scheme assumed for the multiply excited projectile states populated. Good agreement between model and experimental results were obtained. Finally, the model was used to calculate the overall number of electrons lost from the collision system by autoionization as a function of q, and good agreement with experiment was obtained. Overall, the ability of the MCBM to deal so well with such a large and nearly complete set of experimental data, over a large range of projectile charge state, is astonishing and confirms the fundamental soundness of the model. There is at present no other model capable of dealing with this kind of multielectron transfer, since coupled channel calculations for such a system are impossible. A comprehensive paper on this aspect of the work is published in Phys. Rev. A as Publication #90.

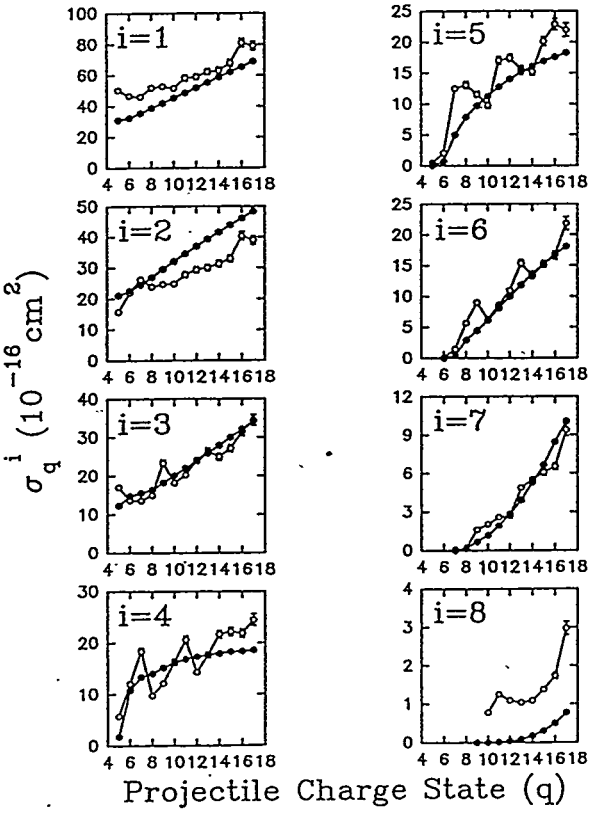

Figure 5.3.1.1. Experimental (open circles) and model (MCBM, Ref. 1) cross sections for the production of Ar^{1+} recoils in Ar^{q+} on Ar at 10 keV/u. The model calculations allow for autoionization of excited target ions.

2. The transverse momentum transfers for Ar^{15+} on Ar, capturing up to 5 electrons, were used to measure angular distributions for this multi-capture situation. As expected, capture of successively more electrons is accompanied by successively greater deflection of the projectile. The data were compared to the predictions of

the MCBM, and excellent agreement in the shapes of the distributions was seen. No systematic under- or over-estimation of the scattering angle by the theory, which had been reported for other systems earlier, was seen.[2,3] These results are shown in Fig. 5.3.1.2. The experiment is published in J. Phys. B as Publication #58.

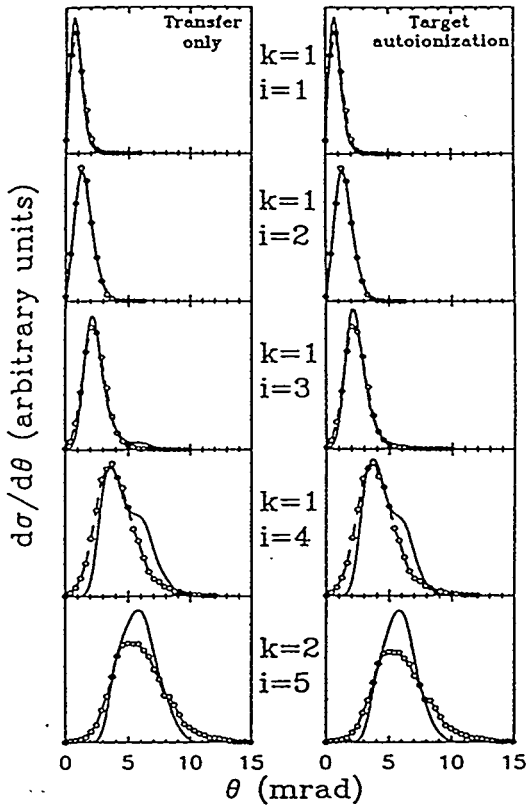

Figure 5.3.1.2. Experimental (points) and model (MCBM, Refs. 1, 3) differential cross sections for production of recoils of charge state i, with the projectile keeping k electrons, for 50 keV Ar^{15+} on Ar. The right hand calculation allows target autoionization, while the left one does not.

3. The longitudinal momentum transfer to the recoil ion for Ar^{15+} on Ar was used to determine the average Q value for these capture reactions for up to 5 electron capture. To our knowledge, this was the first time the longitudinal momentum of the recoil ion was actually used to determine a Q value, after the suggestion of this application by Schmidt-Böcking *et al.*[4] It works for low energy capture because no electrons are ejected directly into the continuum in such collisions and thus two-body kinematics is valid. In the past two years, this technique has become quite widely used by groups at Frankfurt and KSU. The technique can easily be applied to the capture of any number of electrons (previous measurements on the projectile energy gain were generally restricted to single or double projectile capture) and automatically isolates the more important recoil charge state rather than the projectile charge state. It does not require a precisely defined projectile energy. The

results showed average Q values up to 150 eV, in good agreement with the predictions of the MCBM. This work is published in Phys. Rev. Lett. as Publication #36.

All three of the above publications form part of the Ph.D. thesis of R. Ali.

5.3.2 Radiative Stabilization in Slow Double-Electron Capture Collisions of Highly Charged Ions with Neutral Atoms

C.L. Cocke and M.P. Stockli

We have measured the radiative stabilization fractions for double electron capture collisions for the systems 10 keV/u Kr^{q+} (q=13-34) and Ar^{q+} (q=6-17) on Ar. The measured probability shows pronounced structures as a function of q. We have constructed a model which incorporates the initial populations and reasonable assumptions concerning the variation with q of the radiative decay rates. In general, the radiative stabilization is attributed to the initial population of very asymmetric states (e.g., $6\ell\ 20\ell'$). The inner electron is expected to radiatively stabilize first, followed by the outer electron, finally populating a two-electron excited state which may often be metastable against E1 decay. These states are assumed to Auger decay, while all allowed E1 stabilizations lead to true double capture. The model gives a rather good qualitative account of the data for both collision systems. The implication is that the precursors of radiative stabilization[5,6] are likely to indeed be these very asymmetric states, which would have to be populated in the range of 7 to 25% in these experiments to explain the data. This work is published in Publication #68.

5.3.3 Multiple Ionization of Ne by 1 MeV/u F^{9+} Projectiles

C.L. Cocke

We have measured cross sections for the capture from and ionization of Ne by fast (v=6.3 a.u.) bare fluorine projectiles. Such data ultimately reveal the microscopic basis for such average quantities as stopping powers, angular straggling,

equilibrium charge state distributions, etc. which are widely used to characterize the passage of fast ions through matter. The measurements were performed with a gas jet whose geometry is such that the charge states of the projectile and recoil, the vector momentum of the recoil ion and the transverse momentum of the projectile are all registered for each collision event. The data were sorted according to their position in the final charge state matrix. For each point in this matrix, the question of momentum transfer, and of momentum balance between projectile and target, was then examined. The only calculational technique presently capable of dealing with such a very non-perturbative collision is the CTMC calculation, and we have collaborated with R. Olson (Rolla, Missouri) in making a comparison between his CTMC calculations and our results.

A few of the major results may be summarized as follows:

1.) The cross sections, sorted according to projectile capture and recoil charge state, are in excellent agreement with the model for no projectile charge change, and deviate increasingly from the model results for single and double capture. The model seems to give too large capture cross sections.

2.) Transverse momentum balance between projectile and recoil obtains to a high degree in all cases. There is no indication that an appreciable momentum is carried away from the collision by the continuum electrons, within the experimental resolution of typically 8 a.u. This could be the case if substantial correlated emission of continuum electrons were to occur in the same direction. No evidence for this is seen in any of our spectra.

3.) The transverse momentum distributions for the recoils (which have higher resolution than the projectiles) are in rather good agreement with the calculations, with some discrepancies appearing for the hardest collisions. It appears that the model gives a good account of the impact parameter dependence for even rather heavily ionizing events. A summary of these data are shown in Fig. 5.3.3.1. (next page).

4.) The longitudinal momentum transfer to the recoil shows clear evidence for the v/2 translational factor which is expected to characterize electron capture. To our knowledge, this was the first experimental observation of this result, although it has now been seen in many cases at both KSU and Frankfurt. The recoil is thrown backwards with a momentum of this size for each electron captured by the projectile, and this characteristic is in agreement with the model. However, as the ionization state of the recoil increases, the model predicts that the recoil will be thrown increasingly more backwards, while the data show the opposite trend. This is simply a failure of the model for which no explanation is yet forthcoming. This aspect of the work has been published as Publication #74. The more comprehensive data set are part of the Ph.D. thesis of V. Frohne and are being prepared for publication.

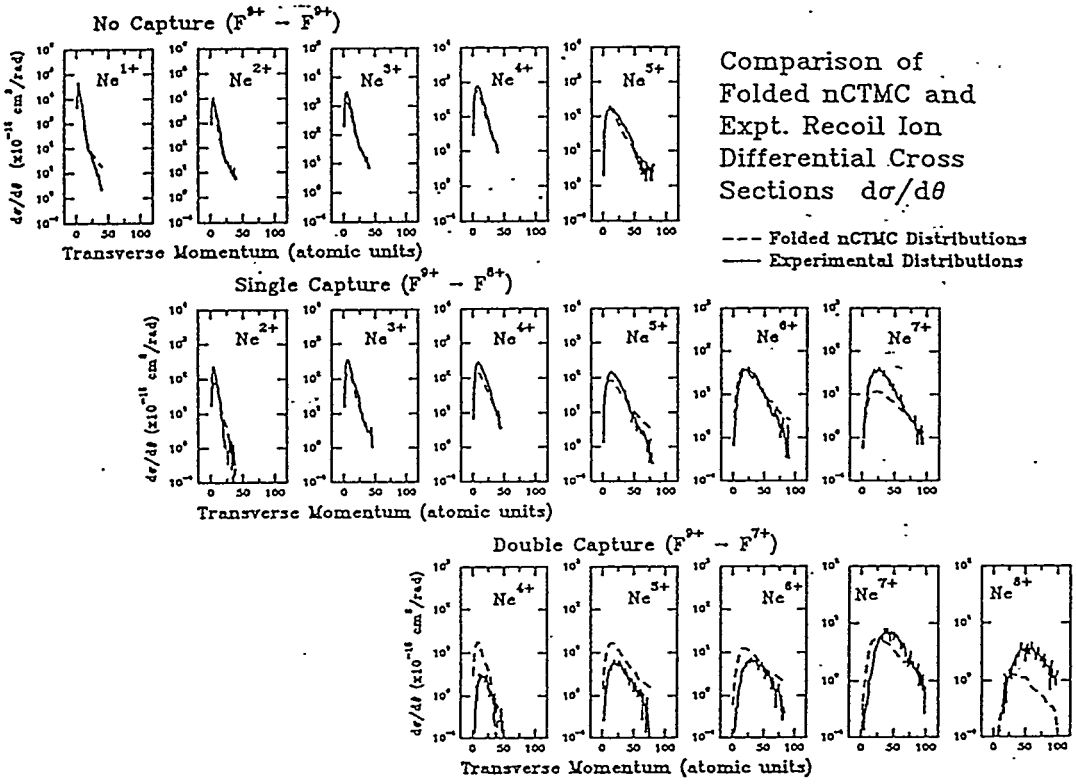

Figure 5.3.3.1. Overview of differential cross sections for the production of Ne^{r+} recoils by 1 MeV/u F^{9+} on Ne. The experimental data, solid lines, are compared with CTMC calculations, folded into the experimental resolution, dashed lines. The cross sections are plotted vs the transverse momentum transferred to the recoil ion.

5.3.4 Velocity Dependence of One- and Two-Electron Capture Processes in Intermediate Velocity Collisions of Highly Charged Ions with He

J.P. Giese, I. Ben-Itzhak, C.L. Cocke, P. Richard,
M.P. Stockli, and H. Schöne

We have completed our study of one and two electron capture processes which occur in collisions of Ar^{16+}, $O^{7,8}$, and N^{7+} ions with He atoms at velocities between 0.19 and 1.67 a.u.[1] These processes were identified by measuring the final charges of the projectile and recoil ions in coincidence. Single electron capture (SC) is the dominant process at all our velocities. Transfer ionization (TI), where the He loses

both electrons but the projectile captures only one, is next largest. Double capture (DC) is about 10 times smaller. None of the cross sections for these processes show any dramatic velocity dependence. This result is consistent with the MO model. The density of final states is fairly uniform for these highly charged projectiles. As the collision velocity changes, there are always states within the reaction window for capture and thus the cross section is insensitive to velocity.

We have also determined the q values for the pure capture processes of SC and DC and for the TI process by measuring the longitudinal recoil ion momenta.[2] TI at these velocities probably occurs via capture of two electrons to doubly excited projectile states. These states can decay radiatively leading to DC or via autoionization leading to TI. We have calculated the q values for TI assuming that TI is a result of a double capture process. The q values for all these capture processes decrease significantly as the collision velocity is increased, as shown in Fig. 5.3.4.1 for SC and TI by O^{8+} and Ar^{16+}. Our results indicate that all capture processes populate less tightly bound states as the projectile velocity is increased. This result is somewhat surprising as both simple low energy models and high energy perturbative models predict an increase in q value with velocity.

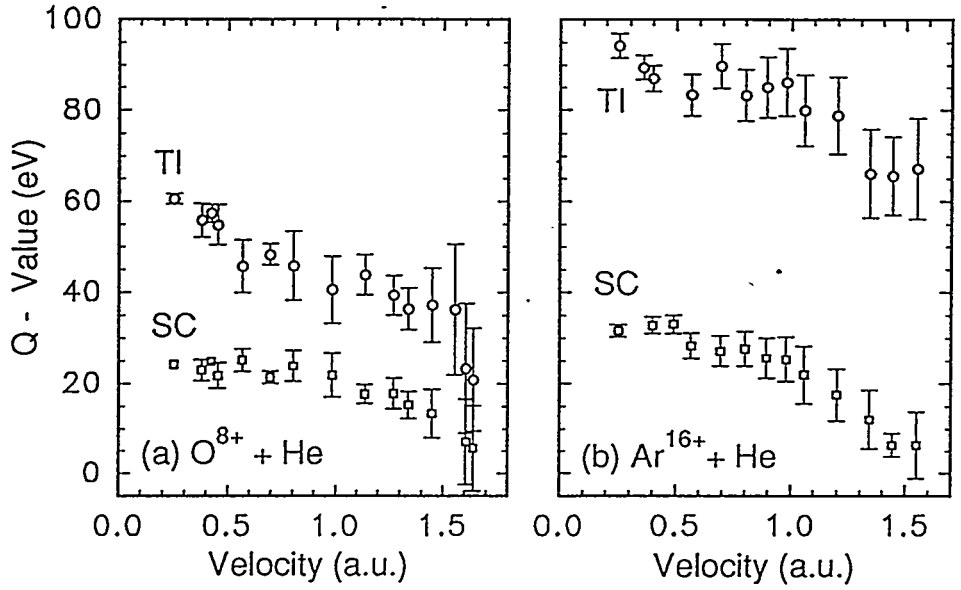

Figure 5.3.4.1. The measured q values for O^{8+} and Ar^{16+} on He for SC (squares) and TI (circles).

Our result can be qualitatively understood as due to the increasing amount of work which must be done to accelerate the captured electron up to the projectile velocity. This effect should be accounted for by the electron translational factors

used in detailed molecular orbital (MO) calculations. Our experimental results are compared in Fig. 5.3.4.2 to the results of a recent close-coupling calculation for O^{8+} and N^{7+} by Chen *et al.*[3] The agreement in absolute magnitude and in the velocity dependence is very good for both collision systems. These authors demonstrate that the decrease in the q value as the velocity is increased is due to increasing population of relatively high n states (n > 6) following capture. These states have higher n than predicted by the Over-Barrier Model (OBM) and form only a small part of the total cross section. However, these states do strongly affect the measured "average" q value.

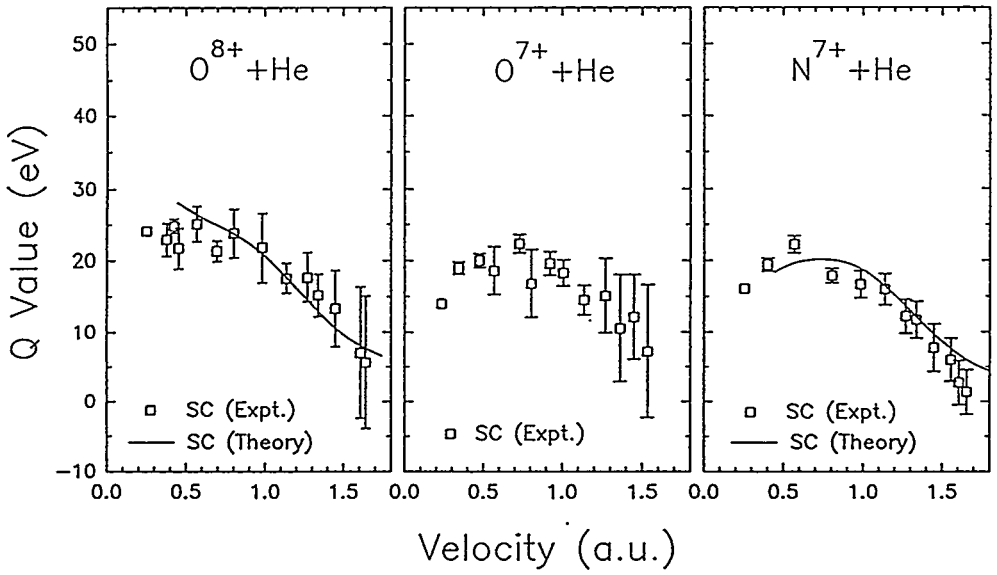

Figure 5.3.4.2. SC q values for O^{8+}, O^{7+}, and N^{7+} on He. Open squares: experiment; solid lines: close-coupling calculation.[3]

References for Section 5.3.4

1. W. Wu, J.P. Giese, I. Ben-Itzhak, C.L. Cocke, P. Richard, M. Stockli, R. Ali, and H. Schöne, Phys. Rev. A, accepted for publication (1994).
2. R. Ali, V. Frohne, C.L. Cocke, M. Stockli, S. Cheng, and M.L.A. Raphaelian, Phys. Rev. Lett. 69, 2491 (1992).
3. Z. Chen, C.D. Lin, and N. Toshima, Phys. Rev. A, accepted for publication (1994).

5.3.5 Evidence for Population of Highly Asymmetric States in Double Electron Capture in Collisions of $O^{8,7+}$ and N^{7+} with He at Intermediate Velocities

J.P. Giese, C.L. Cocke, P. Richard, and M.P. Stockli

Double electron capture processes in collisions of $O^{8,7+}$, and N^{7+} with He at velocities of 0.23 to 1.67 a.u. have been studied by coincident recoil momentum spectroscopy.[1] The final charges of the projectile and recoil were measured simultaneously along with the recoil longitudinal and transverse momenta. The recoil longitudinal momenta determined average q values, from which the approximate final states for each process were estimated. The recoil transverse momenta were used to calculate angular differential cross sections.

Comparisons of TI and DC are interesting because TI at these velocities is generally thought to occur when the projectile captures two electrons into doubly excited states. These states decay by either autoionization, leading to TI, or by radiative stabilization, leading to "true" double capture. As seen in Fig. 5.3.5.1, our measured q values for TI and DC are identical for O^{8+} + He collisions, suggesting that the same range of doubly excited states is populated in each process. However, the q values for DC by O^{7+} and N^{7+} are significantly larger than those for TI. This indicates that the electrons are captured to more tightly bound levels in DC than in TI for these projectiles.

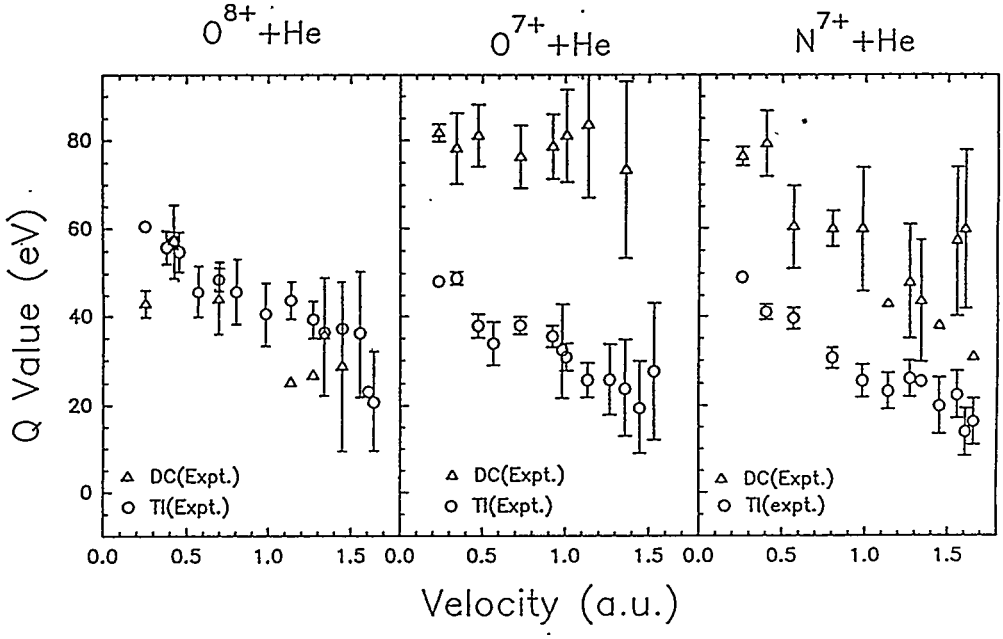

Figure 5.3.5.1. q values for TI and DC by O^{8+}, O^{7+}, and N^{7+} on He. Open circles: TI; open triangles: DC.

The angular differential cross sections of TI and DC are plotted in Fig. 5.3.5.2. The angular distributions for O^{8+} are almost identical for both TI and DC, while for both O^{7+} and N^{7+} DC has a larger scattering angle than TI. These results are consistent with our q value measurements within the MO model. TI and DC have about the same q values for O^{8+} + He collisions, indicating the same range of two-electron states is populated. The crossings of the initial states and these final states must occur at about the same internuclear separation. Thus, one would expect about the same angular dependence as observed. The q value for DC is higher than for TI in O^{7+} and N^{7+} + He, indicating that the crossings leading to DC occur at smaller separations, resulting in larger projectile scattering angles.

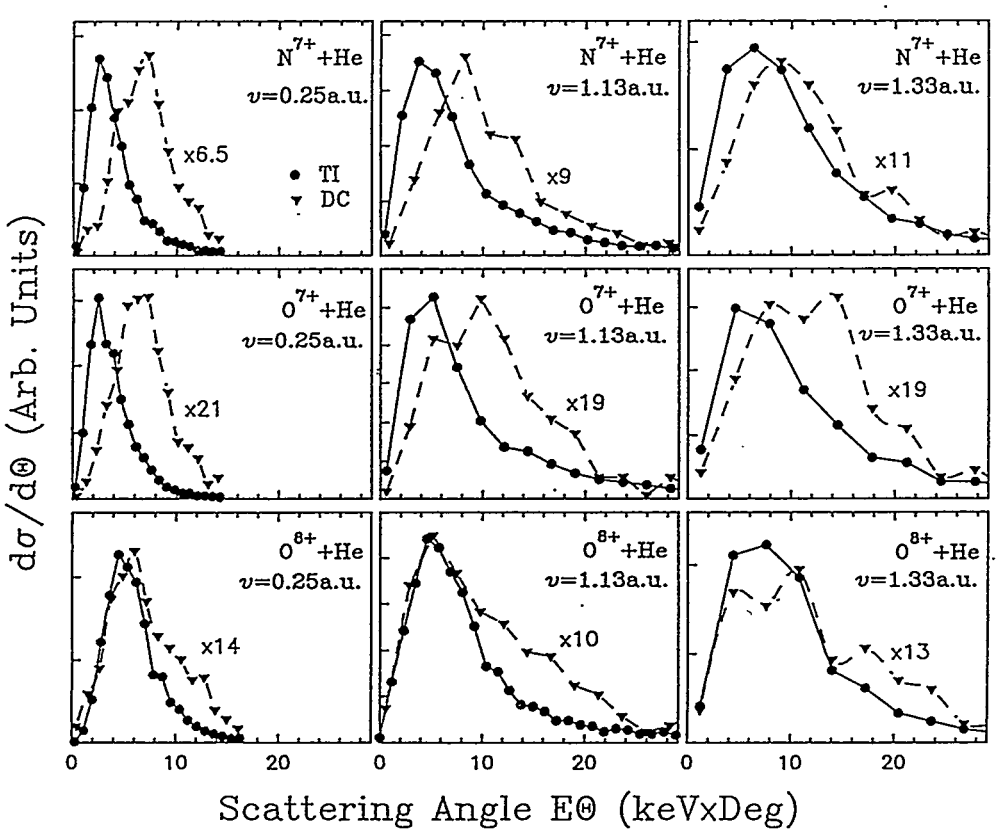

Figure 5.3.5.2. The angular differential cross sections for DC (circles) and TI (triangles).

Using the measured average q value for TI, the final states of the captured electrons were estimated to be (n, n′) = (3, 4) and (4, 4) for O^{8+} + He. While (3, 4) states decay dominantly via autoionization, the (4, 4) states have substantial radiative stabilization due to overlap with the (3, n) series.[2,3] Since DC has approximately the same q value and angular distribution as TI, these capture and

decay mechanisms are probably the main processes of the observed DC. Population of the (4, 4) states is rather unlikely for O^{7+} and N^{7+} + He, because this reaction would be endoergic. The measured average q values for TI in this case suggest that the electrons are captured to the (n, n′) = (3, 3) and (3, 4) states, which have no overlap with any Rydberg states. Thus, radiative stabilization is unlikely. The larger q value and scattering angle observed for DC imply that lower lying asymmetric (2, n) states, are populated in DC.

If the same range of two-electron states is populated for TI and DC by O^{8+}, then the ratio of true double capture to all two-electron capture, $\sigma_{DC}/(\sigma_{TI} + \sigma_{DC})$, is the radiative stabilization probability (P_{rad}) or average fluorescence yield for these states. P_{rad} as a function of the collision velocity is plotted in Fig. 5.3.5.3(a) and initially decreases with increasing velocity before reversing direction at about v = 0.8 a.u. This behavior can be qualitatively attributed to the velocity dependence of the relative populations of the final states. Assuming that radiative decay came mainly from asymmetric states with (n,n′; n′ > n+2), we calculated the sum of the predicted (close coupling) cross sections for these states[4] normalized to the corresponding total cross section for all states (i.e. $\Sigma\sigma_{n,n'>n+2}/\Sigma\sigma_{n,n'}$). As seen in Fig. 5.3.5.3(b), this ratio has a velocity dependence very similar to that of the data. Even our simple estimate of P_{rad} strongly suggests the population of asymmetric states in two electron capture.

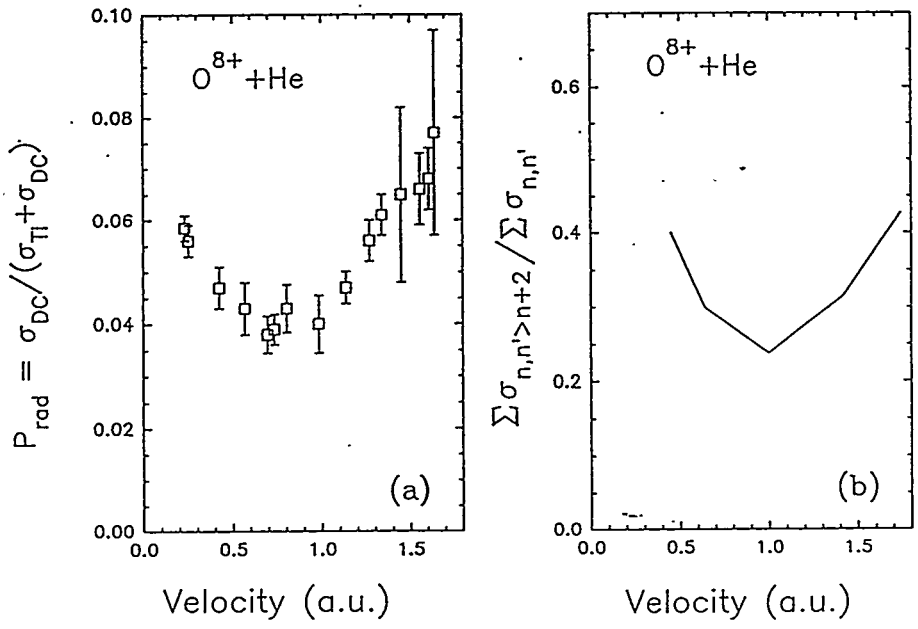

Figure 5.3.5.3. (a) measured radiative stabilization probability P_{rad} after double capture by O^{8+} from He. (b) Calculated ratios of the cross section due to asymmetric states ($\Sigma\sigma_{n,n'>n+2}$) to total cross section ($\Sigma\sigma_{n,n'}$) from the close-coupling calculations of Chen *et al.*[4]

References for Section 5.3.5

1. W. Wu, J.P. Giese, I. Ben-Itzhak, C.L. Cocke, P. Richard, M. Stockli, R. Ali, and H. Schöne, Phys. Rev. A, accepted for publication (1994).
2. P. Roncin, M.N. Gaboriaud, and M. Barat, Europhys. Lett. 16, 551 (1991).
3. H. Bachau, P. Roncin, and C.Harel, J. Phys. B 25, L109 (1992).
4. Z. Chen, C.D. Lin, and N. Toshima, Phys. Rev. A, accepted for publication (1994).

5.3.6 Double Ionization of He by Very High Velocity, Highly Charged Ions

S. Hagmann and C.L. Cocke
(in collaboration with J. Ullrich *et al.*, GSI, Darmstadt, Germany)

We have investigated single and double ionization of He for relativistic heavy ions Ne^{10+}, Ni^{28+}, and U^{90+} using beams from the Bevalac (Berkeley) and SIS-Darmstadt. The mechanism for multi-electron emission into the continuum for charged particle or photon impact has been in the center of interest for a long time and it is well established that the perturbation strength q/v plays a central role in the description. Whereas for electron induced ionization the perturbation strength can only be varied by varying the collision velocity (equivalent to varying collision time) for heavy ions available at relativistic colliders one has the option of varying charge and velocity. This opens the possibility to vary for asymptotically high velocities the charge state of the projectile beam to explore the existence of a high velocity limit of the ratio of double to single ionization for He. Recoiling He ions were charge state separated using conventional time of flight techniques. For Ne^{10+} the ratio decreases from $3.3 \cdot 10^{-3}$ at 0.39 c (80 MeV/u) to $2.6 \cdot 10^{-3}$ for velocities above 0.71 c (= 400 MeV/u).[1,2] This value is in agreement with the asymptotic value for electron and proton induced ionization and the calculation by Ford and Reading.[3] For Ni^{28+} beams the high velocity limit reached for same velocity Ne ions cannot be reached anymore, even at 0.93 c. This is due to the larger perturbation by the higher charge state. For U^{90+} ions then the ratio of double to single ionization of He was found to decrease from $6 \cdot 10^{-2}$ to $3 \cdot 10^{-2}$ for projectile velocities increasing from 0.34 to 0.73 c and thus remains far above the values found for relativistic electron ionization. It is believed that the strong projectile charge in the U^{90+} leads to dominant

contributions of simultaneous and independent interaction of the U^{90+} with both target electrons. We plan to investigate this further by measuring doubly differential cross sections for two-electron emission for widely different perturbations q/v and see whether the perturbation strength affects the momentum distribution of multielectron continua. (see proposal section also).

References for Section 5.3.6

1. H. Berg *et al.*, Phys. Rev. A 46, 5539 (1992).
2. J. Ullrich *et al.*, Phys. Rev. Lett. 71, 1697 (1993).
3. J. Reading *et al.* J. Phys. B 20, 3747 (1987).

5.4 Collisions with Excited, Aligned, and Rydberg Targets

5.4.1 Measurement of Absolute Capture Cross Sections for the Systems Ar^{7+} + Na(3s) and Na(3p)

B.D. DePaola and M.P. Stockli

We have measured absolute cross sections for charge capture by slow Ar^{7+} ions incident on Na(3s) and Na(3p) atoms. The process of electron capture in systems of slow highly charged ions with 1 electron (or effectively 1 electron) target atoms is generally described using a simple over barrier model, or CTMC calculations. These are both semi-classical models. The CTMC approach in particular is known to have difficulties at very low velocities where quantum effects begin to take place. True quantum mechanical models such as coupled channel (CC) calculations using atomic or molecular (or combinations of the two) become problematic for too high a projectile charge because the basis set needed to accurately describe the final projectile state becomes prohibitively large. It was the purpose of these experiments to determine absolute capture cross sections for the two systems Ar^{7+} + Na(3s) and Na(3p). These systems lie near the limit of applicability of CC calculations. Furthermore, the experiments were done with projectile velocities between 0.1 and 1.0 atomic units, near the lower limit of applicability of CTMC calculations. The cross sections were found to be reasonably consistent with CTMC results, particularly for the Na(3p) target. The experimental procedure and results have been published.[1,2]

References for Section 5.4.1

1. B.P. Walch, S. Maleki, R. Ali, M.P. Stockli, M.L.A. Raphaelian, C.L. Cocke, and B.D. DePaola, Phys. Rev. A 47, 3499 (1993).
2. S. Maleki, M.L.A. Raphaelian, M.P. Stockli, B.P. Walch, and B.D. DePaola, Phys. Rev. A 48, 1185 (1993).

5.4.2 Measurement of Alignment Dependence of Charge Capture Cross Sections in Collisions of Highly Charged Ions with Laser Aligned Sodium

B.D. DePaola

We have made measurements of the alignment parameter for charge capture by Ar^{7+} incident on laser-aligned Na(3p). In the system of Ar^{7+} + Na(3p), the capture cross section was measured as a function of the angle between the quantization axis of the laser aligned sodium and the projectile beam. The result was that no alignment effects were seen. This is a bit puzzling since in a subsequent experiment[1] with the similar system of O^{6+} + Na(3p) alignment was seen. We will pursue this line of experiments and try to resolve this discrepancy.

Reference for Section 5.4.2

1. A.R. Schlatmann, S. Schippers, R. Hoekstra, R. Morgenstern, XVIII ICPEAC, Abstracts of Contributed Papers, T. Andersen, B. Fastrup, F. Folkmann, and H. Knudsen, eds., page 545, (1993).

5.4.3 CTMC-Based Empirical Scaling Law for Ion-Rydberg Capture Cross Sections

B.D. DePaola

In preparation for an experiment in which the capture cross sections for slow highly charged ions incident on Rydberg target atoms will be measured, we performed a series of CTMC calculations on similar collision systems. Comparison of many CTMC results on a wide variety of systems let to the determination of an empirical scaling law for highly charged ions-Rydberg atom charge capture cross sections:

$$\sigma = 150\ q^{2.5} n^4 / v_e^{\,9}$$

where v_e is the scaled velocity (the velocity of the projectile divided by the bohr

velocity of the electron), and q is the projectile charge.

This is a bit different from the prediction of a simple application of the Bohr-Lindhard model[1] which gives

$$\sigma = 8\pi\, q^3 n^4 / v_e^7$$

Experiments will be performed to determine which (if either) accurately describes the correct scaling with charge and velocity.

The results of these calculations have been written up and will be submitted for publication.

Reference for Section 5.4.3

1. A nice explanation of the Bohr-Lindhard model for capture cross sections is given in H. Knudsen, H.K. Haugen, and P. Hvelplund, Phys. Rev. A 23, 597 (1981); B40, 187 (1989).

5.4.4 Experimental Velocity Dependence of Charge Capture Cross Sections for Slow, Highly Charged Ions with a Rydberg Target

B.D. DePaola and M.P. Stockli
(in collaboration with S. Lundeen and C. Fehrenbach, Colorado State University)

We have measured absolute capture cross sections for the system of Xe^{q+} + Rb(10F). To date no absolute cross sections for multiply charged ions incident on Rydberg target atoms have been reported in the literature. This is an interesting collision system since it is expected to behave almost classically. CTMC calculations have been performed for this sort of system and, until now, remain untested. Using a rubidium Rydberg target developed by collaborators from Colorado State University, and a beam of Xe^{q+} (q=8, 16, 32, 40) ions from the KSU CRYEBIS at velocities of 0.1 to 0.6 atomic units, we have measured absolute cross sections for charge capture. The results, which have not yet been fully analyzed, appear to be roughly in agreement with CTMC calculations performed at KSU. Following more careful analysis, the experimental results will be submitted for publication.

5.4.5 Development of a Sodium Rydberg Target for use in Collisions with Slow Highly Charged Ions

B.D. DePaola

We have developed a sodium Rydberg target which we plan to use with slow, highly charged ions from the KSU CRYEBIS to measure charge capture and target ionization cross sections. Using an existing homemade copper vapor laser-pumped tunable dye laser to drive the 3s - 3p transition, followed by a nitrogen laser-pumped newly built homemade tunable dye laser to drive the 3p - nℓ transition, we have developed a target of Rydberg atoms. This target will be used to measure capture cross sections by slow highly charged ions as a function of projectile charge and velocity, and as a function of target n, ℓ, and alignment.

5.5 Ion-Ion Collisions

5.5.1 KSU Ion-Ion Collision Facility Installation

J.P. Giese, F. Melchert, and C.L. Cocke

One of the most important questions in the study of ion-ion collisions is whether it is possible to understand, model, and predict the outcomes of ion-ion collisions from the isoelectronic ion-atom collisions. Most ion-ion experiments have been on the lowest charged members of these isoelectronic sequences, i.e. systems where both of the beams were composed of singly or doubly charged ions. It has therefore not been possible to test the predicted cross sections or scaling rules over a broad range of ion-ion collision systems. A facility to study collisions between multiply charged ions is being constructed at the Macdonald Lab. The KSU EBIS and ECR accelerators will provide multiply charged ions over a wide velocity range in order to study electron capture along several isoelectronic sequences.

The proposal to build the KSU Ion-ion Facility was first submitted to DOE as a new initiative in our FY 1992-95 Renewal Proposal in August 1991. This proposal was funded as a University Research Instrumentation Program in September 1993. Considerable progress has been made within the last year to turn the ideas and designs of the proposal into a working experiment. The general layout of the ion-ion collision facility, showing the beam transfer lines from the EBIS and the ECR and the post collision analysis hardware, is shown in Fig. 5.5.1.1. Our facility crosses beams from the EBIS and ECR at right angles to each other in a UHV environment. The products of charge changing reactions in the ion-ion collisions are magnetically and electrostatically analyzed after the collision, and detected in time coincidence.

The major accomplishment of the past year was the installation and testing of our new 5 GHz ECR ion source. This source sits on a 10 kV platform and can provide intense beams of moderately charged ions. Initial tests have produced in excess of 100 nA of Ar^{4+} using an incomplete ion-optics system. Construction of the remaining optical components is underway and final ion source tests should be completed this Fall.

A major difficulty in any ion-ion collision experiment is that the ion beams are tenuous compared to even the residual gas remaining in a UHV environment. We attempt to overcome this problem by decelerating the ECR ion beams to a few hundred eV per charge in order to enhance the effective target density. The ECR requires an extraction voltage of at least 5 kV in order to produce acceptable beam

emittances. The most difficult technical challenge of this facility is to slow the ECR ions without having the beam blow up due to its own space charge. We have modelled the ion-optics of the ECR and EBIS beams from the sources through the deceleration columns and the post collision analyzers. These indicate that it is possible to decelerate the slow, intense ECR beam and maintain both a reasonable focus at the collision region and 100% transmission of the collision products.

The primary equipment and majority of the cost of the facility consists of the UHV vacuum chambers and low ultimate pressure vacuum pumps needed to produce pressures of about 10^{-10} Torr in the collision region. The major components of our vacuum system have been purchased and are being assembled. The deceleration columns and remaining ion optics components are being fabricated in our shops. The assembly and testing of all these components will continue through the Fall with initial ion-ion collision tests beginning sometime in 1995.

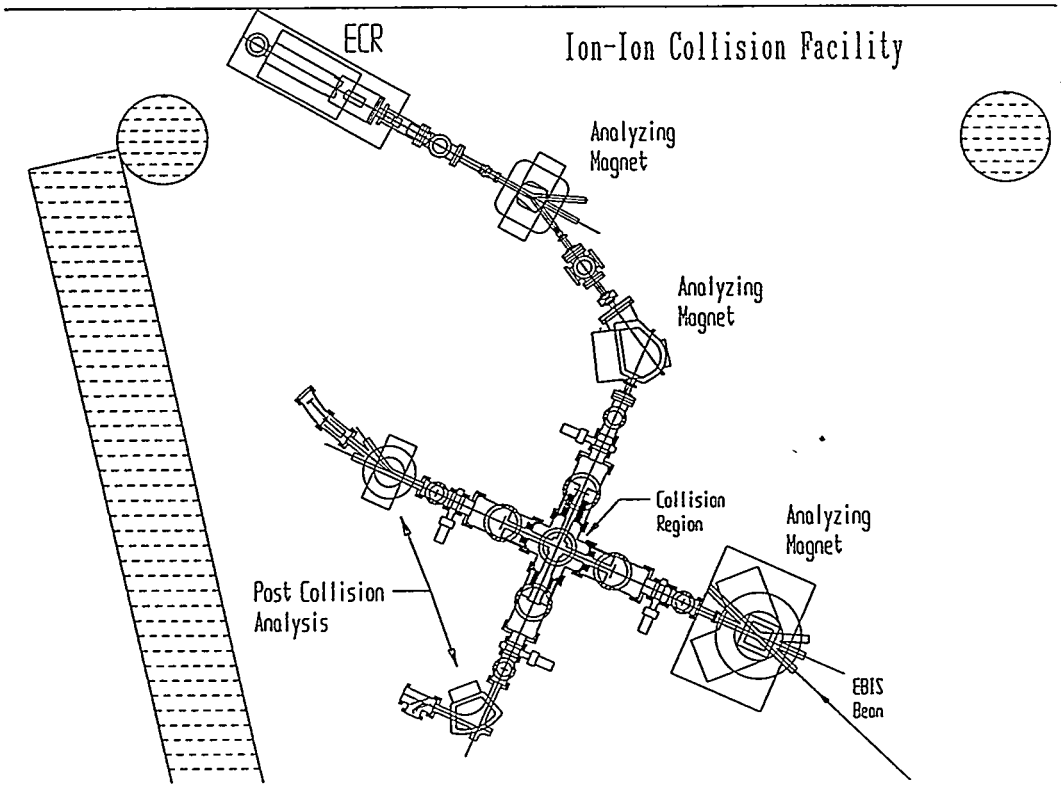

Figure 5.5.1.1. The KSU Ion-Ion Collision Facility.

5.6 Ion-Molecule Collisions

5.6.1 The Coincidence Time-Of-Flight (CTOF) Method for Studies of Ion-Molecule Collisions

I. Ben-Itzhak

During the previous three year period we have spent most of our time developing an experimental method and apparatus which enables us to record the times-of-flight of many ions formed in a single collision. This is accomplished using multi-hit timing electronics for the signals produced by the recoil ions while the time reference signal is produced either by the projectile (particle coincidence mode) or a signal synchronized with the beam bunch (bunched beam mode). A detailed description of the experimental method,[1] used extensively during the last few years, and of a device developed for multi-hit measurements[2] have been reported. The analysis of the multi-dimensional time data, shown for example in the figures below for $H^+ + CH_4$ collisions, enables the determination of the relative cross sections of the different fragmentation channels of a target molecule.[3,4]

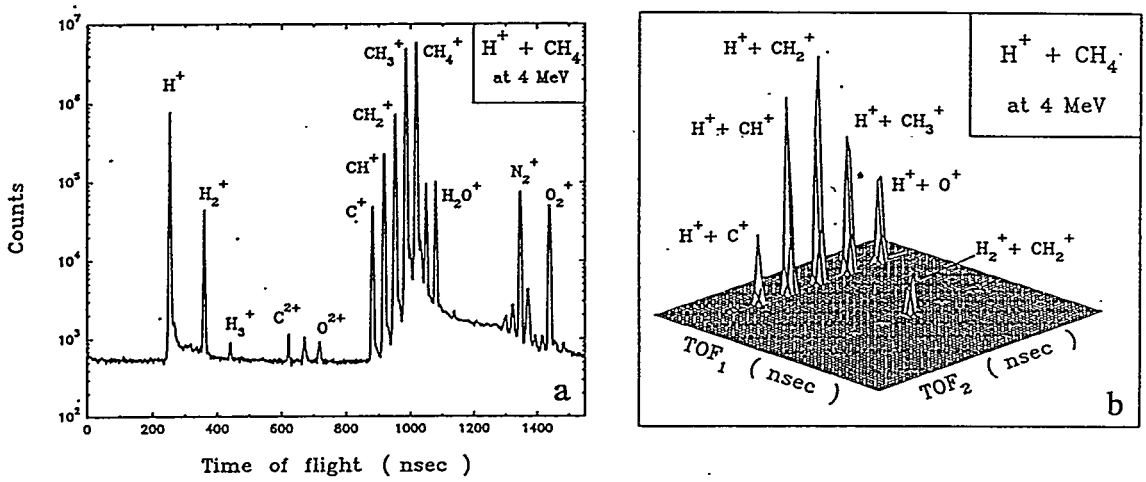

Figure 5.6.1.1. (a) TOF single-ion spectrum of methane fragmentation, produced by 4-MeV proton impact, measured with a strong extraction field of 1250 V/cm. (b) Coincidence TOF spectrum of methane fragmentation, produced by 4-MeV proton impact, measured with a strong extraction field of 1250 V/cm.

The efficiency for detecting events with different multiplicity, n (i.e. number of charged fragments produced in a single collision) is proportional to ϵ^n, where ϵ is

the efficiency for detecting a single ion. In order to reduce the raw data one needs to know this efficiency ϵ as precisely as possible. We have developed a direct method to determine this efficiency.[5]

In addition to the information about production cross sections, the distribution of kinetic energies carried by the fragments can also be determined for each breakup channel (singles, ion-pairs ion-triplets, etc.).[6] This additional information can be used to determine the possible fragmentation pathways in a polyatomic molecule, as we have done for CH_4,[4] or the different dissociation mechanisms, as demonstrated for the diatomic CO molecule.[7] For example, the times-of-flight of the two fragments in a two-body breakup are linearly correlated with a correlation coefficient of -1, as can be seen for $CH_4^{2+} \rightarrow H_2^+ + CH_2^+$ breakup in the figure. By measuring the deviation of the distributions of the different breakup channels, shown in the figure, from such lines, one can estimate the momentum carried away by the neutral fragments, and thus exclude certain fragmentation pathways.[4]

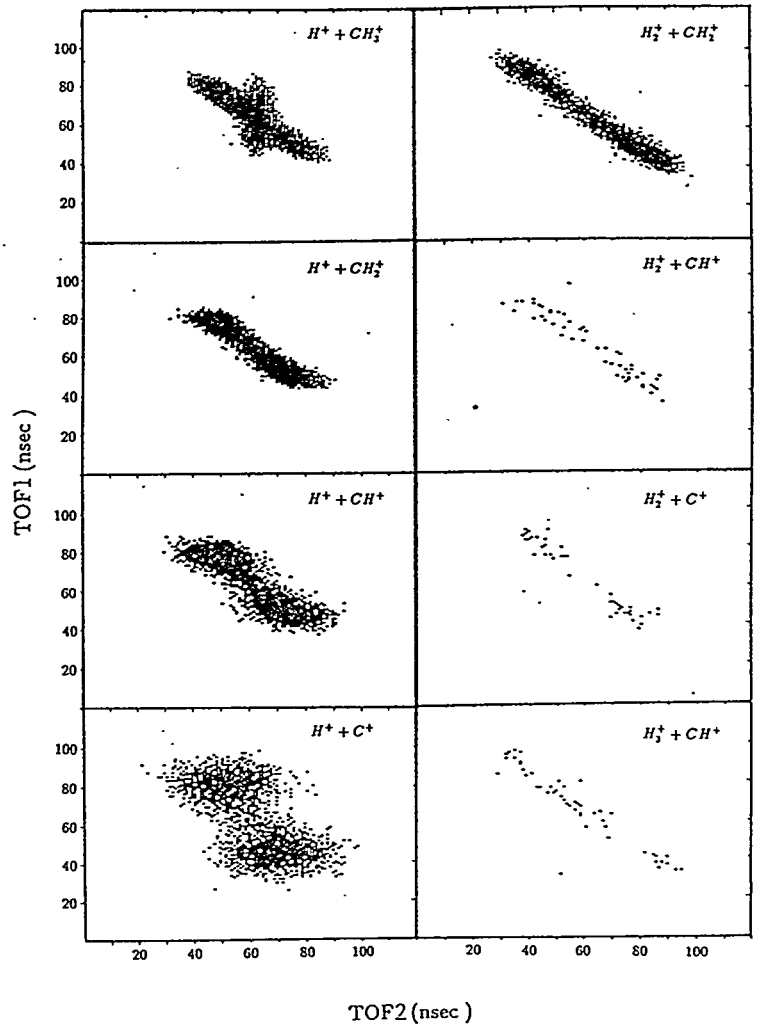

Figure 5.6.1.2. The time-of-flight spectra of the main ion-pair break-up channels, produced by 4-MeV proton impact. Plotted as a density plot of intensity as a function of TOF_1 and TOF_2.

Recently, we have designed, assembled and started testing a multi-hit position sensitive detector. Adding such a detector to our setup will improve the resolution of our kinetic energy measurements, which is limited by the coupling between a fragment's speed and its initial direction. Thus, better measurements of the kinetic energy distributions of the different dissociation channels will be possible. Furthermore, from the measurement of the times-of-flight and position of both fragments the angle between the molecular axis and the beam direction can be determined with 4π collection efficiency.[8] This new information will provide us with a new direction for research, which will be focused on the dependence of processes like ionization, capture, and transfer-ionization on the alignment of the electron cloud relative to the beam direction.

References for Section 5.6.1

1. I. Ben-Itzhak, S.G. Ginther, and K.D. Carnes, Nucl. Instrum. and Meth. B66, 401 (1992).
2. I. Ben-Itzhak, K.D. Carnes, and B.D. DePaola, Rev. Sci. Instrum. 63, 5780 (1992).
3. I. Ben-Itzhak, S.G. Ginther, and K.D. Carnes, Phys. Rev. A 47, 2827 (1993).
4. I. Ben-Itzhak, K.D. Carnes, S.G. Ginther, D.T. Johnson, P.J. Norris, and O.L. Weaver, Phys. Rev. A 47, 3748 (1993).
5. I. Ben-Itzhak, K.D. Carnes, S.G. Ginther, D.T. Johnson, P.J. Norris, and O.L. Weaver, Nucl. Instrum. and Meth. 79, 138 (1993).
6. I. Ben-Itzhak, S.G. Ginther, and K.D. Carnes, p-343 VIth International Conference on the Physics of Highly-Charged Ions, Edited by P. Richard, M. Stockli, C.L. Cocke, and C.D. Lin (American Institute of Physics, New York, 1993).
7. I. Ben-Itzhak, S.G. Ginther, V. Krishnamurthi, and K.D. Carnes, submitted to Phys. Rev. A (1994).
8. S. Cheng, C.L. Cocke, V. Frohne, E.Y. Kamber, and S.L. Varghese, Nucl. Instrum. and Methods B56/57, 78 (1991).

5.6.2 Velocity Dependence of CO and CH_4 Fragmentation Caused by Fast Proton Impact

I. Ben-Itzhak, K.D. Carnes, V. Krishnamurthi, and T.J. Gray

Cross sections of the breakup channels of CO and CH_4, caused by fast (0.5-14 MeV) proton impact, have been measured in order to probe the high impact velocity behavior of molecular fragmentation.[1-3] Single ionization is the dominant channel in these collisions while double ionization is of the order of 1%. The cross sections for multiple ionization of these molecules are well described by simple SCA calculations within the independent electron approximation. (Hydrogenic wave functions were used to calculate the ionization probability of the active electron).

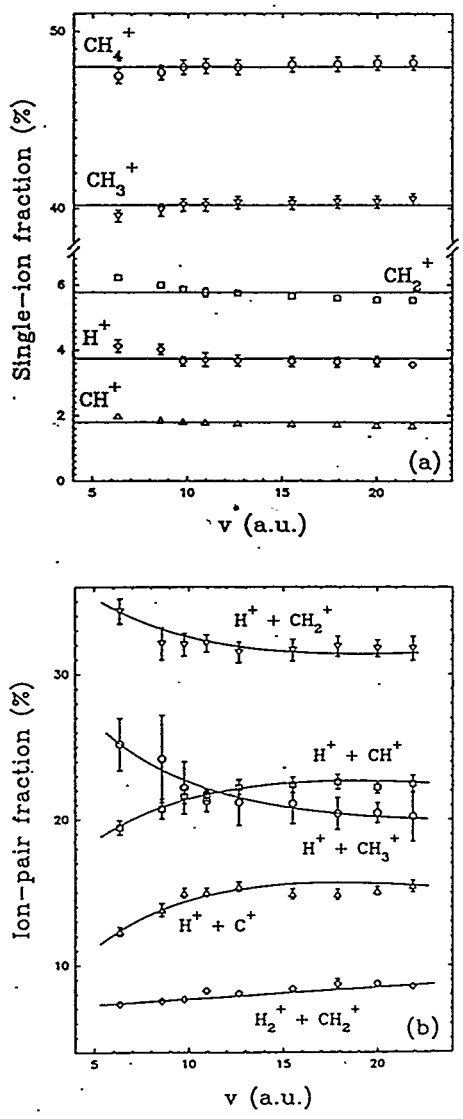

Figure 5.6.2.1. The fraction of (a) the main single-ion channels out of the total number of single ions, and (b) the main ion pairs out of the total number of ion pairs, as a function of the collision velocity. The lines are drawn to guide the eye.

The branching ratios of the main breakup channels of the multiply charged CO and singly charged CH_4 molecular ions are independent of the collision velocity. Surprisingly the branching ratios of the main breakup channels of CH_4^{2+} show some velocity dependence, as can be seen from the Fig. 5.6.2.1 above.

The velocity dependence of the ratio of CO^{2+} to CO^+ (*stabilized* ionization), shown in the figure is in excellent agreement with the equation $R_\infty + R_0/v^2$. The first term is the constant limit expected at high velocities, where direct double ionization is negligible and all double ionization is due to e-e interactions. The second term is what one would expect for the ratio of direct double to single ionization, which are proportional to $(q/vb)^4$ and $(q/vb)^2$, respectively.

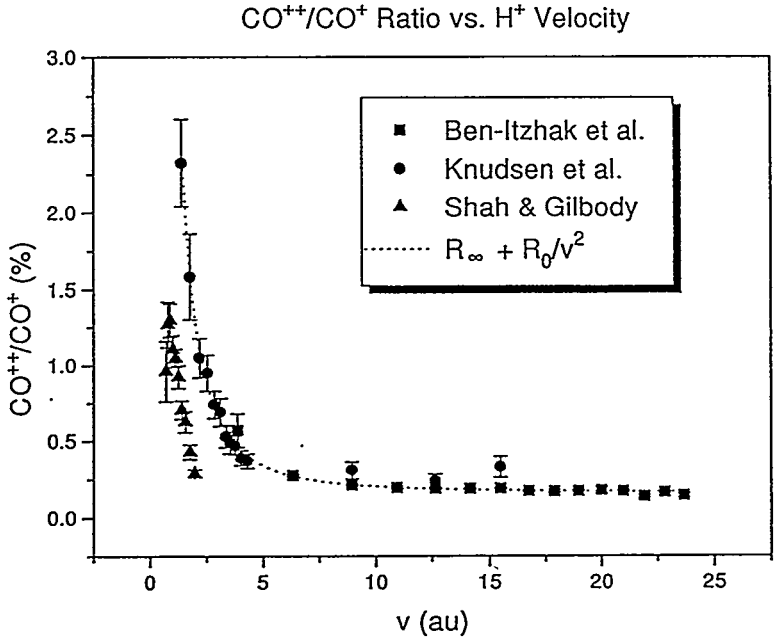

Figure 5.6.2.2.

A few coincidence measurements are still needed at lower energies in order to test this behavior for the *total* ionization. This study has been presented in the ICPEAC 1993 meeting, and recently published in Phys. Rev. A 47, 3748 (1993); and ibid 49, 881 (1994).

Our studies of $H^+ + CO$ and $H^+ + CH_4$ collisions were further motivated by a presentation of Professor Knudsen at the Denton 1992 meeting in which he presented preliminary studies of CO and CH_4 ionization and dissociation caused by $e^\pm$ and $p^\pm$ impact.[4] The ionization cross sections caused by electron,[5-8] positron,[4] proton,[1-4] and antiproton[4] impact are the same as expected at the high velocity limit where the first Born approximation is valid. On the other hand, at intermediate

velocities (i.e. 1-3 a.u.) differences have been observed.[4] These differences, studied extensively for the He target, have been attributed to an interference between the first and second Born terms.[9] The surprising result for molecular targets is the difference between the dissociation of CO^{+*} into either $C^+ + O$ or $C + O^+$, shown below, for the different projectiles. This difference might suggest that the second Born term is not negligible for these single ionization processes.

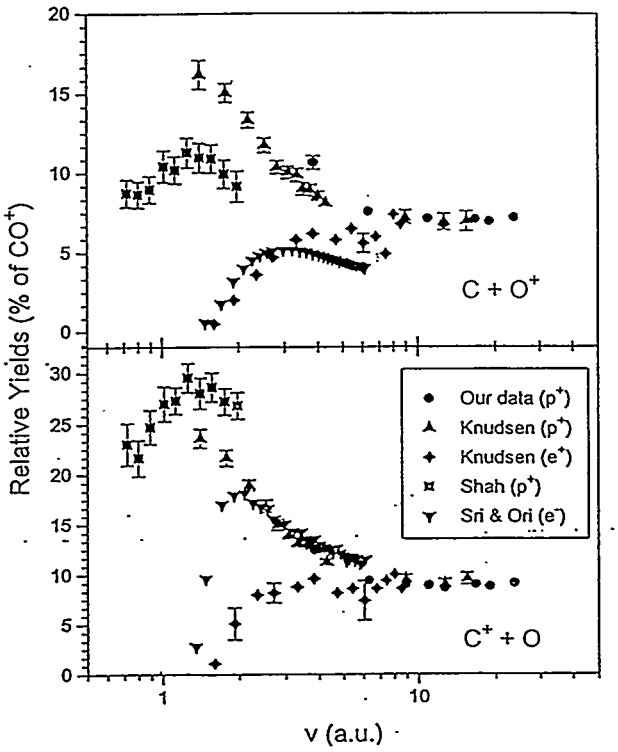

Figure 5.6.2.3.

We are extending our measurements of proton impact ionization and dissociation to lower velocities in order to probe these differences. In particular, we are studying the fragmentation of multiply ionized molecules using the Coincidence Time-of-Flight technique. These ions are expected to have a stronger dependence on the sign of the projectile charge. Unfortunately such coincidence measurements are scarce, but some groups are in the process of starting such measurements for electron and positron impact.

References for Section 5.6.2

1. I. Ben-Itzhak, K.D. Carnes, S.G. Ginther, D.T. Johnson, P.J. Norris, and O.L. Weaver, p-339 VIth International Conference on the Physics of Highly-Charged Ions, Edited by P. Richard, M. Stockli, C.L. Cocke, and C.D. Lin (American Institute of Physics, New York, 1993).
2. I. Ben-Itzhak, K.D. Carnes, D.T. Johnson, P.J. Norris, and O.L. Weaver, Phys. Rev. A 49, 881 (1994).
3. I. Ben-Itzhak, K.D. Carnes, V. Krishnamurthi, K.M. Bloom, and T.J. Gray, to be submitted to Phys. Rev. A (1994).
4. H. Knudsen, The XII International Conference of the Application of Accelerators in Research and Industry, Denton, Texas, November (1992), and private communication.
5. B. Adamczyk, A.J.H. Boerboom, B.L. Schram, and J. Kistemaker, J. Chem. Phys. 44, 4640 (1966).
6. K.E. McCulloh, T.E. Sharp, and H.M. Rosenstock, J. Chem. Phys, 42, 3501, (1965).
7. C. Backx and M.J. Van der Weil, J. Phys. B 8, 3020, (1975).
8. O.J. Orient and S.K. Srivastava, J. Phys. B 20, 3923 (1987).
9. H. Knudsen and J.F. Reading, Phys. Rep. 212, 107 (1992), and references therein.
10. M.B. Shah and H.B. Gilbody, J. Phys. B 23, 1491 (1990).

5.6.3 q-Dependence of CO and CH_4 Ionization and Fragmentation in Fast Collisions

V. Krishnamurthi, I. Ben-Itzhak, and K.D. Carnes

Cross sections for electron removal from CO and CH_4, as well as the cross sections of the different breakup channels, have been measured for collisions with fast highly charged ions (q=1-18) at a fixed velocity of 6.3 a.u. (1 MeV/amu). Single ionization is the dominant channel in these collisions and its cross section increases rapidly with increasing q, as shown in Fig. 5.6.3.1 below. This increase, however, is slower than the q^2 scaling predicted by the first Born approximation. Even though this perturbative approximation is not a good one for the high values of q the *total* and *non-dissociating* single ionization cross sections still scale like $\sigma_0 q^\alpha$, where σ_0 is the proton impact cross section and α is a little smaller than 2, for both atoms[1,2] and

molecules.[3] The values of α, (α~1.5-1.8), however, vary somewhat from one target to the other and no explanation for these values have been found so far. This scaling is the same for bare and dressed projectiles indicating that for the soft collisions associated with single ionization the projectile can be treated as a point charge. This work has been accepted for publication in J. Phys. B Lett.[3]

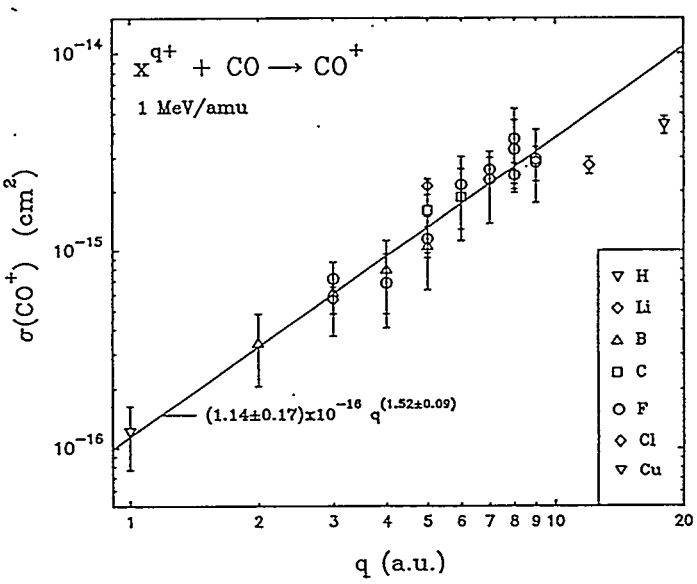

Figure 5.6.3.1.

Multiple electron removal from the many electron CO target falls off exponentially with increasing number of missing electrons in a similar way as a Ne target undergoing the same collisions, as can be seen from Fig. 5.6.3.1. The transient CO^{Q+} molecular ions tend to break into $C^{i+} + O^{j+}$ ion-pairs peaked around i=j, as can be seen from Fig. 5.6.3.2. The branching ratios of the different breakup channels of CO^{Q+*} show a weak dependence on the projectile charge which is consistent with a slight shift toward higher excitation energies with increasing q. This increase is slower than the q^2 increase expected for energy transfer to a single electron, $\Delta E \sim (q/b\ v)^2$, because n-electron ionization of a many electron target happens within an impact parameter range defined by the condition that $P^n(b)\ [1-P(b)]^{N-n}$ is large enough.[4] These "windows" increase when q changes from 1 to 2 but for larger values of q they remain approximately constant and later even decrease, thus suppressing the change in excitation energy. These results have been presented in the DAMOP 1994 meeting. Further data analysis and theoretical calculations are underway.

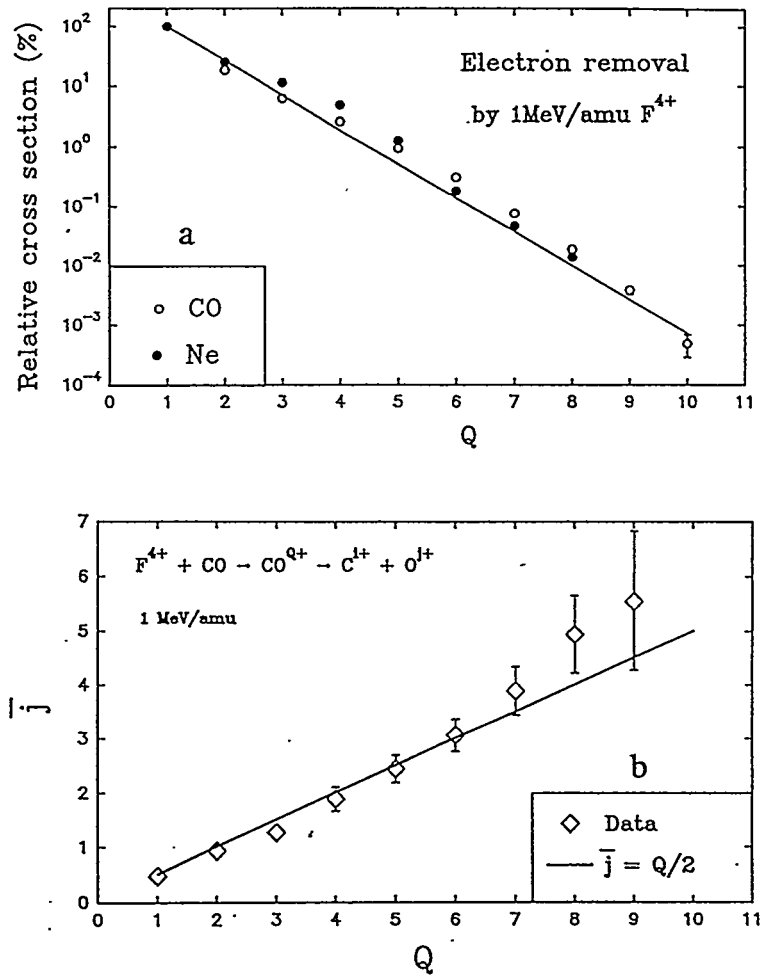

Figure 5.6.3.2. (a) Cross sections for removing electrons from either CO or Ne, by 1-MeV/amu F^{4+} impact, relative to the singly charged CO^+ and Ne^+ cross section, respectively, as a function of the number of electrons removed Q. The line represents as exponential fit to the CO data: ——, $100e^{-1.31Q}$. (b) Average charge state of the oxygen fragment produced by 1-MeV/amu F^{4+} impact as a function of the number of electrons removed Q. The solid line represents $\bar{j} = Q/2$.

References for Section 5.6.3

1. S.H. Be, T. Tonuma, H. Kumagai, H. Shibata, M. Kase, T. Kambara, I. Kohno, and H. Tawara, J. Phys. B 19, 1771 (1986).
2. O. Heber, G. Sampoll, B.B. Bandong, R.J. Maurer, R.L. Watson, I. Ben-Itzhak, J.M. Sanders, J.L. Shinpaugh, and P. Richard, Submitted to Phys. Rev. A (1994).
3. V. Krishnamurthi, I. Ben-Itzhak, K.D. Carnes, and B.M. Barnes, J. Phys. B Lett., accepted for publication (1994).
4. I. Ben-Itzhak, T.J. Gray, J.C Legg, and J.H. McGuire, Phys. Rev. A 37, 3685 (1988).

5.6.4 Kinetic Energy Release in $CO^{q+} \rightarrow C^{i+} + O^{j+}$ Dissociation

I. Ben-Itzhak, S.G. Ginther, V. Krishnamurthi, and K.D. Carnes

The kinetic energy released in the dissociation of a molecule can provide additional information about the breakup mechanism. We have used the coincidence time-of-flight technique (CTOF) in order to determine the distribution of this energy for the main ion-pair dissociation channels of CO. A commonly used model to estimate this energy release is the Coulomb explosion model, in which the two dissociating ions of a diatomic molecule are treated as point charges starting from the equilibrium distance R_0. However, recently Sampoll *et al.*[1] have shown that this model underestimates the average value of the energy release in the breakup of CO caused by fast Ar^{14+} impact. In similar studies by Mathur *et al.*[2] the model failed to predict the end point of the kinetic energy release distributions. The values calculated for the different breakup channels of CO ionized by 19 MeV F^{4+} impact (solid line in the figure) are in reasonable agreement with the most likely value of the kinetic energy released, indicating that repulsive states which are approximately Coulombic are the main dissociation route.

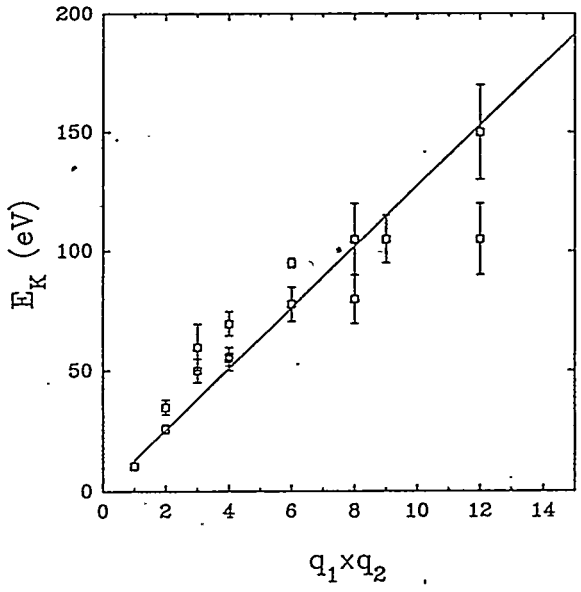

Figure 5.6.4.1. Most likely kinetic energy release E_K as a function of the product of the fragments charges; solid line, Coulomb explosion model.

Furthermore, additional peaks appear in the kinetic energy distributions of breakup channels where only a few electrons have been removed. These peaks are at energies corresponding to Coulomb explosion values associated with higher charge states (see the figure below) suggesting that one electron (or more) is highly excited and thus it does not contribute to the screening of the nuclear charge. This study has

been submitted for publication in Phys. Rev. A.[3]

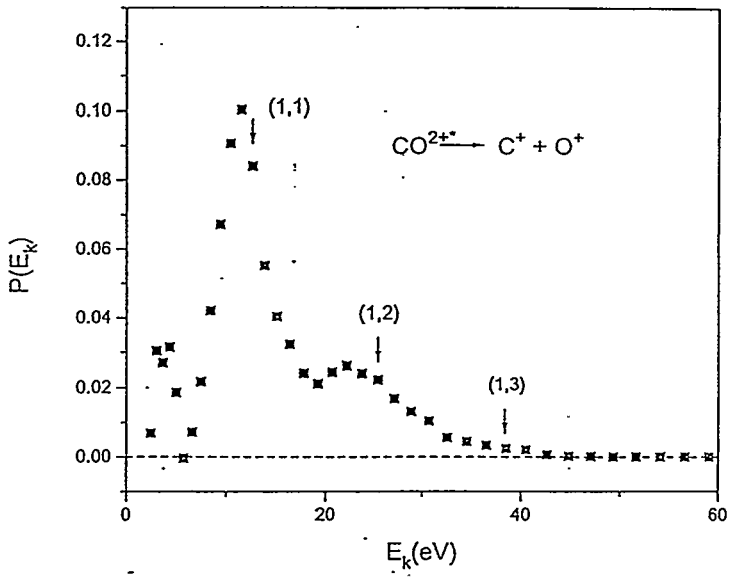

Figure 5.6.4.2. Kinetic energy release distribution of $C^+ + O^+$ breakup. The arrows represent the predicted values for $C^{q_1} + O^{q_2}$ breakup.

References for Section 5.6.4

1. G. Sampoll, R.L. Watson, O. Heber, V. Horvat, K. Wohrer, and M. Chab, Phys. Rev. A 45, 2903 (1992).
2. D. Mathur, E. Krishnakumar, K. Nagesha, V.R. Marathe, V. Krishnamurthi, F.A. Rajgara, and U.T. Raheja, J. Phys. B 26, L141 (1993).
3. I. Ben-Itzhak, S.G. Ginther, Vidhya Krishnamurthi, and K.D. Carnes, Phys. Rev. A, submitted for publication.

5.6.5 Alignment Effects in One and Two Electron Processes in Slow Collisions between Ar^{q+} and Hydrogen Molecules

I. Ben-Itzhak, R. Ali, K.D. Carnes, M.P. Stockli, and C.L. Cocke

The effect of the alignment of a hydrogen internuclear axis and the beam axis are the focus of this study. The highly charged Ar^{8+} projectiles produced by the KSU CRYEBIS were charge state analyzed after the collision and measured in coincidence with the recoil ions. The recoil ions were extracted in a Time-of-Flight spectrometer toward a position sensitive MCP detector with 4π collection efficiency, thus allowing us to distinguish between dissociating and non-dissociating channels. The position

and time information of the molecular fragments enables the determination of the internuclear axis direction relative to the beam axis.[1,2] Preliminary measurements of 400 keV Ar^{11+} + HD collisions using a resistive anode position sensitive detector indicated that everything in our apparatus works fine except the slow response time of the resistive anode. A new detector which will allow multi-hit position information detection is now under development. We hope that this new detector will allow the completion of our first measurement and further work in the same direction.

References for Section 5.6.5

1. S. Cheng, C.L. Cocke, V. Frohne, E.Y. Kamber, S.L. Varghese, Nucl. Instrum. and Methods B56/57, 78 (1991).
2. S. Cheng, C.L. Cocke, V. Frohne, E.Y. Kamber, J.H. McGuire, and Y. Wang, Phys. Rev. A 47, 3923 (1993).

5.6.6 One and Two Electron Processes in Ion-Hydrogen Collisions

I. Ben-Itzhak, V. Krishnamurthi, and K.D. Carnes

Studies of one- and two-electron processes, such as single and double ionization, electron capture, and transfer ionization, in collisions of fast and slow highly charged ions and helium, X^q + He, have been at the center of attention of our community.[1-3] The hydrogen molecule provides another simple two electron target for which some similar studies have been performed.[3-8] This molecular target differs from the atomic He target in a few aspects:

1. The hydrogen molecule has a weaker binding energy than He.

2. The spatial wave function of the electrons of the hydrogen molecule is distributed along the molecular axis, thus some alignment effects are possible.

3. All excited states of the H_2^+ are dissociative, thus one can easily study the ionization-excitation channel (another two electron process).

We have recently started studies of fast X^{q+} + HD collisions, using the coincidence time-of-flight method. The choice of the HD heteronuclear hydrogen molecule makes it easy to distinguish for example the double ionization from the single ionization channel in a time-of-flight measurement. Furthermore, taking advantage of the different kinetic energy release we can distinguish between the dissociation of the $1s\sigma$ ground state from that of all the excited states. Preliminary results from H^+, O^{3+}, and F^{7+} impact at 1 MeV/amu indicate that:

1. The non-dissociative ionization is the main channel, i.e. the transition from HD to the $HD^+(1s\sigma)$.

2. Some of the HD^+ in the $1s\sigma$ electronic ground state dissociates because they were produced at very small internuclear separation. Even though this channel is negligible in comparison with the non-dissociative channel it is still a significant contribution to the dissociative-ionization.

3. The dissociative ionization varies from about 1% for proton impact to above 10% for F^{7+} impact, suggesting that projectiles with higher charge can excite the hydrogen molecule more efficiently.

4. Double ionization, which is measured easily because of the $H^+ + D^+$ coincidence condition, varies from about 0.1% for proton impact to a few percent for F^{7+} impact.

We are planning to continue this line of investigation and to determine the dependence of these channels on the projectile charge and the collision velocity. Furthermore, by measuring the final charge state of the projectile in coincidence with the recoil ions we hope to correlate the final states of the hydrogen target with the process which removed the electrons from it. The study of the velocity dependence of the double to single ionization ratio of hydrogen caused by proton impact will be presented as an invited talk at the Denton 1994 meeting.

References for Section 5.6.6

1. H. Knudsen and J.F. Reading, Phys. Rep. 212, 107 (1992), and references therein.
2. H. Knudsen, L.H. Andersen, P. Hvelplund, G. Astner, H. Cederquist, H. Danared, L. Liljeby, and K.-G. Rensfelt, J. Phys. B 17, 3545 (1984).
3. P. Hvelplund, H. Knudsen, U. Mikkelsen, E. Morenzoni, S.P. Moller, E. Uggerhoj, and T. Worm, J. Phys. B 27, 925 (1994).
4. R.L. Ezell, A.K. Edwards, R.M. Wood, M.W. Dittmann, J.F. Browning, and M.A. Mangan, Nucl. Instrum. and Methods, B56/57, 292 (1991).
5. A.K. Edwards, R.M. Wood, A.S. Beard, and R.L. Ezell, Phys. Rev. A 37, 3697 (1988).
6. H. Kossmann, H. Schwarzkopf, and V. Schmidt, J. Phys. B 23, 301 (1990).
7. E. Krishnakumar and S.K. Srivastava, J. Phys. B 27, L251 (1994).
8. L.H. Andersen, P. Hvelplund, H. Knudsen, S.P. Moller, J.O.P. Pedersen, S. Tang-Petersen, E. Uggerhoj, K. Elsner, and E. Morenzoni, J. Phys. B 23, L395 (1990).

5.6.7 Formation and Decay Mechanisms of the HeH^{2+}, $^3He^4He^{2+}$, $HeNe^{2+}$, and $NeAr^{2+}$ Molecular Ions

I. Ben-Itzhak, Z. Chen, and C.D. Lin
(in collaboration with I. Gertner, B. Rosner, Technion, Israel, where the experiments are carried out and in collaboration with: O. Heber (Weizmann, Israel), W. Koch (Berlin, Germany), and G. Frenking (Marburg, Germany).

Weakly bound doubly charged rare gas dimmers, like $^3He^4He^{2+}$, $HeNe^{2+}$, $NeAr^{2+}$, and the three body system HeH^{2+} are the focus of our collaborative studies. These molecular ions are formed in fast charge-stripping collisions of the singly charged molecular ion in Ar gas. The mean lifetimes of these molecular ions are a stringent test of the potential curves and the process via which they decay.

During the last few years we have conducted experiments in which experimental evidence for the existence of long lived $NeAr^{2+}$ and $HeNe^{2+}$ doubly charged rare gas dimmers has been presented.[1,2] Furthermore, we have measured the mean lifetimes of these molecular ions directly by measuring the number of molecular ions as a function of the distance from the target cell where they were formed, as shown in the figure for $NeAr^{2+}$ ions.

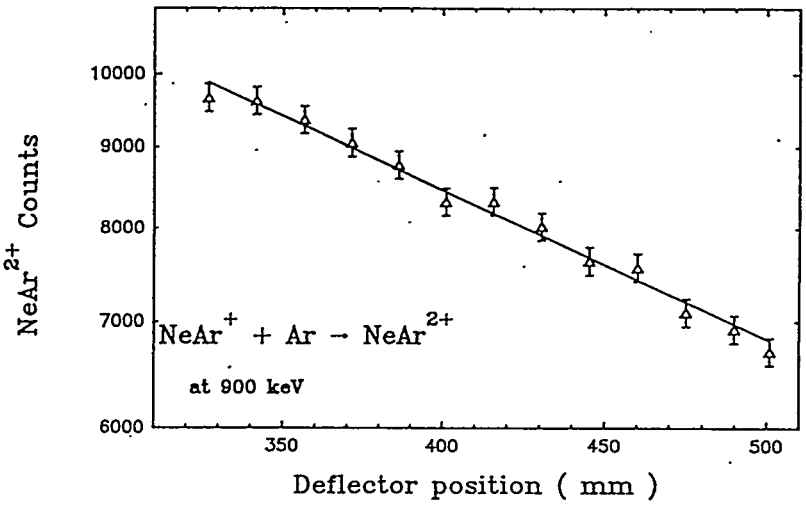

Figure 5.6.7.1. The number of $NeAr^{2+}$ ions as a function of the distance between the exits of the target cell and the electrostatic deflector.

Methods for such measurements have been developed and reported.[3] These molecular ions were formed in collisions of 900 keV singly charged molecular ions with Ar gas. These experiments have been performed in the Van de Graaff accelerator at the Technion, Israel, in which such molecular ions can be produced and accelerated (in contrast to the Tandem Van de Graaff accelerator in our laboratory).

A short while after the discovery of the $NeAr^{2+}$, Koch, Frenking and Gobbi calculated its electronic ground state, which is metastable and decays by tunneling through the potential barrier.[4] We have developed the phase shift method so that it can be applied for such narrow resonances as the ones expected for the highly excited vibrational states of the calculated $NeAr^{2+}$ potential ($\Gamma \sim 10^{-10}$ a.u.). The calculated mean lifetimes show that the $v=12$ vibrational state is populated in the charge stripping collision forming this dication. Even though the calculation is still not in perfect agreement with the measurement one can exclude the other states because the mean lifetimes change by about 3 orders of magnitude from one state to the other. The calculated mean lifetime is about 3 times smaller than the measured one which indicates that the $^1\Sigma^+$ potential of this 26 electron system has been calculated to a precision of a few meV. It is hard to expect significantly better calculations because of the large number of electrons involved. These calculations were published recently in Phys. Rev. A, 49, 3472 (1994).[5]

The long lived $HeNe^{2+}$ molecular ion remains somewhat of a mystery with regard to the electronic state which has been detected. Since its discovery Heinemann and Koch[6] have performed elaborate multi-reference configuration

interaction calculations of the electronic ground state and the lowest excited electronic states of each symmetry. Even though the ground state is predicted to sustain one vibrational state, in contrast to none in previous calculations,[7] this state has a mean lifetime of 11 psec which is too short to be detected in the experiment. A couple of excited bound states, $B^1\Delta$ and $c^3\Sigma^-$, which decay by dipole transitions to the repulsive states below ($B^1\Delta \rightarrow A^1\Pi$ and $c^3\Sigma^- \rightarrow a^3\Pi$, have also been calculated. Mean lifetime calculations for these states are underway. Preliminary results, however, indicate that these states have mean lifetimes of the order of a few μsec, much longer than the measured 180 nsec. The effort to resolve this mystery will continue and we are also planning to repeat the measurement using the $^3He^{20}Ne$ isotope, which will enable us to use a different experimental method.

Using experimental methods similar to those used in the $NeAr^{2+}$ and $HeNe^{2+}$ measurements,[1,2] we have recently measured the mean lifetime of $^3He^4He^{2+}$. This metastable molecular ion decays by tunneling through the potential barrier, and its theoretically predicted mean lifetime[8-10] for the v=2 state, which is about 16 nsec, is within the range of mean lifetimes that we can measure. On the other hand, the v=3 state will dissociate too rapidly to be detected and the lower vibrational states will not dissociate within the flight time through the apparatus. (These states have been reported to have mean lifetimes longer than a few μsec, by Belkacem *et al.*[11])

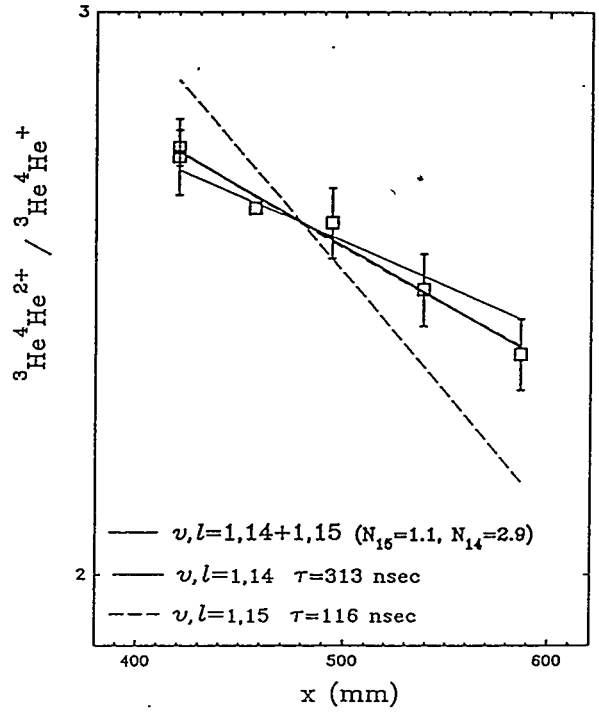

Figure 5.6.7.2.

Surprisingly, the reduction of the $^3He^4He^{2+}$ molecular ions as a function of distance traveled suggests a mean lifetime of about 200 nsec. Using the phase shift method to calculate the decay rate by tunneling of this molecular ion we have shown that a distribution of highly excited rotational states, peaked around $\ell = 14$, is in agreement with the measurement, as shown in Fig. 5.6.7.2. It is suggested that this population of rotational states is a result of the mechanism for $^3He^4He^+$ formation in the rf ion source.[12] This project has been presented in the DAMOP 1994 meeting.

While performing the mean lifetime calculations for many v,ℓ states, we have established that they scale as $e^{-\alpha\ell(\ell+1)}$ for a fixed v, as can be seen from the figure. This simple scaling was explained using a simple parabolic potential barrier. A brief report presenting this scaling law will be submitted to Phys. Rev. A, shortly. For this two electron system one hopes that the potential curves will be better known than for the many electron systems, and that further mean lifetime measurements will help determine which of the calculated potential curves is closer to the *exact* one.

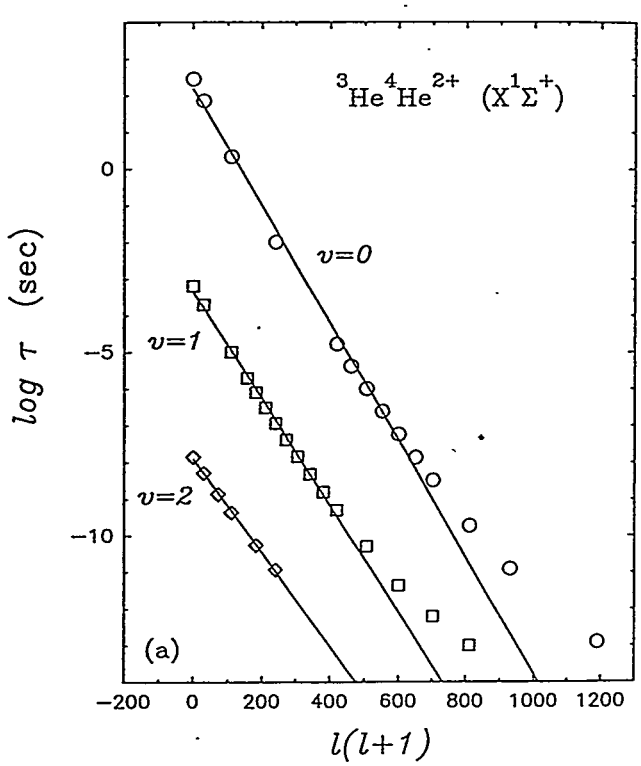

Figure 5.6.7.3.

The HeH^{2+} three body system is bound in the first excited $2p\sigma$ state and decays via an electronic transition to the $1s\sigma$ repulsive ground state. This theoretical prediction was first published by Bates and Carson[13] and the mean lifetime of this molecular ion can be estimated to be about 1 nsec using the dipole transition rates calculated by Arthurs *et al.*[14] We have recently reported the first experimental observation of this

molecular ion which has eluded experimentalists for decades, in Phys. Rev. Lett. 71, 1347 (1993).[15] A novel method was developed for the measurement which is based on the detection of both the H^+ and He^+ fragments in coincidence and the use of a very small magnetic analyzer, shown schematically below. The H^+ + He^+ coincidences have a clear peak at the expected deflection angle as can be seen from the figure.

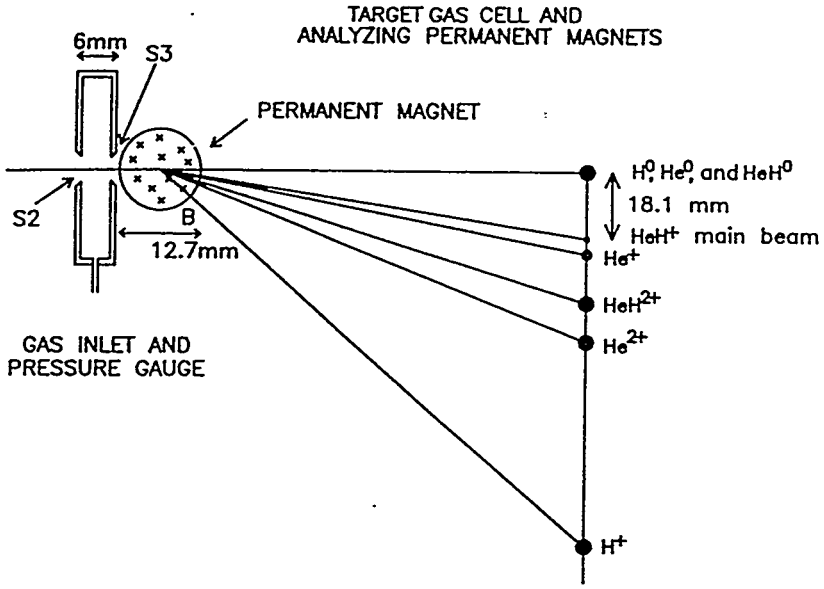

Figure 5.6.7.4. Experimental setup and schematic trajectories of the different ions after the analyzing magnet.

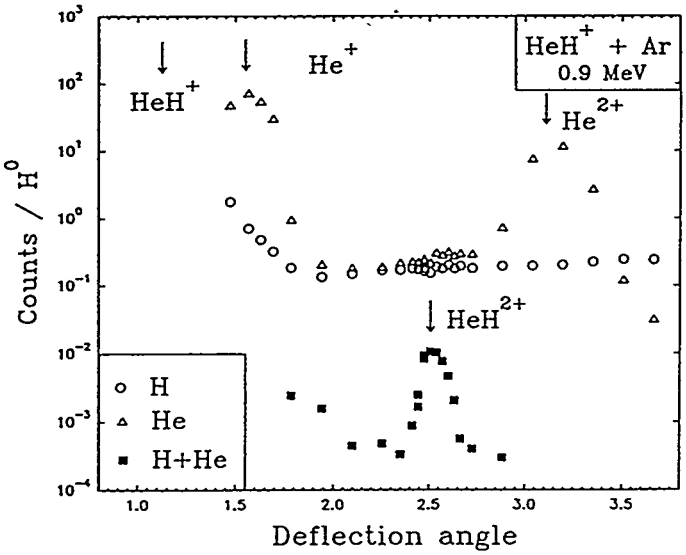

Figure 5.6.7.5. Normalized number of counts of hydrogen ions, helium ions, and H^+ + He^+ coincidence events as a function of the deflection angle. The deflection angle of the main HeH^+ beam is marked for reference.

Measurements of the mean lifetime of HeH^{2+} have been conducted and they compare well with our calculations of the electronic transition rates from the bound $2p\sigma$ state to the $1s\sigma$ repulsive ground state. Surprisingly the calculated mean lifetimes depend strongly on the vibrational state, especially for the highly excited states, as can be seen from Fig. 5.6.7.6 below.

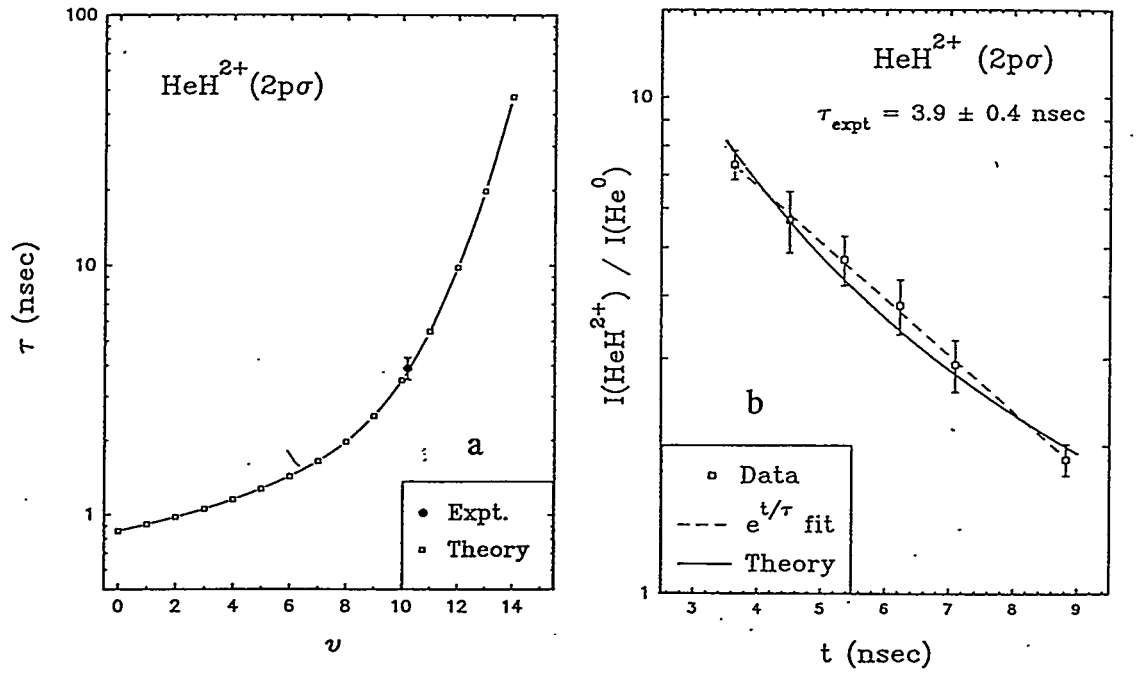

Figure 5.6.7.6. (a) The mean lifetimes of the different vibrational states of $HeH^{2+}(2p\sigma)$. (b) The ratio of HeH^{2+} to He^0 as a function of the flight time from the target cell to the magnet exit. The solid line is the model calculation for an effective temperature of 1530 K in the ion source. The dashed line is a single exponential decay fit to the data with τ_{expt}=3.9±0.4 nsec.

The measured number of HeH^{2+} molecular ions, shown in the figure above, decreases with increasing flight time but not as a single exponential decay. This dependence is well described by a population of vibrational states created in the charge stripping collisions from a HeH^+ beam with a Boltzman distribution of vibrational states at an effective temperature of about 1500 K. These mean lifetime measurements and calculations have been presented as an invited talk in the "hot topics" session of the ISIAC 1994 meeting, and have recently been published in Phys. Rev. A 49, 1774 (1994).[16] Similar mean lifetime measurements have just been completed, using an improved experimental setup (a wider range of distances between the target cell and the small magnet), for 3 isotopes of this molecular ion, namely, $^4HeH^{2+}$, $^4HeD^{2+}$, and $^3HeD^{2+}$. The differences between the decay curves of the different isotopes is very small and further calculations are needed in order

to understand this similarity. Professor B. Rosner from the Technion has been invited to give a talk about this mean lifetime measurement of the short-lived HeH^{2+} at the Denton 1994 meeting, and a paper for publication in Phys. Rev. A is in preparation.

Reference for Section 5.6.7

1. I. Ben-Itzhak, I. Gertner, and B. Rosner, Phys. Rev. A 47, 289 (1993).
2. I. Ben-Itzhak, I. Gertner, O. Heber, and B. Rosner, Chem. Phys. Lett. 212, 467 (1993).
3. I. Gertner, B. Rosner, and I. Ben-Itzhak, accepted for publication in Nucl. Instrum. and Meth. B (1994).
4. W. Koch, G. Frenking, and A. Gobbi, Chem. Phys. Lett. 203, 212 (1993).
5. Z. Chen, I. Ben-Itzhak, C.D. Lin, W. Koch, G. Frenking, I. Gertner, and B. Rosner, Phys. Rev. A 49, 3472 (1994).
6. C. Heinemann and W. Koch, private communication.
7. M.C.B. Montabonel, R. Cimiraglia, and M. Persico, J. Phys. B 17, 1931 (1984).
8. J.F. Babb and M.L. Du, Chem. Phys. Lett. 167, 273 (1990).
9. J. Ackermann and H. Hogreve, J. Phys. B 25, 4069 (1992).
10. C.A. Nicolaides, Chem. Phys. Lett. 161, 547 (1989).
11. A. Belkacem, E.P. Kanter, R.E. Mitchell, Z. Vager, and B.J. Zabransky, Phys. Rev. Lett. 63, 2555 (1989).
12. I. Ben-Itzhak, Z. Chen, I. Gertner, O. Heber, C.D. Lin, B. Rosner, and D. Zajfman, to be submitted to Phys. Rev. A (1994).
13. D.R. Bates and T.R. Carson, Proc. R. Soc. London, Ser A 234, 207 (1956).
14. A.M. Arthurs, R.A.B. Bond, and J. Hyslop, Proc. R. Soc. London, Ser A 70, 617 (1957).
15. I. Ben-Itzhak, I. Gertner, O. Heber, and B. Rosner, Phys. Rev. Lett. 71, 1347 (1993).
16. I. Ben-Itzhak, Z. Chen, I. Gertner, O. Heber, C.D. Lin, and B. Rosner, Phys. Rev. A 49, 1774 (1994).

5.7 Ion-Atom Collision Theory

5.7.1 One- and Two-Electron Processes in Ion-Atom Collisions

C.D. Lin

In the last three years we have carried out a number of theoretical studies in an effort to understand the mechanism of several ion-atom collision systems that have been measured at the JRM laboratory or elsewhere. In particular, we have employed the close-coupling method where the time dependent electronic wave function is expanded in terms of travelling atomic orbitals in the two collision centers to study both the excitation, electron capture and ionization processes. Together with the independent electron model we also examined the two-electron processes such as transfer ionization, and in particular, double electron capture processes. For the latter, the process populate doubly excited states which often decay by autoionization and the resulting electronic spectra were measured.

We have carried out theoretical studies to predict the ejected electron spectra from the double electron capture processes (see Publication nos. #24, #25, #53 and #70). Such calculations require the knowledge of electron capture amplitude to each individual doubly excited state, the Auger yield of each state and the inclusion of post-collision effect. The two-electron capture amplitudes are determined using the independent electron approximation and each doubly excited state wave function is expressed as configuration interaction of two-electron orbitals. The calculated electron spectra are found to be in quite good agreement with experimental data.

Experimentalists have also measured the double electron capture processes by multiply charged ions. There a large number of doubly excited states are populated. The stabilization of these states, especially when the principal quantum numbers of the two electrons are both large, can favor the Auger emission or the photon radiation, depending on the nature of the specific doubly excited states. Since the number of doubly excited states is large when both principal quantum numbers are large, it is necessarily to examine the fluorescence yield of a large number of states. This was carried out and the results are given in Publication #54.

The excitation process in collisions between He^{++} on H to the n=2 and n=3 states of H are of interest in the study of high-temperature plasmas. We have made a careful study of such processes and the results were presented in Publication #23.

5.7.2 Electron Capture from Oriented or Aligned Excited States

C.D. Lin

We have examined the dependence of electron capture cross sections and/or probabilities on the unisotropy of the initial target state in ion-atom collisions. In conjunction with earlier experiments where the unisotropy was determined only for the final states (see Publication #26), we have also investigated the validity of the classical trajectory Monte Carlo approximation for the orientation and alignment parameters and found that the latter are not reliable in general (Publication see #32).

We have since extended the investigation to study the dependence of electron capture probabilities on the magnetic quantum numbers of the initial target states, focussing on identifying propensity rules that are characteristic of all the collision systems. Initially the calculations were carried out for simple systems where there were no experimental data (see Publication #73). There it was established that there are no general propensity rule if the quantization axis of the magnetic substates is defined with respect to the direction of the incident beam. On the other hand, if the quantization axis is defined with respect to the direction perpendicular to the scattering plane, then there is a strong propensity rule where the negative m susbstates are predominantly populated. This propensity rule has been used to study the dependence of electron capture cross sections from the oriented circular states and elliptic states. These studies are used to interpret the experimental results on such collisions involving circular and elliptic Rydberg states.* Reports from these newer studies are now in preprint form. (See manuscripts to be published #6 and #7.)

In connection with experimental studies of collisions with laser-excited target atoms, we have also examined the dependence of electron capture cross sections on the magnetic quantum numbers of the target atom in the collision of K^+ ions with Na in 4d states. (See Publication #4.) The results are used to interpret and analyze the experiments of Campbell *et al.* (Z. Phys. D16, 21 (1990)).

5.7.3 Calculations of Mean Lifetimes of Molecular Ions

C.D. Lin

In connection with the experimental studies of the lifetimes of doubly charged molecular ions, we have carried out theoretical calculations of the lifetimes of the molecular ions in different rotational and vibrational states. New numerical techniques have to be developed in order to obtain accurate lifetimes which depend very sensitively on the molecular potential curves. The results of such studies are given in Publications #86 and #89.

5.8 Ion-Surface Interactions

5.8.1 Electron Capture from C_{60} by Slow Multiply Charged Ions

C.L. Cocke
(in collaboration with E. Salzborn and R. Völpel,
Justus Liebig Universität, Giessen, Germany)

We have measured electron capture from C_{60} by 80 keV Ar^{8+} projectiles. Two experiments have been carried out:

1. At the University of Giessen, the experiment consisted in crossing a jet of C_{60} with the multi-charged ion beam and measuring in coincidence the charge-state-analyzed projectile and the time of flight of the C_{60} ion or ion fragment. The latter gives the charge-to-mass ratio of the fragment. The two-dimensional spectrum so obtained is shown in Fig. 5.8.1.1. We identify two collision mechanisms or regions: For large impact parameters, the projectile removes electrons gently from the C_{60} cage, leaving the cage intact but charged. The C_{60} ion, which we observe to lose up to 6 electrons, is then seen in coincidence with an Ar^{7+} or 6+ projectile, since, as discussed for the Ar^{q+} on Ar system, the projectile typically loses all but one or two of its captured electrons by autoionization. For small impact parameters, the projectile destroys the C_{60} cage, signalled by the appearance of many C^{+}, C^{2+}, etc. fragments, and exists as Ar^{1+} or Ar^{2+}, as it would had it passed through a thin graphite foil.
2. In order to place these data on an absolute cross section scale, at KSU we constructed a small C_{60} gas cell and measured the absolute cross sections for projectile capture by Ar^{8+} on C_{60}, using published vapor pressure curves for the C_{60}. These cross sections were then compared to expectations from a modified classical barrier model for capture from a spherical conductor with known work function. (The ionization potentials for C_{60} can be closely described as due to a work function near that of graphite plus a contribution due to the Coulomb attraction of the removed electron by the residual ion. See Ref. 1 for an early discussion.) Agreement between experiment and prediction is sufficiently good that we feel confident that our qualitative interpretation of the soft collision mechanism is correct. The total cross section for the hard collision component is a factor of two larger than the geometrical size of the C_{60} cage, suggesting that a substantial part, of the catastrophic destruction of the cage begins before the projectile actually touches the cage. This work is published as Publication #85.

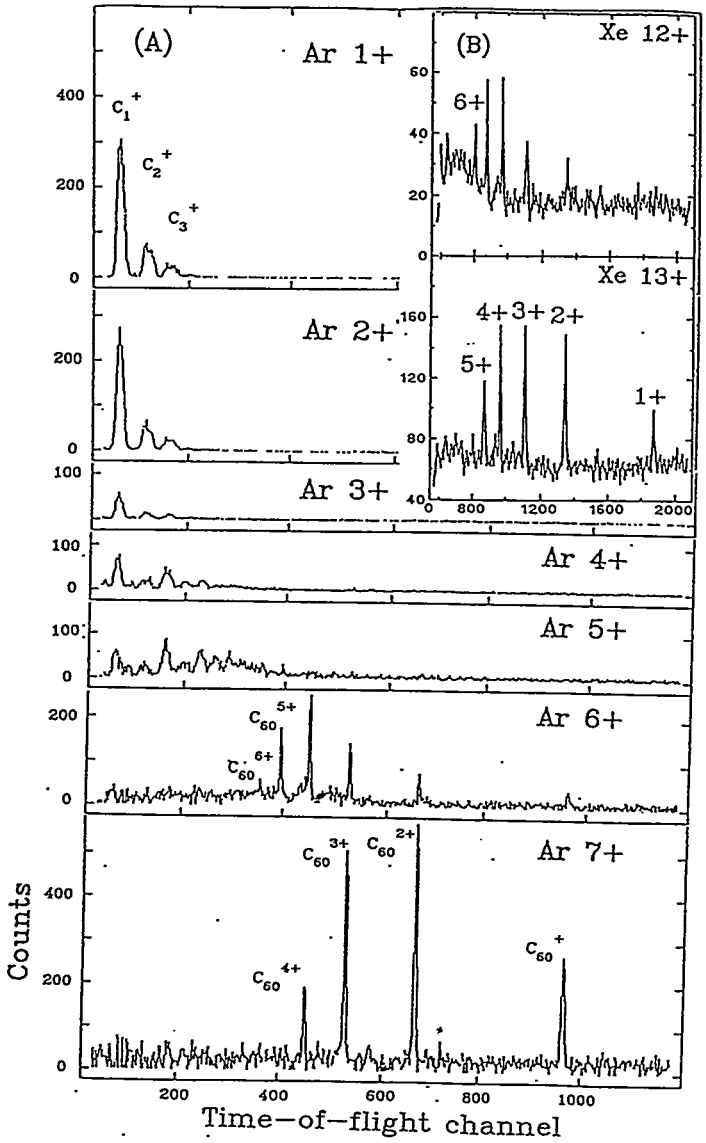

Figure 5.8.1.1. (A) Time-of-flight (charge-to-mass) spectra of C_{60} and fragment ions produced by Ar^{8+} ions on C_{60}. The spectra are labelled according to the final charge state of the Ar projectile downstream. (B) Similar spectra for Xe^{14+} on C_{60}, showing evidence for C_{60}^{6+}.

Reference for Section 5.8.1

1. F.T. Smith, J. Chem. Phys. 34, 793 (1961).

5.8.2 Experimental Compton Profile of C_{60}

B.D. DePaola and P. Richard

C_{60} can be thought of as a curved surface material as discussed in the accompanying proposal. For this reason we include this experiment in the section on ion-surface interactions.

We used the novel method of binary encounter electron spectroscopy to measure the Compton profile of C_{60} clusters. Through the many investigations done over the past several years by several different research groups, it is well understood that the shape of the binary encounter electron (BEe) peak simply reflects the Compton profile of the target. For the first time this fact was exploited to determine the unknown Compton profile a target, in this case C_{60}.

Buckminster Fullerenes represent a new class of clusters which has received a tremendous amount of attention since their recent discovery. A great deal of speculation on the properties of C_{60} is based on an assumed form of the electronic wavefunctions of this cluster. In order to provide a test for these assumed wave functions, we measured the Compton profile of C_{60} and compared it to wave functions made available to us by collaborators. The Compton profile generated from the theoretical wave functions matched the experimental one beautifully. The results, both theoretical and experimental have been submitted to Physical Review Letters. It should be noted that this represents a very general technique for the experimental determination of the Compton profile of a substance. It is particularly useful for vapor targets since conventional Compton scattering, with its low count rates is extremely time consuming, while BEe production is very quick. See Submitted for Publication #1.

---

6. JRM Laboratory Operations

6.1 Tandem Van de Graaff Accelerator

Tom J. Gray

The EN tandem Van de Graaff accelerator continues to operate reliably up to 6.5 MV. Both ion sources have required only standard maintenance. The tandem did have a charging belt failure with 9,231 hours on the belt. A new belt was installed at 77,008 hours and a set of new column resistors was installed between three planes on the high energy column to evaluate their performance. These column resistors are of the University of Washington design with 400 MΩ EBG resistors. They have performed well over greater than 1,000 hours of operation. An upgrade of all column resistors is planned for the fall of 1994 with the system developed by Oak Ridge National Laboratory for their EN tandem being the design of choice due to a combination of the running experience at ORNL and fabrication cost considerations for the shielded resistor mounting system.

Modifications of the terminal stripping box were made to allow for the installation of an additional 256 position stripping foil terminal beam stripper. This stripper is on order with delivery and installation scheduled for fall, 1994. Studies of the use of gridded carbon stripping foils have been made. The failure of unsupported carbon stripping foils represents a major limitation on available experimental beam time. We use 5μg unsupported carbon foils in the foil stripper. The unsupported foils have an average life time of order 1½ hour maximum for ~10μA of 6 MeV Si^- beam. Limited studies to date show that the gridded foils have a life time of 1½ times that for the unsupported foils. The real benefit of the gridded foils is found, however, in the fact that when the foil fails, only the foil under the beam spot is damaged, therefore leaving the undamaged portion useable for beam stripping. The design of the foil holder has been changed so that the portion exposed to the beam is all grid, thus giving two to three useable portions per gridded foil in lieu of the one useable portion per ungridded foil. Tests with the new totally gridded stripping foil system are under way. We expect to increase the effective stripping foil useability by a factor of three to four over the present ungridded foil system, thus converting the current 60 position foil stripper to an effective ~230 position stripper and the new additional 256 position NEC foil stripper to an effective 700 position foil stripper. These improvements will greatly reduce down time for foil replacement and thereby vastly improve research beam time availability.

This represents a major improvement in system efficiency and reliability.

6.2 Superconducting LINAC

T.J. Gray

The superconducting LINAC has been providing beams of C, O, F, Si, and Cℓ with an effective gradient of up to 4.5 MV. We have had problems with one high ß resonator which was sent back to Argonne National Laboratory for inspection and repair. That resonator had a perforated weld on the mounting base for the drift tube arms. It is currently being repaired. The failure of one fast energy control unit has negated an additional resonator and one other resonator has continued to be plagued with high rf leakage problems. A rework of the rf drive power coax cables is planned for the next shut down which is scheduled for October, 1994. Recurrent problems with joints in the rf drive cables will be eliminated during this rework by redoing the cables to eliminate cold joints.

During the last shut down of the LINAC, all resonators were washed in place and realigned. Beam transmission was improved with 100% of the injected beam now transmitted through the LINAC. Beam steering by the superconducting solenoids was eliminated.

6.3 Cryogenics

T.J. Gray

The LHe system has performed very well with no major problems. We had been plagued with connecting rod failures on the warm expansion engine on the LHe cold box. Realignment of the crankshaft mounting blocks to correct an error occurring at the manufacturing level and the use of a harder aluminum alloy for the connecting rod has solved this problem. The LHe plant continues to provide LHe refrigeration ample to meet all needs without LN_2 precool operation. We provide LHe for the operation of CRYEBIS also. We have installed a He warm gas recovery

system for CRYEBIS thus allowing essentially 100% recovery of He used by that device. The He losses under normal operation have been reduced to of order 10 ℓ/week. Power failures continue to be the major source of large He losses with a typical power failure costing between 100 to 300 ℓ of LHe.

4. System upgrades

We are beginning a series of major system upgrades on the LINAC, tandem Van de Graaff, and CRYEBIS. These upgrades include:

a. Building a new compressor enclosure for the large Sullaire compressor for the LHe system and moving the compressor off of the laboratory roof to eliminate noise and vibration problems.
b. Installing an additional 900 KVA power substation to provide power for the compressor and future expansion plans as well as solving present electrical power problems associated with the age of the original power system and laboratory growth.
c. Upgrading the tandem Van de Graaff with modern column resistors for more reliable high voltage operation up to 7.5 MV.
d. Adding terminal foil stripping capacity for improved efficiency.
e. Upgrading the rf control electronics on the LINAC to provide for auto barrier burn through on the resonators and more user friendly control.
f. Upgrading the LINAC cryostat turbo pumps to provide for higher system reliability and lower maintenance costs.

These projects are currently in progress at various stages of either planning and design, component procurement, or implementation. The LINAC and Van de Graaff projects are planned for completion by late spring, 1995.

6.4 CRYEBIS

M.P. Stockli and C.L. Cocke

The productivity of the KSU CRYEBIS facility increased substantially with the addition of the beam line system, which was installed late in 1990, and the resulting

increase in the number of users. During the three year period covered in this report, the source was used for atomic physics experiments 791 days which is over 70% of all available time. A total of 86 beam times were awarded with an average length of 9 days, requested by 6 outside and 11 KSU users for 28 different experiments. The experiments used 8 different species of ions with masses between 1 and 136, and charge states between 1+ and 45+, and with energies between 1 and 160 keV per charge. Fifteen refereed papers (see Publication nos. 1, 10, 13, 36, 37, 43, 55, 56, 57, 58, 68, 76, 78, 90, O.C.R. #2) were published in this report period describing the results of those atomic physics experiments performed with ions from the KSU CRYEBIS, which is a 600% increase of the yearly publication rate over the previous reporting period. Four refereed papers (see Publication nos. 5, 11, 17, 42), a 53% decrease, were published in this report period, describing the KSU CRYEBIS facility or related topics.

The increase in productivity is in part due to the continuous analysis of the difficulties encountered with our CRYEBIS operation, the ion beam transport, and the ongoing experiments. The continuous analysis allows us to frequently identify the weakest links in our system and to focus our scarce resources on the improvements of those most important problems. For example, the broad range of ion masses, charge states and energy per charge is very demanding for any ion transport system, and many changes have been implemented to simplify the control system, as well as to improve the resolution and stability of the ion optical transport elements, especially the analyzing and switching magnets. Those two magnets are the most important elements and therefore were upgraded in December 1991 and January 1992 with specially fitted hall probes which provide accurate, high resolution measurements of the central magnetic field. Those accurate measurements allow for reliable identification of all ion beams if the beam energy per charge and the analyzing magnet constant are calibrated with common, easy identifiable ion beams from residual gases. A computer program was implemented in September 1992 which lists, after proper calibration, the exact magnetic field values required for all ion beams of interest as well as of all undesired residual gas ion beams and therefore greatly facilitates the ion beam analysis.

Another reason for the increased productivity is the ion beam diagnostics which has been improved in many small, but manageable and affordable steps. The most important step was the addition of a current preamplifier and a digital storage oscilloscope in early 1992 which display the instantaneous and the time-averaged currents of the pulsed, low-energy, highly-charged ion beams during the tuning process. The addition of a ramp generator in 1993 automated the calibrated recording of charge state distributions which greatly enhanced the reliability of the

ion beam identification. A simple, $167 modular ramp generator replaced a sophisticated computer based system which was previously used to measure charge state distributions, but which was not able to record absolute ion currents and accurate magnetic field values and hence did not always allow for a reliable identification of all ion beams. The simplified and improved diagnostics greatly accelerated the tuning of the low intensity highest charge states. For example, it took approximately 5 days in 1992 to tune Ar^{17+} or Xe^{44+} and to focus it into a collision chamber, whereas the same task has been accomplished several times in 1994 in 1 or 2 days.

The low-energy, highly-charged ion beams are very sensitive to magnetic and electric fields as well as to the residual gas pressure which were indeed the guiding reasons in the design of our compact UHV (ultra high vacuum) ion transport system. The transport system brings the ions in a residual gas pressure of less than 10^{-8} Torr as close as 2-5 cm in front of the interaction region. Several differentially pumped target systems have been developed which use compactness to minimize the charge exchange with residual gas and hence allow for the convenience of O-ring sealed target chambers. The CRYEBIS is partially protected by interlocked gate valves, which cannot be opened or close whenever the beam line pressure exceeds $5*10^{-7}$ Torr.

The personnel safety precautions have improved substantially, especially with respect to the high voltages required for the operation of the source. Improved, calibrated metering eliminated the need for measuring high voltages with hand-held probes, and therefore allows us to shield all high voltage connections during normal operations. The electric control circuit for the electron beam has been modified to improve the safety of the electron gun, which now is and remains deactivated after failures through an interlock with an ionization gauge. Many other changes aimed at an improved voltage stability or at an extension of the voltage limits which allowed us to push the upper limit of the electron beam ionization power from 5.4 kV in 1991 to 9.5 kV in 1994. This is sufficient to ionize the L-shell of Xe, and we produced 0.2pA of Xe^{46+} and supplied an experiment with 2 pA of Xe^{45+}.

The highest charge states require a very careful adjustment of the seed gas flow in the range of 10^{-9} cc/s, which can be accomplished with a manual ultra-fine control UHV leak-valve as long as the gas is dry. Sometimes this flow needs to be stable over long time periods and therefore a stable valve inlet pressure is required. Expensive, isotopically enriched seed gases are often favored to obtain the desired high purity ion beams. During the last 3 years we have implemented a seed gas supply system based on ultra high purity components and techniques which minimizes contamination and losses of those gases. A positive seal regulator minimizes creep

and droop of the reduced pressure in the manifold for standard gases (Ar, He, H). An absolute pressure regulator minimizes the loss of expensive isotopically enriched gases by regulating a pressure below atmosphere in the manifold for low pressure gases ($^{13}CH_4$, $^{15}N_2$, $^{18}O_2$, ^{22}Ne, ^{86}Kr). A manifold without regulator is used for the 99% enriched ^{136}Xe which is stored below atmospheric pressure. The consumption of this very expensive gas ($30/cc STP) is minimized by immersing its storage bottle in liquid nitrogen to recover all gas from the manifold before changing the seed gas. A negligible consumption and level of contamination has been reached for all seed gases.

The operational costs for cryogens have been essentially eliminated over the last three years by recovering 97% of the evaporated He gas (up from 70% in 1991) and reliquefying it with the inhouse liquefier. The cryogenic procedures, and the cryogenic personnel and equipment safety precautions have been upgraded several times and have reached a level near perfection. For example, a revised cool down procedure condenses most of the residual gas on the cryoshields and correspondingly less on the drift tubes, which substantially shortened the electron beam conditioning required for the production of the highest charge states. Most cryogenic procedures are described in a concise operation manual, which is important as some of the tasks are executed very infrequently. The manual allows students to provide most cryogenic services after an initial training period of a few weeks.

The most serious problems encountered in the three year period were the failures which incapacitated the CRYEBIS during 16% of the total time. The leading reason was high voltage power supplies and amplifiers which failed 14 times, followed by low voltage supplies, which failed 7 times. The aging cryogenerator failed 5 times with accelerating frequency before the compressor and later the cold head were replaced with new units. An additional 7 failures were caused by pushing the operational conditions too close to the limits of the present design, mainly the high voltages on the drift tubes, the electron gun and the high voltage platform. In addition there were numerous failures of various meters, often caused by transients during high voltage discharges. Insufficient manpower forced us initially to limit the repairs to the most essential equipment, which reduced the instrumentation to a level where the operation became very difficult. The recent addition of a full time engineering position to the CRYEBIS staff has reversed this difficult situation, and the hiring of Paul E. Gibson, a former undergraduate research assistant, brought great relief. In addition we have addressed the question of the high voltage supplies and amplifiers which are responsible for the largest fraction of down time, although the number of failures is not excessive if one considers the number of units which are in operation 24 hours a day, 7 days a week. We have identified and started to

implement other modular, low-cost high-voltage supplies which seem to have the desired higher reliability. In addition we have modularized the high voltage units and many of the remote controls and improved some of the instrumentation to simplify the diagnostics of failures and to speed up the replacement of faulty units. Our resources do not allow for shelved spare units and therefore we often replace inoperable units with units which are useful but not vital for the operation. This method permits us to resume operation in a very short time with experiments which do not require the ultimate performance.

The most astounding fact of this report period is that the bulk of the operation and maintenance have been provided by, and the bulk of developments have been accomplished by our enthusiastic and dedicated students, namely S. Lampenscherf, R. Mack, L. Rebohle, N. Renard, J. Werick, and foremost R. Ali, W. Wu, and S. Winecki.

6.5 Data Acquisition and Analysis Systems

K.D. Carnes

The data acquisition computer system in the laboratory has now been in operation for over six years. Its power, flexibility, and built-in redundancy have confirmed our initial configuration choices. Over the years, faculty and students alike have become proficient in operating the system with little or no guidance. The system consists of three identical DEC MicroVAX II minicomputers, linked via DECNET, each with its own 19" monitor, system disk, program disk, 205 MB removable user disk, 9-track tape drive, and DEC LN03Plus laser printer. Each computer also has its own MBD (Microprogrammable Branch Driver), which serves as an interface to the CAMAC electronics and as an intelligent front end to handle the real-time aspects of data acquisition. Our multiparameter acquisition and analysis software continues to be the XSYS package.

Our data analysis capabilities have improved dramatically in the past three years. Originally, data analysis was performed on a VAX 8250 or on an idle MicroVAX II. As activity at the lab increased, this became an unacceptable bottleneck. In 1992, with funds from a special instrument grant, we were able to purchase four DEC VAXStation 4000 workstations, one Model 60 and three VLC's. The workstations are configured as a Local Area VAXCluster. The Model 60 is the

boot node and serves two 1 GB disks for user file storage. Each machine has its own 5 GB 8mm tape drive for analysis of list mode data and for backups. The VLC's have roughly 6 times the processing speed of a MicroVAX II and over three times the speed of the 8250. In addition, they use DEC's version of X windows, which makes the display of graphics data, such as spectra, much more convenient All of the VAXStations are connected to the campus network via the TCP/IP protocol. This is essential for data transfer, given the fact that our departmental computing environment now consists of networked VAXStations, Sun workstations, and PC's. The 8250, which was once our only data analysis system, has been relegated to the role of a data transfer computer. Since it is the only machine that provides access to all three types of storage media used in the lab (removable disk, 9 track and 8mm tape), it is used primarily for copying files from a removable disk over the network to the newer analysis workstations, for backing up removable disks to 8mm, and for transferring 9-track tapes to 8mm for analysis on the new workstations.

6.6 Laboratory Safety

T.N. Tipping

From a combination of the LINAC and CRYEBIS becoming operational research tools and the dynamic nature of the regulatory environment, several changes have taken place over the past three years with regard to laboratory safety.

Progress in the operation of the LINAC and CRYEBIS has made new radiation monitoring needs appear. Two additional area radiation monitors have been installed on a portable "beam dump" for monitoring the LINAC experimental area. This beam dump was constructed in-house and may be positioned at the end of any of the LINAC beam lines. The dump will attenuate neutron radiation from the final beam stop by more than a factor of 100. Correct positioning of the dump on a beam line is assured by connection of the monitors to the LINAC radiation interlock system. The interlock system will not allow the beam to enter an experimental beam line unless the dump and its associated area monitors are properly positioned and operational. Two area radiation monitors were also installed in the CRYEBIS experimental area. These monitors are connected to the radiation interlock system to provide personnel protection in the CRYEBIS experimental area.

In addition to the new monitors, the radiation interlock system in the LINAC

and CRYEBIS areas has had several new access gates added. These gates are interlocked such that the beam will be stopped before entering the LINAC if the radiation level in one of the LINAC areas or the CRYEBIS experimental area (downstream from the LINAC experimental area) is above a preset value and an access gate to that area is opened. These additional gates have required that a new interlock status panel be designed and constructed.

Illuminated "CAUTION-BEAM ON" warning signs are located at the new LINAC access gates. These signs are on when the beam is directed into the LINAC. To maintain consistency and facilitate understanding of the warning signs, the access gate warning signs in the tandem facility were changed from simply "RADIATION" to the same wording as the LINAC signs. Also, almost every alarm and warning light in the laboratory had a sign installed next to it which explains what the device indicates and the appropriate action to take when the device is activated.

With the first beam on target from the LINAC, we found that the LINAC had become a useful tool for research and the radiation produced was well within the design parameters of our shielded beam dump and interlock system. Even with this demonstration of relative safety from the LINAC, we decided to erect a concrete block shielding wall to separate the LINAC target area from the CRYEBIS area. This required the addition of another access gate and interlock to our expandable interlock status panel.

The construction of an Electron Cyclotron Resonance (ECR) ion source has brought about additional safety needs. The ECR operates at high voltage and produces large quantities of x-rays. A shield was designed to act as both a radiation shield and an enclosure for the high voltage platform of the source. This shield is installed and will be interlocked with source power supplies before the source becomes fully operational. An additional area radiation monitor has been installed in the ECR area and it will also be interlocked with the source power supplies in the near future.

A unique safety issue which arose from the ECR construction was designing a cooling system for the ECR plasma chamber. Since the chamber is at high voltage, a non-conductive coolant must be used. Unfortunately, the coolant of choice produces flammable vapors at high temperatures. This required that a closed cooling system be designed to prevent contact between the flammable vapors and air. This system uses a nitrogen gas blanketed reservoir to prevent the introduction of air into the cooling system.

Due to the sabbatical leave of Prof. C.L. Cocke who served as the laboratory's radioactive material licensee, Prof. P. Richard has taken over these responsibilities. We used this transition as an opportunity to "clean house" in our radioactive source

inventory. We transferred numerous "dead" sources to our university radiation safety office for disposal. As a result, we have reduced our inventory of radioactive sources substantially.

The approximately twenty-year-old, lead-acid, wet-cell emergency light units in the tandem facility were replaced in early 1991 with modern, maintenance-free units. This eliminated two hazards. The first was the increasingly poor reliability of the old units and the second is the problem of dealing with heavy, acid filled batteries. The emergency lights in the CRYEBIS/LINAC area also became a concern. The original emergency lights are built into the fluorescent light fixtures on the ceiling. These low bid (pronounced, "CHEAP") fixtures are failing at a rapid rate. Additional emergency lights have been installed in the CRYEBIS/LINAC area to alleviate this problem.

Numerous structured training programs have also been implemented in the laboratory. We are fortunate that our university campus safety department makes available to our laboratory personnel, numerous safety workshops and seminars. The campus safety department annually presents a seminar on radiation safety in the research laboratory. In the spring of 1991, the campus safety department hosted a satellite teleconference sponsored by the American Chemical Society entitled, "Complying with the OSHA Lab Standard." Our campus safety department also presents a summer safety seminar series which covers various issues such as hazardous material spill control, confined space entry, compressed gas cylinder safety, and numerous other topics. In addition, Tracy Tipping (Laboratory Safety Officer) attended "Laboratory Safety-Principles, Practice, and Compliance" presented in Chicago by the safety consultant firm of Kaufman and Associates. In addition to training programs sponsored by our campus safety department, we offer in-house safety training which includes written safety material and safety training on topics specific to the Macdonald Laboratory.

With recent emphasis from regulatory agencies on controlling hazardous materials, we have implemented a laboratory-wide hazardous materials procurement program. Under this program, all hazardous materials are ordered, received, inventoried, and distributed by the laboratory safety officer. This program has prevented duplication of orders which has greatly reduced the amount of hazardous materials on hand in the laboratory. In some cases, less hazardous substitutes have been found for some of the materials ordered, again, reducing the amount of hazardous material in the laboratory.

In this day of increased safety and health awareness, we are continuing to review and upgrade as necessary, our ES&H programs. The State of Kansas Department of Health and Environment is preparing a new set of safety guidelines

specific to particle accelerators. These guidelines are scheduled for distribution in the near future. In the interim, we are using the DOE Safety of Accelerator Facilities order (DOE 5480.25) as a guide in preparation for our new state guidelines. The normal, scheduled testing and maintenance of the various safety systems in the J.R. Macdonald Laboratory continues with modifications as necessary due to changing regulations and laboratory operations.

7. List of JRM Publications

For grant period June 15, 1991 - June 14, 1994

1. "X Rays from Electron Bombardment of Heliumlike Argon"
   R. Ali, C. P. Bhalla, C. L. Cocke, M. Schulz, and M. Stockli
   Z. Phys. D: Atoms, Molecules and Clusters 21, S207-208 (1991).

2. "KLL Resonant Transfer Excitation to $F^{6+}(1s2\ell 2\ell')$ Intermediate States"
   D. H. Lee, P. Richard, J. M. Sanders, T.J.M. Zouros, J. L. Shinpaugh, and S. L. Varghese
   Phys. Rev. A 44, 1636 (1991).

3. "Space and Time Correlation in High Velocity Multiple Electron Transitions"
   J. H. McGuire and Jack C. Straton
   NIMS B56/57, 192 (1991).

4. "Ion Neutral Reactions: Collision Spectrometry of Multiply Charged Ions at Low Energies"
   E. Y. Kamber and C. L. Cocke
   Springer Series in Chemical Physics, Vol. 54, 91 (1991).

5. "The Status of the Electron Beam Ion Sources"
   M. P. Stockli
   Z. Phys. D: Atoms, Molecules and Clusters 21, S111-115 (1991).

6. "Strong Directional Out-of-Plane Scattering in Multiple Ionizing Highly-Charged Ion-Atom Collisions"
   A. Gonzalez, S. Hagmann, T. Quinteros, B. Krassig, R. Koch, A. Skutlartz, and H. Schmidt-Bocking
   Z. Phys. D: Atoms, Molecules and Clusters 21, S299-300 (1991).

7. "Variation of Dielectronic Satellite Intensity Factors with n for $1s\epsilon\ell$-$2\ell'n\ell''$-$1sn\ell''$ Dielectronic Recombination Processes in Selected Hydrogen-like Ions"
   K. R. Karim, C. P. Bhalla, M. Suesink, S. Biel, and M. Wilson
   J. Phys. B 24, L375 (1991).

8. "Contribution of Exchange on Charge-State Dependence of Large-Angle Electron-Ion Elastic Scattering"
   C. P. Bhalla and R. Shingal
   J. Phys. B 24, 3187 (1991).

9. "Electron Capture by O^{8+} from aligned Molecular Deuterium"
S. Cheng, C. L. Cocke, V. Frohne, E. Y. Kamber, and S. L. Varghese
Nucl. Instrum. & Methods B56/57, 78 (1991).

10. "X-Ray Emission from Slow Highly Charged Ar Ions Interacting with a Ge Surface"
M. Schulz, C. L. Cocke, S. Hagmann, M. Stockli, and H. Schmidt-Bocking
Phys. Rev. A 44, 1653 (1991).

11. "The KSU-CRYEBIS: A Unique Accelerator System for Low Energy, Highly Charged Ions"
M. P. Stockli, R. M. Ali, K. R. Buck, A. C. Canelos, C. L. Cocke, P. E. Gibson, P. E. Lammert, G. J. Lehman, C. L. Lewis, R. A. Mack, B. C. McLaren, M. D. Morrison, M. Schulz, J. M. Socolofsky, and S. D. Worm
Proceedings of Symposium of North Eastern Accelerator Personnel, October 22-25, 1991 (ed. Tracy N. Tipping and Robert D. Krause), published by World Scientific, p. 79.

12. "δ-Electron Emission in Fast, Highly-Charged Heavy Ion-Atom Collisions"
C. Kelbch, S. Hagmann, R. Koch, G. Kraft, R. E. Olson, H. Schmidt-Bocking, and J. Ullrich
Z. Phys. D 21, S301 (1991).

13. "K X-Ray Auger Emission from H-like Ar Ions Slowly Approaching a Ge Surface"
M. Schulz, C. L. Cocke, M. Stockli, S. Hagmann, and H. Schmidt-Bocking
Z. Phys. D 21, S341 (1991).

14. "Measurement of the L-Shell X-Ray Production Cross Sections of Yb and Au by Li, Be, C, N, F, and Si Bombardments"
N. B. Malhi and T. J. Gray
Phys. Rev. A 44, 7199 (1991).

15. "Electron Capture and Target Ionization in Collisions of Bare Projectile Ions Incident on Helium"
J. L. Shinpaugh, J. M. Sanders, J. M. Hall, D. H. Lee, H. Schmidt-Bocking, T. N. Tipping, T.J.M. Zouros, and P. Richard
Phys. Rev. A 45, 2922 (1992).

16. "Recent Trends in Ion Atom Collisions"
C. L. Cocke
1992 IOP Publishing Ltd, ICPEAC XVII, Brisbane, Australia (July 1991).

17. "The KSU CRYEBIS: A Unique Ion Source for Low-Energy Highly-Charged Ions"
Martin P. Stockli, R. M. Ali, C. L. Cocke, M.L.A. Raphaelian, P. Richard, and T. N. Tipping
Rev. Sci. Instrum. 63, 2822 (1992).

18. "Target Centered Coupled Channel Calculations for L_1 Subshell X Ray Production Cross Sections by Heavy Ions"
R. Shingal, N. B. Malhi and T. J. Gray
J. Phys. B: At. Mol. Opt. Phys. 25, 2055 (1992).

19. "Coincidence Time-of-Flight Studies of Molecular Fragmentation"
I. Ben-Itzhak, S. G. Ginther, and K. D. Carnes
NIMS B66, 401 (1992).

20. "Cross Sections for Resonant Transfer and Excitation in Fe^{q+} + H_2 Collisions"
M. W. Clark, J. A. Tanis, E. M. Bernstein, N. B. Badnell, R. D. Dubois, W. G. Graham, T. J. Morgan, V. L. Plano, A. S. Schlachter, and M. P. Stockli
Phys. Rev. A 45, 7846 (1992).

21. "Comparison of Explicit Calculations for n = 3-8 Dielectronic Satellites of the FeXXV Kα Resonance Line with Experimental Data from the Tokamak Fusion Test Reactor"
V. Decaux, M. Bitter, H. Hsuan, K. W. Hill, S. von Goeler, H. Park, and C. P. Bhalla
Phys. Rev. A 44, R6987 (1991).

22. "Electron-Electron Interactions in Two-Electron Phenomena in Collisions of Fast Ions with He Atoms"
J. P. Giese and J.O.P. Pedersen
Nucl. Instrum. & Methods B56/57, 176 (1991).

23. "Close-Coupling Study of Electron Excitation in 1-300 keV/u He^{2+} - H Collisions"
W. Fritsch, R. Shingal and C. D. Lin
Phys. Rev. A 44, 5686 (1991).

24. "Ejected Electron Spectra of Doubly Excited States from Double Capture in Collisions of Bare Ions with Helium Atoms"
C. D. Lin, Z. Chen, and R. Shingal
Proceedings of ICPEAC XVII, Brisbane, Australia, July 1991, p. 683.

25. "State-Selective Double Capture in Collisions of Bare Ions with Helium Atoms at Low Energies: I. Total Cross Sections"
Z. Chen, R. Shingal and C. D. Lin
J. Phys. B 24, 4215 (1991).

26. "H(n=2 and 3) Density Matrices Produced in Proton-Helium Collisions at Intermediate Energies"
R. Shingal and C. D. Lin
J. Phys. B 24, 963 (1991).

27. "Ion-Neutral Reactions: Collision Spectrometry of Multiply Charged Ions at Low Energies"
E. Y. Kamber and C. L. Cocke
Springer Series in Chemical Physics 54, 91 (1991).

28. "Multiple-Electron Excitation, Ionization, and Transfer in High-Velocity Atomic and Molecular Collisions"
J. H. McGuire
Advances in Atomic, Molecular, and Optical Physics, Vol. 29, 217 (1992), Academic Press.

29. "Delta-Electron Emission in Fast Heavy Ion-Atom Collisions: Observations of New Phenomena and Breakdown of Common Scaling Laws"
C. Kelbch, R. Koch, S. Hagmann, H. Schmidt-Bocking, C. O. Reinhold, D. R. Schultz, R. E. Olson, and G. Kraft
Z. Phys. D 22, 713 (1992).

30. "Quasi-Discretization of the Electron Continuum Emitted in Collisions of 0.6 MeV u^{-1} Au^{11+} with Noble Gases"
S. Hagmann, W. Wolff, J. L. Shinpaugh, H. E. Wolf, R. E. Olson, C. P. Bhalla, R. Shingal, C. Kelbch, R. Herrmann, O. Jagutzki, R. Dorner, R. Koch, J. Euler, U. Ramm, S. Lencinas, V. Dangendorf, M. Unverzagt, R. Mann, P. Mokler, J. Ullrich, H. Schmidt-Bocking, and C. L. Cocke
J. Phys. B 25, L287 (1992).

31. "K-Shell Ionization of O^{4+} and C^{2+} Ions in Fast Collisions with H_2 and He Gas Targets"
D. H. Lee, T.J.M. Zouros, J. M. Sanders, P. Richard, J. M. Anthony, Y. D. Wang, and J. H. McGuire
Phys. Rev. A 46, 1374 (1992).

32. "Orientation Parameters and Dipole Moments of $He^+(n=2)$ States in He^{2+} + H Collisions: Comparison of CTMC and Close-Coupling Results"
N. Toshima, R. Shingal, and C. D. Lin
J. Phys. B 25, L11 (1992).

33. "Multiple-Electron Excitation, Ionization, and Transfer in High-Velocity Atomic and Molecular Collisions"
J. H. McGuire
Advances in Atomic, Molecular, and Optical Physics Vol. 29, 217 (1992), Academic Press.

34. "Absolute Cross Sections for Helium Single and Double Ionization in Collisions with Fast, Highly Charged Projectiles"
H. Berg, J. Ullrich, E. Bernstein, M. Unverzagt, L. Spielberger, J. Euler, D. Schardt, O. Jagutzki, H. Schmidt-Bocking, R. Mann, P. H. Mokler, S. Hagmann, and P. D. Fainstein
J. Phys. B 25, 3655-3670 (1992).

35. "Dielectronic Recombination from High-Lying Resonance States in H-like Silicon, Calcium, and Iron"
K. R. Karim, M. Ruesink, and C. P. Bhalla
Phys. Rev. A 46, 3904 (1992).

36. "Q-Value Measurements in Charge-Transfer Collisions of Highly Charged Ions with Atoms by Recoil Longitudinal Momentum Spectroscopy"
R. Ali, V. Frohne, C. L. Cocke, M. Stockli, S. Cheng, and M.L.A. Raphaelian
Phys. Rev. Letters 69, 2491 (1992).

37. "Electron Ion Recombination Experiments on the KSU EBIS"
R. Ali, C. P. Bhalla, C. L. Cocke, M. Schulz, and M. Stockli
"Recombination of Atomic Ions," edited by W. G. Graham et al.
(Plenum Press, New York, 1992) p. 193-202.

38. "Angular Effects in Dielectronic Recombination and Resonance Transfer Excitation"
C. P. Bhalla
"Recombination of Atomic Ions," edited by W. G. Graham et al.
(Plenum Press, New York, 1992) p. 87-97.

39. "Discussion of Resonant Transfer and Excitation"
P. Richard
"Recombination of Atomic Ions," edited by W. G. Graham et al.
(Plenum Press, New York, 1992) p. 327-334.

40. "Double Ionization of Helium by High-Velocity U^{90+} Ions"
H. Berg, O. Jagutzki, R. Dorner, R. D. DuBois, C. Kelbch, H. Schmidt-Bocking, J. Ullrich, J. A. Tanis, A. S. Schlachter, L. Blumenfield, B. d'Etat, S. Hagmann, A. Gonzalez, and T. Quinteros
Phys. Rev. A 46, 5539 (1992).

41. "Fast Timing Signal Sorter for Multiple Hit Coincidence Time-of-Flight Spectroscopy"
I. Ben-Itzhak, K. D. Carnes, and B. D. DePaola
Rev. Sci, Instruments 63, 5780 (1992).

42. "The KSU-CRYEBIS: A Unique Ion Source for Low-Energy Highly-Charged Ions"
Martin P. Stockli, R. M. Ali, C. L. Cocke, M.L.A. Raphaelian, P. Richard, and T. N. Tipping
5th International Symposium on Electron Beam Ion Sources and Their Applications (Dubna, USSR) 1992, p. 82.

43. "Atomic Physics Experiments on the KSU EBIS"
C. L. Cocke, M. Stockli, R. Ali, M. Schulz, and C. P. Bhalla
5th International Symposium on Electron Beam Ion Sources and Their Applications (Dubna, USSR) 1992, p. 101.

44. "A Measurement of the Dielectronic Recombination of He^+ Ions"
J. R. Mowat, J. A. Tanis, R. R. Haar, J. L. Forest, T. Ellison, C. Foster, W. Jacobs, T. Rinckel, P. F. Dittner, W. G. Graham, M. W. Clark, D. E. Schneider, and M. P. Stockli, in "Recombination of Atomic Ions," edited by W. G. Graham et al. (Plenum Press, New York, 1992) p. 203.

45. "Ripple Corrections on a 6 MV Tandem Accelerator and its Influence on Nuclear Resonance Measurements"
A. D. Gonzales, J. P. Giese, and E. Horsdal
Nucl. Instrum. & Meth. B71, 224 (1992).

46. "Development of Ion-Ion Collisions at KSU"
J. P. Giese, C. Y. Chen, A. Landers, M. Stockli, P. Richard, and C. Miller
AIP Conference Proceedings, "VIth International Conference on the Physics of Highly Charged Ions," Manhattan, KS, ed. by P. Richard, M. Stockli, C. L. Cocke, and C. D. Lin
(American Institute of Physics, New York, 1993) p. 497.

47. "Fragmentation of CO Caused by Fast F^{4+} Impact"
I. Ben-Itzhak, S. G. Ginther, and K. D. Carnes
AIP Conference Proceedings, "VIth International Conference on the Physics of Highly Charged Ions," Manhattan, KS, ed. by P. Richard, M. Stockli, C. L. Cocke, and C. D. Lin
(American Institute of Physics, New York, 1993) p. 343.

48. "Interference Between RTEA and Elastically Scattered Target Electrons in 20 MeV F^{6+} + H_2 Collisions"
T.J.M. Zouros, H. I. Hidmi, J. M. Sanders, P. Richard, S. L. Varghese, M.L.A. Raphaelian, and C. P. Bhalla
AIP Conference Proceedings, "VIth International Conference on the Physics of Highly Charged Ions," Manhattan, KS, ed. by P. Richard, M. Stockli, C. L. Cocke, and C. D. Lin
(American Institute of Physics, New York, 1993) p. 331.

49. "Electron-Electron Interactions in K-Shell Excitation of F^{6+} Ions in Fast Collisions with H_2 Targets"
D. H. Lee, T.J.M. Zouros, J. M. Sanders, and P. Richard
AIP Conference Proceedings, "VIth International Conference on the Physics of Highly Charged Ions," Manhattan, KS, ed. by P. Richard, M. Stockli, C. L. Cocke, and C. D. Lin
(American Institute of Physics, New York, 1993) p. 323.

50. "Energy Shifts in the Binary Encounter Peak of 0.5 MeV/amu Cu^{q+} + H_2"
H. I. Hidmi, P. Richard, J. M. Sanders, and T.J.M. Zouros
AIP Conference Proceedings, "VIth International Conference on the Physics of Highly Charged Ions," Manhattan, KS, ed. by P. Richard, M. Stockli, C. L. Cocke, and C. D. Lin
(American Institute of Physics, New York, 1993) p. 319.

51. "Diffraction Structures in Delta Electron Spectra Emitted in Heavy-Ion Atom Collisions"
C. Liao, S. Hagmann, Ch. Bhalla, R. Shingal, H. Schmidt-Bocking, R. Mann, J. Shinpaugh, W. Wolff, and H. Wolf
AIP Conference Proceedings, "VIth International Conference on the Physics of Highly Charged Ions," Manhattan, KS, ed. by P. Richard, M. Stockli, C. L. Cocke, and C. D. Lin
(American Institute of Physics, New York, 1993) p. 281.

52. "Experimental Evidence for the Formation of the $2p\sigma$ Bound State of HeH^{2+}"
I. Ben-Itzhak, I. Gertner, and B. Rosner
AIP Conference Proceedings, "VIth International Conference on the Physics of Highly Charged Ions," Manhattan, KS, ed. by P. Richard, M. Stockli, C. L. Cocke, and C. D. Lin
(American Institute of Physics, New York, 1993) p. 214.

53. "Theoretical Studies of Double Electron Capture in Collisions of Ne^{8+} with He Atoms"
Z. Chen and C. D. Lin
AIP Conference Proceedings, "VIth International Conference on the Physics of Highly Charged Ions," Manhattan, KS, ed. by P. Richard, M. Stockli, C. L. Cocke, and C. D. Lin
(American Institute of Physics, New York, 1993) p. 34.

54. "Fluorescence Yields of High-Lying Doubly Excited States of Ar^{16+}"
Z. Chen and C. D. Lin
J. Phys. B 26, 957 (1993).

55. "One and Two Electron Processes in 0.9 keV/u to 60 keV/u Ar^{16+} + He Collisions"
W. Wu, J. P. Giese, P. Richard, M. Stockli, R. Ali, C. L. Cocke, and H. Schone, in "VIth International Conference on the Physics of Highly Charged Ions," Manhattan, KS, ed. by P. Richard, M. Stockli, C. L. Cocke, and C. D. Lin
(American Institute of Physics, New York, 1993) p. 147.

56. "Velocity Dependence of Absolute Cross Sections for Charge Capture by Ar^{7+} from Ground-State and Excited-State Sodium"
S. Maleki, M.L.A. Raphaelian, M. P. Stockli, B. P. Walch, and B. D. DePaola
Phys. Rev. A 48, 1185 (1993).

57. "Enhancement of Charge Capture from a Laser-Excited Target by Highly Charged Ions"
B. P. Walch, S. Maleki, R. Ali, M. P. Stockli, M.L.A. Raphaelian, C. L. Cocke, and B. D. DePaola
Phys. Rev. A 47, R3499 (1993).

58. "Angular Distribution in Charge-Transfer Collisions of 50 keV Ar^{15+} with Ar"
R. Ali, C. L. Cocke, M.L.A. Raphaelian and M. Stockli
J. Phys. B 26, L685 (1993).

59. "Formation and Mean Lifetime of the Metastable Doubly Charged Rare-Gas Dimer $NeAr^{2+}$"
I. Ben-Itzhak, I. Gertner, and B. Rosner
Phys. Rev. A 47, 289 (1993).

60. "Secondary Electron Emission in Swift Heavy-Ion Atom Collisions"
Siegbert Hagmann, Chun-lei Liao, Chander Bhalla, Rajiv Shingal, Jeff Shinpaugh, Wanja Wolff, Hans Wolf, Rido Mann, Ron Olson, Horst Schmidt-Bocking
Radiation Effects and Defects in Solids 126, 35-40 (1993).

61. "Effect of Exchange on the Binary-Encounter-Electron Double-Differential Cross Section in C^{q+} - H_2 Collisions at 0.75 MeV/amu"
H. I. Hidmi, C. P. Bhalla, S. R. Grabbe, J. M. Sanders, P. Richard, and R. Shingal
Phys. Rev. A 47, 2398 (1993).

62. "Angular Distribution of Dissociated Deuterons by Impact of 2-16 MeV O^{8+}"
S. Cheng, C. L. Cocke, V. Frohne, E. Y. Kamber, J. H. McGuire, and Y. Wang
Phys. Rev. A 47, 3923 (1993).

63. "Fragmentation of CH_4 Caused by Fast-Proton Impact"
I. Ben-Itzhak, D. K. Carnes, S. G. Ginther, D. T. Johnson,
P. J. Norris, and O. L. Weaver
Phys. Rev. A 47, 3748 (1993).

64. "Quasimolecular X-Ray Spectrum from 117 keV Ne^{9+} + Ne Collisions"
M. H. Prior, R. Dorner, H. Berg, H. Schmidt-Bocking,
J.O.K. Pedersen, and C. L. Cocke
Phys. Rev. A 47, 2964 (1993).

65. "Multiple-Electron Removal and Molecular Fragmentation of CO by Fast F^{4+} Impact"
I. Ben-Itzhak, S. G. Ginther, and K. D. Carnes
Phys. Rev. A 47, 2827 (1993).

66. "Zero-Degree Binary Encounter Electrons in Fast Collisions of Highly Charged F and O Ions with H_2 Targets"
D. H. Lee, T.J.M. Zouros, J. M. Sanders, H. Hidmi, and P. Richard
NIMS B79, 11 (1993).

67. "Impulse Approximation Treatment of Electron-Electron Excitation and Ionization in Energetic Ion-Atom Collisions"
T.J.M. Zouros, D. H. Lee, J. M. Sanders, and P. Richard
NIMS B79, 166 (1993).

68. "On the Radiative Stabilization in Slow Double-Electron Capture Collisions of Highly Charged Ions with Neutral Atoms"
R. Ali, C. L. Cocke, M.L.A. Raphaelian, and M. Stockli
J. Phys. B: 26, L177 (1993).

69. "Theory of Projectile Ionization by Molecular Hydrogen Targets"
Y. D. Wang, J. H. McGuire, T.J.M. Zouros, D. H. Lee,
J. M. Sanders, and P. Richard
NIMS B79, 124 (1993).

70. "Double Electron Capture and the Angular Distribution of Ejected Electrons in Ne^{8+} - He Collisions"
Z. Chen and C. D. Lin
Phys. Rev. A 48, 1298 (1993).

71. "Direct Determination of Recoil Ion Detection Efficiency for Coincidence Time-of-Flight Studies of Molecular Fragmentation"
I. Ben-Itzhak, K. D. Carnes, S. G. Ginther, D. T. Johnson,
P. J. Norris, and O. L. Weaver
NIMS B79, 138 (1993).

72. "Impact Parameter Dependence of Classical Capture Probability from any Initial State by Fast Bare Projectiles"
I. Ben-Itzhak, Ashok Jain and O. L. Weaver
J. Phys. B 26, 1711 (1993).

73. "Close-Coupling Calculations of Electron Capture Cross Sections from the n=2 States of H by Protons and α Particles"
B. D. Esry, Z. Chen, C. D. Lin, and R. D. Piacentini
J. Phys. B 26, 1579 (1993).

74. "Measurements of Recoil Ion Longitudinal Momentum Transfer in Multiply Ionizing Collisions of Fast Heavy Ions with Multielectron Targets"
V. Frohne, S. Cheng, R. Ali, M. Raphaelian, C. L. Cocke, and R. E. Olson
Phys. Rev. Letters 71, 696 (1993).

75. "Formation and Mean Lifetime Measurements of the Long-Lived Doubly Charged $HeNe^{2+}$"
I. Ben-Itzhak, I. Gertner, O. Heber, and B. Rosner
Chem. Phys. Letters 212, 467 (1993).

76. "One and Two Electron Processes in Collisions of Highly Charged Ions with He at Velocities around 1 a.u."
J. P. Giese, W. Wu, I. Ben-Itzhak, C. L. Cocke, R. Ali, P. Richard, M. Stockli, and H. Schone
in "The Physics of Electronic and Atomic Collisions," edited by T. Andersen, B. Fastrup, F. Folkmann, H. Knudsen and N. Andersen, AIP Conf. Proc. No. 295 (American Institute of Physics, New York, 1993) p. 585.

77. "Charge-State Dependence of Binary-Encounter-Electron Cross Sections and Peak Energies"
H. I. Hidmi, P. Richard, J. M. Sanders, H. Schone, J. P. Giese, D. H. Lee, T.J.M. Zouros, and S. L. Varghese
Phys. Rev. A 48, 4421 (1993).

78. "Velocity Dependence of One- and Two-Electron Processes in Intermediate-Velocity Ar^{16+} + He Collisions"
W. Wu, J. P. Giese, I. Ben-Itzhak, C. L. Cocke, P. Richard, M. Stockli, R. Ali, H. Schone
Phys. Rev. A 48, 3617 (1993).

79. "Experimental Evidence for the Existence of the $2p\sigma$ Bound State of HeH_{2+} and Its Decay Mechanism"
I. Ben-Itzhak, I. Gertner, O. Heber, and B. Rosner
Phys. Rev. Letters 71, 1347 (1993).

80. "Binary Encounter Electrons in Ion-Atom Collisions"
C. P. Bhalla, R. Shingal and S. Grabbe
Nucl. Instrum. & Meth. B79, 170 (1993).

81. "Atomic Electron Capture in the Presence of a Narrow Nuclear Resonance: $^{40}Ar(p,p)^{40}Ar$ Reaction"
A. D. Gonzalez, J. P. Giese, E. Horsdal-Pedersen
Phys. Rev. A 48, 3663 (1993).

82. "Resonant Inelastic Scattering of Quasifree Electrons on $C^{5+}(1s)$"
P. Hvelplund, A. D. Gonzalez, P. Dahl, and C. P. Bhalla
Phys. Rev. A 49, 2535 (1994).

83. "The Enhancement of the Binary Encounter Peak for q = 1 to Z in Collisions of Fast C^{q+} and O^{q+} on H_2"
J. H. Posthumus, B. Christensen, N. Glargaard, J. N. Madsen,
L. H. Andersen, P. Hvelplund, S. R. Grabbe, and C. P. Bhalla
J. Phys. B 17, L97 (1994).

84. "Theoretical Auger Spectra of Selected Doubly Excited Li-like Ions"
K. R. Karim and C. P. Bhalla
J. Quant. Spectrosc. Radiat. Transfer 51, #4, 557 (1994).

85. "Electron Capture from C_{60} by Slow Multiply Charged Ions"
B. Walch, C. L. Cocke, R. Voelpel, and E. Salzborn
Phys. Rev. Letters 72, 1439 (1994).

86. "Mean Lifetimes of the Bound $2p\sigma$ State of HeH^{2+}"
I. Ben-Itzhak, Z. Chen, B. D. Esry, I. Gertner, O. Heber,
C. D. Lin, and B. Rosner
Phys. Rev. A 49, 1774 (1994).

87. "Velocity Dependence of Ionization and Fragmentation of Methane Caused by Fast-Proton Impact"
I. Ben-Itzhak, K. D. Carnes, D. T. Johnson, P. J. Norris, and O. L. Weaver
Phys. Rev. A 49, 881 (1994).

88. "Projectile-Charge-State Dependence of 0° Binary-Encounter Electron Production in 30-MeV $O^{q+} + O_2$ Collisions"
T.J.M. Zouros, P. Richard, K. L. Wong, H. I. Hidmi, J. M.
Sanders, C. Liao, S. Grabbe, and C. P. Bhalla
Phys. Rev. A 49, R3155 (1994).

89. "Mean Lifetime Calculations of the Metastable Doubly Charged $NeAr^{2+}$ Rare Gas Dimer"
Z. Chen, I. Ben-Itzhak, C. D. Lin, W. Koch, G. Frenking, I. Gertner, and B. Rosner
Phys. Rev. A 49, 3472 (1994).

90. "Multielectron Processes in 10-keV/u Ar^{q+} ($5 \leq Q \leq 17$) on Ar Collisions"
R. Ali, C. L. Cocke, M.L.A. Raphaelian, and M. Stockli
Phys. Rev. A 49, 3586 (1994).

91. "Experimental Separation of Electron-Electron and Electron-Nuclear Contributions to Ionization of Fast Hydrogenlike Ions Colliding with He"
W. Wu, K. L. Wong, R. Ali, C. Y. Chen, C. L. Cocke, V. Frohne, J. P. Giese, M. Raphaelian, B. Walch, R. Dorner, V. Mergel, H. Schmidt-Bocking, and W. E. Meyerhof
Phys. Rev. Letters 72, 3170 (1994).

93. "Energy Calibration of an Accelerator Using Cusp Electron Spectroscopy"
H. I. Hidmi, P. Richard, and I. Ben-Itzhak
Nucl. Instrum. & Meth. B88, 313 (1994).

94. "Electron-Electron Interaction in Projectile Ionization Investigated by High Resolution Recoil Ion Momentum Spectroscopy"
R. Dorner, V. Mergel, R. Ali, U. Buck, C. L. Cocke, K. Froschauer, O. Jagutzki, S. Lencinas, W. E. Meyerhof, S. Nuttgens, R. E. Olson, H. Schmidt-Bocking, L. Spielberger, K. Tokesi, J. Ullrich, M. Unverzagt, and W. Wu
Phys. Rev. Letters 72, 3166 (1994).

Manuscripts Accepted for Publication

1. "Evidence for Population of Highly Asymmetric States in Double Electron Capture by $O^{7,8+}$ and N^{7+} Colliding with He at Low to Intermediate Velocities"
   W. Wu, J. P. Giese, Z. Chen, R. Ali, C. L. Cocke, P. Richard, and M. Stockli
   Accepted for publication in Phys. Rev. A.

2. "Charge-State Equilibration Length of a Highly Charged Ion Inside a Carbon Solid"
   R. Herrmann, C. L. Cocke, J. Ullrich, S. Hagmann, M. Stockli, and H. Schmidt-Bocking
   Accepted for publication in Phys. Rev. A.

3. "Angular Distribution of δ Electrons Emitted in Collisions of 1.0 MeV/u F^{q+}(q = 4,6,8,9) with Molecular Hydrogen"
   C. Liao, P. Richard, S. R. Grabbe, C. P. Bhalla, T.J.M. Zouros and S. Hagmann
   Accepted for publication in Phys. Rev. A in Vol. 50.

4. "Excitation and Ionization of H(2s) by Proton Impact"
   Z. Chen, B. D. Esry, C. D. Lin and R. D. Piacentini
   Accepted for publication in J. Phys. B.

5. "Charge Exchange and Electron Emission in Slow Collisions of Highly Charged Ions with C_{60}"
   U. Thumm
   Accepted for publication in J. Phys. B, Vol. 27 (1994).

6. "Scaling of Single Ionization Cross Sections of Molecules with the Charge of Fast Projectiles"
   V. Krishnamurthi, I. Ben-Itzhak, K. D. Carnes, and B. M. Barnes
   Accepted for publication in J. Phys. B.

Manuscripts Submitted for Publication

1. "Determination of the Compton Profile of C_{60} through Binary Encounter Electron Spectroscopy"
   B. D. DePaola, R. Parameswaran, B. P. Walch, M. D. Troike, P. Richard, M. J. Puska, and R. M. Nieminen
   Submitted to Physical Review Letters.

2. "Instantaneous- and Time-Averaged Current Measurements of Pulsed Ion Beams from an Electron Beam Ion Source"
   Martin P. Stockli, S. Winecki, and E. D. Donets
   Submitted to Review of Scientific Instruments, American Institute of Physics.

3. "AFM Imaging of Nanometer-size Surface Features Produced on Mica by Single, Highly-Charged, Low-Energy Ions"
   D. Parks, R. Bastasz, R. W. Schmieder and M. Stockli
   Submitted to J. Vac. Sci. Technol.

4. "Electron Capture in K^+ Ion Collisions with Na(4d)"
   M.F.V. Lundsgaard, Z. Chen and C. D. Lin
   Submitted to J. Phys. B.

5. "Close-Coupling Calculations of Alignment Parameters in p + Mg(2p) Collisions"
   Z. Chen and C. D. Lin
   Submitted to Phys. Letters.

6. "Electron Capture from Elliptical Rydberg States"
   M.F.V. Lundsgaard, N. Toshima, Z. Chen and C. D. Lin
   Submitted to J. Phys. B.

7. "Electron Capture from Circular Rydberg States"
   M. Lundsgaard, Z. Chen, C. D. Lin and N. Toshima
   Submitted to Phys. Rev. Letters.

8. "Kinetic Energy Release in Molecular Dissociation of CO Caused by Fast F^{4+} Impact"
   I. Ben-Itzhak, S. G. Ginther, V. Krishnamurthi, and K. D. Carnes
   Submitted to Phys. Rev. A.

9. "Charge Dependence of Electron Capture and Electron Loss in Collisions of 1 MeV/amu O^{q+} and F^{q+} with Ar"
   O. Heber, G. Sampoll, B. B. Bandong, R. J. Maurer, R. L. Watson, I. Ben-Itzhak, J. M. Sanders, J. L. Shinpaugh, and P. Richard
   Submitted to Phys. Rev. A.

Other Collaborative Research

1. "Single and Double K-Shell Ionization and Electron-Transfer Cross Sections for Fe and Ni Bombarded by S Ions and Fe by Si Ions at 1.25-4.70 MeV/amu"
   L. C. Tribedi, K. G. Prasad, P. N. Tandon, Z. Chen, and C. D. Lin
   Phys. Rev. A 49, 1015 (1994).

2. "X-Ray Spectroscopy of Highly Charged Ions Interacting with Surfaces"
   B. d'Etat, J. P. Briand, G. Ban, L. de Billy, P. Briand, J. P. Desclaux, G. Melin, T. Lamy, G. Lamboley, P. Richard, M. Stockli, R. Ali, N. Renard, D. Schneider, M. Clark, P. Beierstorfer, V. Decaux, in "VIth International Conference on the Physics of Highly Charged Ions," Manhattan, KS, ed. by P. Richard, M. Stockli, C. L. Cocke, and C. D. Lin (American Institute of Physics, New York, 1993) p. 592.

3. "The Dirac R-Matrix Method for Scattering of Slow Electrons from Alkali-Metal-Like Targets"
   U. Thumm
   American Institute of Physics Conference Proceedings 295, "XVIII International Conference on the Physics of Electronic and Atomic Collisions," edited by T. Anderson, B. Fastrup, F. Folkmann, H. Knudsen, and N. Andersen (AIP Press, New York 1993).

Abstracts for Grant Period

June 15, 1991 - June 14, 1994

Annual DOE Atomic Physics Program Workshop, Kansas State University, Manhattan (October 15-16, 1991).

1. "Low Energy Collisions Involving Multiply-Charged Ions"
   Macdonald Laboratory Group

2. "High Energy Collisions Involving Multiply-Charged Ions"
   Macdonald Laboratory Group

3. "Theory for Multiply-Charged Ions"
   Macdonald Laboratory Group

Second International Symposium on Swift Heavy Ions in Matter, Bensheim/Darmstadt, Germany (May 19-22, 1992).

4. "Secondary Electron Emission in Swift Heavy-Ion Atom Collisions"
   S. Hagmann, C. L. Liao, C. Bhalla, R. Shingal, J. Shinpaugh, W. Wolff, H. Wolf, R. Mann, R. Olson, and H. Schmidt-Bocking

Annual Meeting of the Division of Atomic, Molecular, and Optical Physics, Chicago, IL (19-22 May 1992).

5. "The Macdonald Laboratory at Kansas State University as a User Facility for Atomic Physics Studies"
   Pat Richard

6. "Charge State Dependence of Double Differential Cross Sections (DDCS) for Binary Encounter Electrons (BEe)"
   H. I. Hidmi, P. Richard, J. M. SAnders, H. Schone, J. P. Giese, D. H. Lee, S. L. Varghese, and T.J.M. Zouros

7. "K-Shell Ionization of O^{4+} and C^{2+} Ions in Fast Collisions with H_2 and He Gas Targets"
   D. H. Lee, T.J.M. Zouros, J. M. Sanders, P. Richard, J. M. Anthony, Y. D. Wang, and J. H. McGuire

8. "A Discussion of the Superconducting LINAC/Tandem Accelerator Facilities for Ion-Atom and Ion-Molecule Collisions Research at JRML"
   T. J. Gray

9. "Secondary Electron Yields from Low Energy, Highly Charged Ions Impacting on a Metal Surface"
   Martin P. Stockli

10. "The KSU-CRYEBIS: A Low Energy, Highly Charged Ion Factory Designed and Operated for Atomic Physics Users"
    Martin P. Stockli, R. M. Ali, C. L. Cocke, M.L.A. Raphaelian, and T. N. Tipping

11. "Multiple Electron Removal and Fragmentation of CO Caused by Fast F^{q+} Impact"
    I. Ben-Itzhak, S. G. Ginther, and K. D. Carnes

12. "Diffraction Structure Observed in Delta Electron Spectra Emitted in Cu^{q+}→H_2, Ne Collisions"
    C. Liao and S. Hagmann

13. "Inverse q-Scaling and Diffraction Patterns in Binary Encounter Electrons in Au^{q+}-Atom Collisions"
    S. Hagmann, J. Shinpaugh, W. Wolf, Ch. Kelbch, J. Euler, R. Mann, P. Mokler, C. L. Cocke, and H. Schmidt-Bocking

14. "Charge Capture from a Laser-Excited Target by Highly Charged Ions"
    B. D. DePaola, B. P. Walch, and S. Maleki

15. "Single and Double Electron Processes with Slow Highly Charged Projectiles"
    W. Wu, J. P. Giese, P. Richard, M. Stockli, R. Ali, and H. Schone

16. "Charge Transfer in Collisions of Alpha Particles with Ground and Excited State Sodium Atoms"
    Rajiv Shingal

17. "Electron Capture in Collisions of High Energy Ions with Atomic and Molecular Hydrogen"
    J. M. Sanders, H. Schone, J. P. Giese, H. I. Hidmi, A. Landers, and P. Richard

18. "Q-Value Measurements in Low Energy Collisions of Highly Charged Ions with Atoms by Recoil Longitudinal Momentum Spectroscopy"
    R. Ali, V. Frohne, C. L. Cocke, M. Stockli, S. Cheng, and M. Raphaelian

19. "Triple-Coincidence Measurements of K X Rays, Recoil and Final Projectile Charge States in Low Energy Collisions of Ar^{17+} with He and Ar Atoms"
    R. Ali, Z. Chen, C. L. Cocke, C. D. Lin, M. Lundsgaard, M. Raphaelian, and M. Stockli

20. "Ar^{q+} ($10 \leq q \leq 17$) Auger Spectra from Low to Intermediate Collisional Velocity with Atomic Argon"
M.L.A. Raphaelian, R. Ali, C. L. Cocke, S. Hagmann, and M. P. Stockli

21. "Velocity Dependence of Charge Capture Cross Sections in Ar^{7+} + Na(3s), Na(3p) Collisions"
S. Maleki, M.L.A. Raphaelian, B. P. Walch, and B. D. DePaola

22. "Observation of Longitudinal Momentum Shifts in Recoil Ions from Collisions of 1 MeV/u F^{9+} + Ne"
V. Frohne, C. L. Cocke, and S. Cheng

23. "The Calculation and Analysis of Fluorescence Yields of High-Lying Doubly Excited States of Highly Charged Ions"
Z. Chen and C. D. Lin

24. "The High-Lying States of Coulombic Three-Body Systems"
Z. Chen and C. D. Lin

25. "Electron Capture in Highly Charged Ion Collisions Reduced Close Coupled Calculations"
M.F.V. Lundsgaard and C. D. Lin

Annual DOE Atomic Physics Program Workshop, Cornell University, New York (October 15-16, 1992).

26. "High Energy Collisions Involving Multiply Charged Ions"
J. R. Macdonald Laboratory Group

27. "Low Energy Collisions Involving Multiply Charged Ions"
J. R. Macdonald Laboratory Group

28. "Theory of Multiply Charged Ions"
J. R. Macdonald Laboratory Group

12th International Conference on the Application of Accelerators in Research and Industry, Denton, Texas (November 2-5, 1992).

29. "Probing the Physics of Low Energy, Highly Charged Ions with the KSU-CRYEBIS"
Martin P. Stockli

30. "Binary Encounter Electrons in Ion-Atom Collisions"
R. Shingal

31. "Angular Distribuitons in Resonant Transfer Excitaitno in Ion-Atom Collisions"
C. P. Bhalla

32. "Fluorescence Yields for Hypersatellite Lines for Variously Ionized Argon"
C. P. Bhalla, K. R. Karim, and M. Wilson

33. "Secondary Electron Yields from Low Energy, Highly Charged Ions Impacting on Metal Surfaces"
Slawomir Winecki and M. P. Stockli

34. "Fast Timing Signal Sorter for Multiple Hit Coincidence Time-of-Flight Spectroscopy"
I. Ben-Itzhak, K. D. Carnes, and B. D. DePaola

35. "Direct Determination of Recoil Detection Efficiency for Coincidence Time-of-Flight Studies of Molecular Fragmentation"
I. Ben-Itzhak, S. G. Ginther, K. D. Carnes, P. J. Norris, D. T. Johnson, and O. L. Weaver

36. "Development of an Ion-Ion Collisions Facility at KSU"
J. P. Giese

37. "Two-Electron Processes in Collisions of Ar^{16+} Ions with He Atoms"
J. P. Giese

38. "Heavy Ion-Atom Collision Phenomena Using Zero Degree Electron Spectroscopy"
Pat Richard

39. "Electron Capture in Collisions of High Energy Ions with Atomic and Molecular Hydrogen"
J. M. Sanders, H. Schone, J. P. Giese, H. I. Hidmi, A. Landers, and P. Richard

40. "Methods for Measuring Mean Lifetimes of Metastable Molecular Ions Formed in Fast Collisions"
I. Gertner, B. Rosner, and I. Ben-Itzhak

<u>International Conference on Highly Charged Ions, Kansas State University, Kansas (September 28 - October 2, 1992).</u>

40. "Direct Measurements of the Decay Time of Ar Hollow Atoms in Solids"
J. P. Briand, B. d'Etat, L. deBilly, Rami Ali, Nathalie Renard, Patrick Richard, and Martin Stockli

41. "Radiative Electron Capture of Slow Argon Ions Inside a Solid"
L. deBilly, J. P. Briand, Rami Ali, Nathalie Renard, Patrick Richard, and Martin Stockli

42. "Energy Loss of 576 keV Ar Ions in Carbon as Function of the Initial Charge State"
R. Hermann, C. L. Cocke, S. Hagmann, J. Ullrich, M. Stockli, and H. Schmidt-Bocking

43. "Development of an Ion-Ion Collisions Facility at KSU"
J. P. Giese, C. Y. Chen, A. Landers, M. Stockli, P. Richard, and C. Miller

44. "Line Fluorescence Yields for Lithiumlike Silicon
K. R. Karim and C. P. Bhalla

45. "Measurement of the Momentum Distributions of Recoil Ions in the 1 MeV/u F^{9+} + Ne Collision System"
V. Frohne, C. L. Cocke, R. Olson, S. Cheng, R. Ali, and M.L.A. Raphaelian

46. "Fragmentation of CO Caused by Fast F^{4+} Impact"
I. Ben-Itzhak, S. G. Ginther, and K. D. Carnes

47. "Velocity Dependence of the Fragmentation of CH_4 Caused by Fast H^+ Impact"
I. Ben-Itzhak, S. G. Ginther, K. D. Carnes, P. J. Norris, D. T. Johnson, and O. L. Weaver

48. "Interference Bewteen RTEA and Elastically Scattered Target Electrons in 20 MeV F^{6+} + H_2 Collisions"
T.J.M. Zouros, H. I. Hidmi, J. M. Sanders, P. Richard, S. L. Varghese, M.L.A. Raphaelian, and C. P. Bhalla

49. "Electron-Electron Interactions in K-Shell Excitation of F^{6+} Ions in Fast Collisions with H_2 Targets"
D. H. Lee, T.J.M. Zouros, J. M. Sanders, and P. Richard

50. "Effect of the Charge State on the Double Differential Cross Section of the Binary Encounter Electrons"
H. I. Hidmi, P. Richard, J. M. Sanders, H. Schone, J. P. Giese, D. H. Lee, T.J.M. Zouros, and S. L. Varghese

51. "Electron Capture from Buckminsterfullerene C_{60} by Multiply Charged Projectiles"
B. Walch, C. L. Cocke, R. Volpel, and E. Salzborn

52. "Experimental Evidence for the Formation of the $2p\sigma$ Bound State of HeH^{2+}"
I. Ben-Itzhak, I. Gertner, and B. Rosner

53. "Single and Double Electron Processes in Ar^{16+} + He Collisions"
W. Wu, J. P. Giese, P. Richard, M. Stockli, R. Ali, C. L. Cocke, and H. Schone

54. "Velocity Dependence of Absolute Cross Sections for Charge Capture by Ar^{7+} from Ground State and Excited Sodium"
S. Maleki, M.L.A. Raphaelian, M. P. Stockli, B. P. Walch, and B. P. DePaola

55. "Q-Value Measurements in Charge Transfer Collisions of Highly Charged Ions with Atoms by Recoil Longitudinal Momentum Spectroscopy"
R. Ali, V. Frohne, C. L. Cocke, M. Stockli, S. Cheng, H. Sharabati, and M.L.A. Raphaelian

56. "Diffraction Structures in δ-Electron Spectra from Heavy Ion-Atom Collisions"
S. Hagmann, C. Liao, C. P. Bhalla, R. Shingal, J. Shinpaugh, W. Wolff, H. Wolf, R. Mann, and H. Schmidt-Bocking

International Conference on the Physics of Electronic and Atomic Collisions, Aarhus, Denmark (July 21-27, 1993).

57. "Diffraction Observed in Heavy-Ion Induced Electron Continua"
C. Liao, S. Hagmann, Ch. Bhalla, R. Shingal, H. Schmidt-Bocking, R. Mann, J. Shinpaugh, W. Wolff, and H. Wolf

58. "Violation of q^2 Scaling in Delta-Electron Emission in Heavy Ion Atom Collisions"
S. Hagmann, C. Liao, Ch. Bhalla, R. Shingal, H. Schmidt-Bocking, R. Mann, J. Shinpaugh, W. Wolff, and H. Wolf

59. "Electron Capture in Collisions of $O^{8,7+}$, N^{7+} with He at Intermediate Velocities"
W. Wu, J. P. Giese, C. L. Cocke, R. Ali, P. Richard, and M. Stockli

60. "Velocity Dependence of CO and CH_4 Fragmentation Caused by Fast Proton Impact"
I. Ben-Itzhak, K. D. Carnes, and V. Krishnamurthi

61. "The Dirac R-Matrix Method for Scattering of Slow Electrons from Alkalai-Metal-like Targets"
U. Thumm

62. "Experimental Evidence for the Formation of Metastable $HeNe^{2+}$"
I. Ben-Itzhak, I. Gertner, O. Heber, and R. Rosner

63. "One and Two Electron Processes in Collisions of Highly Charged Ions with He at Velocities around 1 a.u."
J. P. Giese, W. Wu, I. Ben-Itzhak, C. L. Cocke, R. Ali, P. Richard, and H. Schone

64. "Multi-Electron Processes in 10 keV/u Ar^{q+} ($5 \leq q \leq 17$) on Ar Collisions"
R. Ali, C. L. Cocke, M.L.A. Raphaelian, and M. Stockli

65. "Charge-State q-Dependence of O° Binary Encounter Electron Production in 30 MeV O^{q+} + H_2He,Ne, and O_2 Collisions"
T.J.M. Zouros, K. L. Wong, H. I. Hidmi, J. M. Sanders, C. Liao, P. Richard, S. Grabbe, and C. P. Bhalla

66. "The KSU-CRYEBIS: A User Facility Providing Low-Energy Highly-Charged Ions"
M. P. Stockli, R. M. Ali, C. L. Cocke, M.L.A. Raphaelian, P. Richard, T. N. Tipping, S. Winecki and W. Wu

67. "Mean Lifetime Measurements of the Newly Discovered $2p\sigma$ Lowest Bound State of HeH^{2+}"
I. Ben-itzhak, I. Gertner, O. Heber, and B. Rosner

68. "Electron Capture from C_{60} by Multiply Charged Projectiles"
B. Walch, C. L. Cocke, E. Salzborn, and R. Volpel

Annual Division of Atomic, Molecular, and Optical Physics Meeting, Reno, Nevada (May 16-19, 1993).

69. "Charge Exchange in Large Angle Scattering of C^{6+} on He"
S. Winecki, R. Ali, C. L. Cocke, M.L.A. Raphaelian, P. Richard, H. Schmidt-Bocking, H. Schone, and M. P. Stockli

70. "Angular Distribution of Binary Encounter Electrons"
C. Liao, T.J.M. Zouros, P. Richard, S. Grabbe, C. P. Bhalla, and S. Hagmann

71. "Rydberg Atom Targets in Slow Collisions with Highly Charged Ions"
B. D. DePaola, J. Lauritsen, M.-T. Huang, and S. Maleki

72. "Absolute Cross Sections for Charge Capture by Ar^{8+} from the Fullerenes $C_{60}C_{70}$"
Bernhard P. Walch and C. Lewis Cocke

73. "Secondary Electron Yields from Low Energy, Highly Charged Ions Impacting on Metal Surfaces"
Martin P. Stockli and Slawomir Winecki

74. "Angular Distributions in Ar^{15+} - Ar Collisions at 0.2 a.u. $\leq v_p \leq 2.0$ a.u."
M.L.A. Raphaelian, R. Ali, C. L. Cocke, M. P. Stockli, and W. Wu

75. "Double Electron Capture and Angular Distribution of Ejected Electrons in Ne^{8+}-He Collisions"
Z. Chen and C. D. Lin

76. "Fluorescence Yields for Hypersatellite Lines for Variously Ionized Silicon"
C. P. Bhalla, K. R. Karim, and M. Wilson

77. "Observations of Transverse Momentum Distributions from Fast Collisions of F^{9+} + Ne"
V. Frohne, C. L. Cocke, R. Ali, M. Raphaelian

78. "Energy Shifts of the Binary Encounter Peak (BEP) in 1 MeV/u Si^{q+} + H_2"
H. I. Hidmi, J. M. Sanders, T.J.M. Zouros, and P. Richard

79. "Binary Encounter Electron Production in Ion-Atom Collisions"
S. Grabbe, C. P. Bhalla, and R. Shingal

80. "Observation of Enhanced Zero-Degree Binary Encounter Electron Production with Decreasing Charge-State q in 30 MeV O^{q+} + O_2 Collisions"
T.J.M. Zouros, K. L. Wong, H. I. Hidmi, J. M. Sanders, C. Liao, and P. Richard

81. "Fragmentation of CO Caused by Fast F^{4+} Impact"
V. Krishnamurthi, I. Ben-Itzhak, and K. D. Carnes

82. "Velocity Dependence of CO and CH_4 Electron Removal and Fragmentation Caused by Fast Proton Impact"
I. Ben-Itzhak, K. D. Carnes, and V. Krishnamurthi

83. "Electron Transfer and Ionization in Collisions of Highly Stripped Ions with Neutral Targets at Intermediate Velocities"
C. L. Cocke, R. Ali, V. Frohne, J. P. Giese, M. Raphaelian, P. Richard, M. Stockli, and W. Wu

Annual DOE Atomic Physics Program Workshop, Charlottesville, Virginia (October 15-16, 1993).

84. "High Energy Collisions Involving Multiply Charged Ions"
J. R. Macdonald Laboratory Group

85. "Low Energy Collisions Involving Multiply Charged Ions"
J. R. Macdonald Laboratory Group

86. "Theory of Structure and Collisions of Highly Charged Ions"
J. R. Macdonald Laboratory Group

Annual Division of Atomic, Molecular, and Optical Physics Meeting, Crystal City, Virginia (April 18-22, 1994).

87. "Mean Lifetime of HeH^{2+}"
B. D. Esry, I. Ben-Itzhak, Z. Chen, and C. D. Lin

88. "Charge Exchange in Large Angle Scattering of C^{4+} on He"
S. Winecki, R. Ali, C. L. Cocke, M.L.A. Raphaelian,
P. Richard, H. Schmidt-Bocking, H. Schone, and M. P. Stockli

89. "Scaling Law for Molecular Ionization"
V. K. Krishnamurthi, I. Ben-Itzhak, and K. D. Carnes

90. "Q-Dependence of Molecular Fragmentation"
V. K. Krishnamurthi, I. Ben-Itzhak, and K. D. Carnes

91. "Atomic Parameters of Selected Two-Electron Hollow Ions"
K. R. Karim, T. Barnett, Melanie Henderson, and C. P. Bhalla

92. "Fluorescence Yields for Hypersatellite Lines for Variously Ionized Calcium"
C. P. Bhalla, K. R. Karim, and M. Wilson

93. "Observations of Recoil Ion Momentum Distributions in the 10 MeV C^{6+} + Ne Collision System"
V. Frohne, C. L. Cocke, M. Raphaelian, and W. Wu

94. "Energy Transfer Processes Between Xe^{30+} Projectiles and Argon Target Atoms"
M.L.A. Raphaelian, M. P. Stockli, W. Wu, and C. L. Cocke

95. "Electron-Recoil-Projectile Coincidence Experiments in the J. R. Macdonald Laboratory at Kansas State University"
M.L.A. Raphaelian, M. P. Stockli, and C. L. Cocke

96. "Electron Capture and Target Ionization in Collisions of $C\ell^{9+}$ and $C\ell^{13+}$ Projectile Ions Incident on Helium"
K. L. Wong, W. Wu, V. Frohne, B. Walch, C. Y. Chen, I. Ben-Itzhak, C. L. Cocke, J. Giese, and P. Richard

97. "Experimental Separation of Electron-Electron and Electron-Nuclear Contributions to Ionization of Fast Hydrogenlike Ions Colliding with He"
W. Wu, K. L. Wong, R. Ali, C. L. Cocke, V. Frohne, J. P. Giese, M. L. Raphaelian, B. Walch, R. Dorner, V. Mergel, H. Schmidt-Bocking, and W. E. Meyerhof

98. "Charge Exchange and Electron Emission in Slow Collisions of Highly Charged Ions with C_{60}"
U. Thumm

99. "Electron Capture from Circular Rydberg Atoms"
M.F.V. Lundsgaard, Z. Chen, and C. D. Lin

100. "Calculations of Q Values in Single and Double Charge Transfer Collisions of Highly Charged Ions with Atoms"
Z. Chen, C. D. Lin, and N. Toshima

101. "Excitation and Ionization of H(2s) by Proton Impact"
Z. Chen, B. D. Esry, C. D. Lin, and R. D. Placentini

102. "Correlated Two-Electron Effect in Collisions of 0.3 MeV/u I^{6+} on H_2"
C. Liao, S. Hagmann, P. Richard, C. Bhalla, and S. Grabbe

103. "Diffraction Structure Observed in Binary Encounter Electron Peak"
C. Liao, S. Hagmann, C. Bhalla, S. Grabbe, and P. Richard

104. "Multi-Electron Emission in Heavy-Ion Atom Collisions"
S. Hagmann, C. Liao, J. Ullrich, R. Mann, R. Moshammer, U. Bechthold, A. Bohris, and H. Schmidt-Bocking

105. "The Mean Lifetime of $^3He^4He^{2+}$"
I. Ben-Itzhak, Z. Chen, I. Gertner, O. Heber, C. D. Lin, and B. Rosner

106. "Equivalence Between Born and Impulse Approximations for the Antiscreening Process"
E. C. Montenegro and T.J.M. Zouros

107. "State Selective Measurement of Single Differential Cross Sections for Excitation and RTE in 4 MeV B^{2+} + H_2 Collisions"
T.J.M. Zouros, G. Toth, E. C. Montenegro, P. Richard, S. Grabbe, and C. P. Bhalla

108. "Enhancement of Narrow Resonances in Photoabsorption from He Atom in Metastable States"
Bin Zhou, C. D. Lin, T. Z. Tang, S. Watanabe, and M. Matsuzawa

109. "Photoionization of Beryllium Atoms"
Bin Zhou and C. D. Lin

110. "Electron Capture from Elliptical Rydberg Atoms"
Uwe Thumm

8. Financial Report

It is anticipated that there will be no unexpended funds for the current funding period February 15, 1994 to February 14, 1995 (FY94).